BODY AXIS FORMATION IN *Xenopus laevis*: POSITIVE AND NEGATIVE REGULATION OF CANONICAL WNT-MEDIATED TRANSCRIPTION

MARK KENNEDY


CENTRE FOR NFLD. STUDIES
MEMORIAL UNIVERSITY
OF NEWFOUNDLAND

Title page

Body axis formation in *Xenopus laevis*:

Positive and negative regulation of Canonical Wnt-mediated transcription

By

© Mark Kennedy

A thesis submitted to the

School of Graduate Studies

in partial fulfillment of the

requirements for the degree of

Doctorate of Philosophy

Division of Biomedical Science

Faculty of Medicine

Memorial University of Newfoundland

St. John's Newfoundland

ABSTRACT

Establishment of dorsoventral polarity in *Xenopus* embryos requires activation of the canonical Wnt signal transduction pathway. Accumulated evidence has indicated that the key effector of canonical Wnt signaling, the β-catenin transcriptional activator, is localized in nuclei of dorsally fated cells of the early embryo and is required for dorsal development. The importance of β-catenin as a key element in body axis formation implies that factors which influence β-catenin expression and activity play important roles during dorsal development. Our understanding, however, of the mechanism(s) that govern β-catenin activity, for example, during embryonic development, is incomplete. Therefore, there is a need to identify factors that both inhibit and promote its activity. To this end, I have identified several novel proteins that interact with β-catenin to modulate its transcriptional activity in *Xenopus* embryos.

I first determined that the *Xenopus* Rel/NF-κB proteins, XRelA and XRel3, function as inhibitors of β-catenin activity in embryos. Using gain-of-function assays, I found that both XRelA and XRel3 perturbed dorsal development by repressing the expression of multiple *Xenopus nodal-related* (*Xnr*) genes. Since dorsal development is a canonical Wnt-dependent process and the timing and level of *Xnr* expression is regulated by canonical Wnt signaling, I hypothesized that XRelA/XRel3 inhibits Canonical Wnt activity in embryos to regulate axis formation. Co-expression of either XRelA or XRel3 efficiently antagonized ectopic β-catenin activity, as measured by their ability to prevent supernumerary axis formation in embryos injected at the 2-cell stage with β-catenin and a constitutively active β-catenin mutant. Furthermore, XRel3 directly interacted with

β-catenin, using *in vitro* co-immunoprecipitation assays. These results suggest a mechanism whereby *Xenopus* Rel proteins negatively regulate *Xnr* expression by inhibiting β-catenin-dependent transcription thus controlling dorsal axis development.

In a second set of experiments, I explored the role of a component of the β-catenin transcriptional activation complex called B-cell lymphoma 9 (Bcl9), which is the orthologue to Legless (Lgs) of *Drosophila* and mammals. In *Drosophila* embryos, Lgs/Bcl9 was identified as a bridging protein between the downstream component, Pygopus, and β-catenin. Furthermore, both Lgs/Bcl9 and Pygopus were demonstrated to be indispensable for β-catenin-dependent embryonic patterning in *Drosophila*. Unlike Pygopus, however, the role of Lgs/Bcl9 in vertebrate development is unknown. I determined that like its fly counterpart, *Xenopus* Bcl9 (XBcl9) directly interacted *in vitro*, via conserved peptide sequences with the co-activator proteins, Pygopus and β-catenin. Interestingly, XBcl9 preferentially accumulated in dorsal nuclei at a stage in development later than that reported for β-catenin and just prior to Wnt target gene activation. Gain-of-function assays demonstrated that XBcl9 was dependent on Pygopus to ectopically promote β-catenin target gene transcription, and that β-catenin was dependent on its interaction with XBcl9 for dorsal axis formation. Additionally, loss-of-function assays determined that XBcl9 was required for body axis formation during *Xenopus* development. These results implied that the timing of XBcl9 nuclear localization may indicate an important step in dorsal cell fate determination.

The role of XBcl9 in axis formation suggested that its regulation is important for normal development. In my final set of experiments, I determined that *XBcl9* is post-

transcriptionally regulated in *Xenopus* embryos. The inhibition of XBcl9 translation is dependent on a minimal 29nt element in the 5'UTR, proximal to the putative start of translation, and is well conserved in human Bcl9. The minimal repression element is predicted to form a stable secondary structure, posing as a possible block to constitutive translation. Due to the dependence of β-catenin on XBcl9 for axis development in *Xenopus* embryos, these results suggest a novel mechanism regulating β-catenin-dependent transcription.

ACKNOWLEDGEMENTS

I would like to thank a number of people who have helped me in many ways during the course of my graduate studies. First, I would like to thank current and past members of the Terry Fox labs, Corrine Mercer, Rebecca Ford, and Blue Lake who provided me with confidence early in my studies based on their own experiences. I especially want to acknowledge Phillip Andrews who was always willing to lend a hand or listen to my incessant 'science' babbling.

Also, I would like to thank my entire family for their unwavering and emotional support during my entire university career. Especially my wife, Janice, for her patience, encouragement and understanding through the long hours I spent at the lab in order for me to reach my academic goals.

Lastly, I would like to express my sincere gratitude to Dr. Ken Kao, for his supervision, patience and commitment to me and my studies, especially at times when my research seemed to stumble. As well as for providing me with the opportunity to learn not just how to do research but what it takes to be a successful scientist. And for his continued support and advice that fueled my maturation as a developing researcher and for his many insights that will undoubtedly benefit me in my future career.

TABLE OF CONTENTS

LIST OF TABLES

LIST OF FIGURES

LIST OF ABBREVIATIONS

APC.....Adenomatis polyposis coli
Arm.....Armadillo; *Drosophila* of β-catenin
ATP-[α-^{32}P] .....Adenosine triphosphate; alpha phosphate radiolabelled with ^{32}P
bFGF.....basic Fibroblastic growth factor
BMP.....Bone morphogenetic protein
BRE.....Bruno response element
BSA.....Bovine serum albumin
BUTR.....5'UTR of XBcl9
cAMP.....cyclic Adenosine monophosphate
CamKII.....Camodulin kinase II
Canonical Wnt.....β-catenin mediated transcription
CBP/p300.....CREB binding protein
cDNA.....complimentary DNA
Cer-S.....Mutant form of Cerberus that specifically inhibits Xnrs
CKI/II.....Casein Kinase I/II
CNS.....Central nervous system
Co-IP.....Co-immunoprecipitation
CPE.....Cytoplasmic polyadenylation element
CPEB.....Cytoplasmic polyadenylation element binding protein
Cpm.....counts per minute
CREB.....cAMP response element binding protein
CtBP.....C-terminal binding protein
D_2O.....Deuterium oxide (a.k.a heavy water)
DAI.....Dorsoanterior index
DAPI.....4',6-diamidino-2-phenylindole
Dl.....*Drosophila* Dorsal protein
DMEM.....Dulbecco's modified eagle's medium
DNA.....Deoxyribonucleic acid
Dsh.....Dishevelled
DTT.....Dithiothreitol
EDTA.....ethylenediaminetetraacetic acid
eFGF.....Embryonic Fibroblastic growth factor
EGA.....Embryonic genome activation
EGF-CFC.....Nodal co-receptor
EGFP.....Enhanced green fluorescent protein
EGTA.....ethylene glycol tetraacetic acid
eIF.....eukaryotic initiation factor
FBS.....Fetal bovine serum
FGF.....Fibroblastic growth factor
FITC.....Fluorescein isothiocyanate
Fz.....Frizzled receptor

GBP.....GSK3β binding protein
Gsd.....goosecoid
GST.....Glutathione S-transferase
GTP.....Guanosine triphosphate
GVBD.....Germinal vesicle breakdown
H4.....Histone 4
HD.....Homology domain
HDAC.....Histone deacetylase
HEK293T.....Human embryonic kidney cells (Transformed)
HMG.....High mobility group
HRP.....Horseradish peroxidase
HSPG.....Heparan sulfate proteoglycans
IκB .....Inhibitor κ B (*i.e.* inhibitor of NF-κB)
IKK.....IκB kinase
IL.....Interleukin
IP.....Immunoprecipitation
IRE.....Iron responsive element
IRES.....Internal ribosome entry site
IRP.....Iron responsive element binding protein
IVT.....*In vitro* translated
KCl.....Potassium chloride
kD.....kilodaltons
KLC.....Kinesin light chain
L-15.....Leibovitz medium
LAP.....Leukemia associated protein
Lgs/Bcl9.....Legless/B-cell lymphoma 9
LH.....Luteinizing hormone
Li^+.....Lithium ion
LPS.....Lipopolysaccharide
LRP.....Low density lipoprotein related receptor
m^7G.....7-methylguanosine
MAPK.....Mitogen activated protein kinase
MBT.....Midblastula transition
Med12/13.....Mediator complex subunits 12/13
MEK.....MAPK kinase
MEMFA.....Fixative: Mops, EDTA, $MgSO_4$, formaldehyde
µg.....micrograms
$MgCl_2$.....Magnesium dichloride
$MgSO_4 \cdot 7H_2O$.....Magnesium sulphate heptahydrate
MII.....Metaphase II
miRNA.....micro RNA
µl.....microliter
mM.....millimolar
mm.....millimeter

MMLV-RT.....Moloney murine leukemia virus reverse transcriptase
MO.....Morpholino
MOPS.....3-(N-morpholino) propanesulfonic acid
MPF.....Maturation promoting factor
mRFP.....monomeric red fluorescent protein
mRNA.....messenger ribonucleic acid
MT.....Myc tagged
$Na_2HPO_4 \cdot 7H_2O$.....Disodium phosphate heptahydrate
$NaH_2PO_4 \cdot H_2O$.....Sodium dihydrogenphosphate monohydrate
NAM.....Normal amphibian medium
NaN_3.....Sodium azide
Native PAGE.....Non-denaturing polyacrylamide gel electrophoresis
NC.....Nieuwkoop Center
NF stages.....Nieuwkoop and Faber embryonic staging atlas
ng.....nanogram
NLS.....Nuclear localization sequence
nt.....nucleotide
OCM.....Oocyte culture medium
ODC.....Ornithine decarboxylase
Oligo dT.....18mer thymidine oligonucleotide
ONPG.....*ortho*-Nitrophenyl-β-galactoside
ORF.....Open reading frame
PABP.....Poly(A) tract binding protein
PBS.....Phosphate buffered saline
PBT.....PBS with Tween-20
PCP.....Planar cell polarity
PCR.....Polymerase chain reaction
pg.....picograms
PHD.....Plant homology domain
PI.....Prophase I
PKA.....Protein kinase A
PKC.....Protein kinase C
PMT.....Photomultiplier tube
qPCR.....quantitative/real time polymerase chain reaction
R85.....dominant negative GSK3β; Lysine 85 mutated to Arginine
Rel/NF-κB.....Reticuloendotheliosis/Nuclear factor κB
RHA.....RNA Helicase A
RHD.....Rel homology domain
RISC.....RNA-induced silencing complex
RNA Pol I.....RNA polymerase I
RNAi.....RNA interference
RT-PCR.....Reverse transcription coupled polymerase chain reaction
SDS-PAGE.....Denaturing polyacrylamide gel electrophoresis
SEP.....Sperm entry point

SLBP.....Stem loop binding protein
SO.....Spemann organizer
SRE.....Smaug response element
TBE.....Tris, borate, EDTA gel electrophoresis buffer
TBS.....Tris buffered saline
TCF/LEF.....T-cell factor/ Lymphoid enhancement factor
TGF-β.....Transforming growth factor β
TLE.....Transducin-like enhancer of split
TLR.....Toll-like receptor
TNF-α.....Tumor necrosis factor α
TOV-112D.....human epithelial ovarian cancer cell line
tPA.....Tissue plasminogen activator
trim36.....tripartite motif-containing protein
tRNA.....transfer ribonucleic acid
UTP-[α-^{32}P].....Uracil ribonucleotide radiolabelled with ^{32}P in the alpha position
UTR.....Untranslated region
UV.....Ultra violet
VCC.....Vegetal cortical cytoplasm
Wg.....wingless; *Drosophila* homolog of Wnt
WIF1.....Wnt-inhibitory factor 1
Wnt.....renamed *Drosophila*/mouse wg/int
WT.....wild type
X.EXT1.....Xenopus Exostosin 1; an HSPG
XBC01.....XBcl9 clone #1
XBcl9.....Xenopus B-cell lymphoma 9
XBcl9^{coding}.....XBcl9 coding region cDNA/mRNA
XBcl9$^{\Delta 3'UTR}$.....XBcl9 lacking the 3'UTR cDNA/mRNA
XBcl9$^{\Delta 5'UTR}$.....XBcl9 lacking the 5'UTR cDNA/mRNA
XBcl9$^{F.L...}$.....XBcl9 full length cDNA/mRNA
XBcl9^{H417A,R418A}....XBcl9 mutant; alanine substitution at Histidine 417 and Arginine 418
Xbra.....Xenopus Brachyury
Xdpcp.....Xenopus dok-1 phosphotyrosine binding protein containing protein
Xema.....Ectodermally-expressed mesendoderm antagonist
XFD.....dominant negative Xenopus FGF receptor
Xnr.....Xenopus nodal-related
Xβ-catenin^{D162A,D164A}.....Alanine substitution at aspartic acid residues 162 and 164
Xβ-catenin^{D164A}.....Alanine substitution at aspartic acid residue 164 only
Xβ-catenin^{S37A}.....Alanine substitution at serine residue 37
β-gal.....β-galactosidase
β-TrCP.....β-transducin-repeat containing protein

CO-AUTHORSHIP STATEMENTS

Chapter 2:

Figure 2.2 and Table 2.1 were originally published, in modified form, in Developmental Biology (Kennedy et al. 2007). Experiments were designed, performed and analyzed with the assistance of Dr. K. Kao. The corresponding author of this manuscript was Dr. K. Kao with co-author contribution of results and materials and methods from M. Kennedy, K. Green, R. Ford, L. Gillespie and G. Paterno.

Chapter 3:

This research was published in Developmental Dynamics (Kennedy et al. [epub] 2009), special issue on 'Wnt signaling in Development.' Experimental design and data analysis was performed with the assistance of Dr. K. Kao. Experiments were primarily performed by M. Kennedy. Crude Bcl9 antiserum was generated by P. Andrews. The manuscript was authored by M. Kennedy and edited by Dr. K. Kao, who also helped with the design of several figures, particularly figure 3.6 and figures 3.9-3.11. The experiments presented in Figures 3.9 and 3.10 were performed in collaboration with Dr. Janet Heasman and her post-docs, Sang-Wook Cha and Emmanual Tadjuidje, at the Cincinnati Children's Research Foundation.

Chapter 1: Axis formation in Xenopus development

1.1.1 Foreword

The field of developmental biology aims to describe the highly coordinated morphological and molecular interactions that direct the progressive organization of a multicellular adult organism from a single egg. In lieu of human embryonic research, scientists exploit the use of animal models and *in vitro* cell culture methods to answer questions such as, how does an eye form? or the heart? or pancreas? The answers to these questions are not only important for the basic study of embryonic development, but understanding these processes provides insight into the etiology of congenital birth defects and adult disease.

The establishment of the body plan is a fundamental problem of embryology. It is dependent upon the foundation of a coordinate set of axes on which the embryo can be regionalized into morphogenetic fields that derive the organ systems of the adult organism. Many investigators have greatly contributed to the elucidation of the mechanisms that govern the architectural design of the embryonic blueprint, and the molecular engineering that develops the body plan into a mature organism. However, although we know much about embryonic development our knowledge concerning the genetic and molecular controls of embryogenesis is incomplete.

This thesis is an account of my studies aimed at understanding the precise transcriptional control of gene expression regulated by the canonical Wnt molecular signaling pathway, which directs the formation of the primary body axis. As such, the body axis is the foundation upon which dorsal-ventral and anterior-posterior embryonic pattern formation is imparted.

1.1.2 Xenopus: the experimental model

1.1.2.1 The origins of Xenopus as an experimental model

As recently as the 1950's African clawed frogs of the genus *Xenopus,* were used for pregnancy testing. The injection of urine from a pregnant woman, which contains elevated levels of the hormone chorionic gonadotropin, induced the frogs to lay eggs (Harjola and Toivonen 1949; Joel and Rabau 1949; Polack 1949). As a result, reproductive biology labs began to exploit the ability to obtain frog eggs on demand. The earliest experimental use of these frog eggs can be traced to the 1950's to the labs of Boris Ivan Balinsky (Balinsky 1951), Pieter Nieuwkoop (Nieuwkoop 1955) and Michail Fischberg (Elsdale et al. 1958).

Several critical achievements by biologists have come from studies using *Xenopus*, including the first report of animal cloning by the transfer of somatic nuclei into enucleated eggs (Gurdon et al. 1958) and the identification of the O-*nu* nucleolar mutation important for the study of ribosomal genes (Elsdale et al. 1958;Elsdale et al. 1960). In the 1960s's protocols for the purification of messenger RNA (Brown and Littna 1966) were developed, which led to the discovery that purified mRNA species, when injected into *Xenopus* embryos, were efficiently translated (Gurdon et al. 1971). This discovery allowed researchers to begin to study the expression and requirement of specific genes and the proteins they encoded for embryonic development. As a result of this early work, the practical use of *Xenopus* as a model to study not only classical embryology, but also cell and molecular biology led to its rise as one of the most popular models of vertebrate development.

1.1.2.2 Xenopus as a model system

During the last 50 years, frogs have become an important model organism for developmental biologists interested in the morphological and molecular mechanisms that govern embryonic development. The species *Xenopus laevis*, is an ideal experimental model for studying vertebrate embryogenesis for multiple reasons: A native of South Africa, *X. laevis* are completely aquatic and very resistant to disease. Thus laboratory colonies are relatively easy to maintain. With a diameter of ~1.2-1.3mm, *Xenopus laevis* eggs are large (compared to ~0.1mm for mammalian oocytes) and very robust, making them easily amenable to experimental manipulation. As well, large clutches of eggs can be obtained (~300-2000) per ovulation, at any time of year, can be fertilized *in vitro* and cultured in a simple saline solution. Lastly, and arguably most importantly, the oviparous nature of frogs allow biologists to directly observe embryogenesis in its entirety. The most noted disadvantages of *Xenopus laevis* are its allotetraploid genome and a 1-2 year generation time, making it less desirable for genetic studies.

1.1.3 Overview of Xenopus development

1.1.3.1. From egg to neurula

Embryonic development consists of a progressive series of many highly complex overlapping cellular events that occur through space and time. The egg is a single, spherical, haploid cell. The most conspicuous aspect of the *Xenopus* egg is its pigmentation pattern; the 'animal' hemisphere is darkly pigmented whereas the 'vegetal'

hemisphere is lightly pigmented. During ovulation, the extruding egg is coated with a thick jelly coat required to capacitate sperm cells as they burrow through it. A single sperm fuses to the egg in the animal hemisphere only, and donates the male pronucleus to complete fertilization. Further sperm are prevented from entering by egg membrane-associated blocks to polyspermy. As a result, ploidy is restored and the zygote begins to rapidly divide and proliferate, forming a multicellular embryo.

Early development is divided into 4 overlapping stages: cleavage, blastula, gastrula and neurula stages. Organogenesis commences during neurulation and the embryo begins to significantly increase in size. As my thesis is focused on transcriptional regulation during cleavage-gastrula stages, I will limit this overview to these early embryonic phases.

In *Xenopus*, the first 6 or so cell divisions (referred to as the cleavage stages) results in a 'solid' ball of cells called the morula. The morula does not increase in size with each round of mitosis. Instead, cells become increasingly smaller as the egg cytoplasm is repeatedly partitioned into each new cell. Importantly, the egg cytoplasm is not uniform and contains maternally deposited factors that direct early embryogenesis. This aspect will be further explained, later in this chapter. When the morula reaches about 128 cells (7 cell divisions), it is known as a blastula. Blastula stage embryos have a fluid filled cavity, called the blastocoel that is located in the animal hemisphere.

During blastula stages, cells produce/receive molecular information/signals that specify cell fates, which are related to the cells' positions within the embryo. At this time, all cells are categorized as members of one of the three primordial germ layers, from

which all of the adult tissues and organs are derived. Superficially, the three germ layers, ectoderm, mesoderm and endoderm, form in the animal, equatorial and vegetal regions, respectively, in *Xenopus* blastulae.

Gastrulation begins about 9 hours post-fertilization. This phase of development is characterized by the extensive cellular rearrangements that terminally define the germ layers and properly re-position them for further development. Briefly summarized, the animal pole cells (ectoderm) spread vegetally to encapsulate the entire embryo. This process is called epiboly. Concurrently the mesoderm and endoderm are internalized in such a way that by the end of gastrulation the mesoderm lies between the ectoderm and endoderm. Internalization of the mesendoderm displaces the blastocoel, forms the archenteron (primitive gut) and elongates the embryo to establish anterior and posterior (*i.e.* head to tail) polarity.

On the upper (back or dorsal) side of the embryo, the ectoderm evaginates as two parallel neural folds all along the anteroposterior axis. The neural folds rise up and fuse along the embryo midline to form the neural tube that eventually gives rise to the central nervous system (CNS). The process of neurulation is, unsurprisingly, an extremely intricate and complicated process. Head and CNS development of the frog has been extensively reviewed elsewhere (Lake and Kao 2003a).

1.1.3.2 The formation of embryonic organizer tissue and convergent extension in Xenopus embryos

About 85 years ago, Hans Spemann and Hilde Mangold famously demonstrated that a specific equatorial region of salamander embryos could induce or 'organize' adjacent cells into specific developmental programs necessary for normal embryogenesis. Astonishingly, when this 'organizer' tissue was transplanted to recipient embryos, it was capable of inducing host cells that would normally differentiate into hematopoietic progenitors to duplicate the embryonic body plan, resulting in the formation of conjoined twins. Homologous inductive organizers have since been identified in all vertebrates studied (García-Fernández et al 2007; Meinhardt 2006). For example, in amniotes it is called the Node (mouse) or Hensen's Node (avians), respectively, or the Shield, in fish. In *Xenopus* embryos, and likely all chordates, the heretofore named 'Spemann Organizer' is mapped to a region of the mesoderm known to derive the notochord (future backbone).

The appearance of a darkly pigmented 'arc' just below the mesodermal region of the embryo externally marks the onset of gastrulation. This 'arc' is produced by the apical constriction, with concomitant basal expansion, of cells causing the sparse pigments to be apically concentrated thus giving it the dark appearance and the bottle-shape for which the cells are named (*i.e.* bottle cells) (Hardin and Keller 1988). The formation of bottle cells creates an invagination in the embryo called the 'blastopore' through which the mesoderm and endoderm migrate during gastrulation and which forms the archenteron. The 'dorsal lip' is the patch of cells above the bottle cells and contains

the Spemann organizer activity; it also forms the leading edge of the mesoderm as it migrates inward.

Initially, the blastopore forms as a small arc on one side (*i.e.* dorsal side) of the embryo. As gastrulation proceeds, the blastopore extends laterally and towards the opposite side (*i.e.* ventral side) of the embryo until a complete circumferential invagination/pore is formed (Keller and Danilchik 1988). As the mesendoderm migrates inward, the blastopore closes (Keller and Danilchik 1988). This eventually becomes the proctodeum.

The dorsal mesoderm involutes first and migrates the farthest. As the dorsal mesoderm migrates inwards, a second process called convergent extension, occurs concurrently. Convergent extension is the process whereby cells of the involuting sheet of mesodermal cells intercalate (*i.e.* converge) along the embryo midline, causing the layer of cells, which give rise to the notochord, to extend in the opposite direction, creating an elongated embryo with an anteroposterior axis (Keller and Danilchik 1988; Keller et al. 2008; Wallingford et al 2002).

The Spemann organizer is not a mosaic region of the embryo but rather is formed in response to maternal stimuli (De Robertis 2006). In particular, the Spemann organizer/dorsal mesoderm is induced by the underlying dorsal endoderm denoted as the Nieuwkoop center (Figure 1.1). Similar to the Spemann organizer, the Nieuwkoop center is formed after fertilization. The molecular cues that define the Nieuwkoop center and that induce Spemann organizer formation are described in detail in the section 1.1.3.3.

1.1.3.3 Body Plan Formation

Formation of the primary body axis is the most important step in early embryonic development and is necessary to form the bilateral embryonic body plan. The primary body axis is established as a result of 2 early developmental events. The first event is triggered by fertilization and imposes a molecular Dorsal-Ventral asymmetry in the embryo. The second event is the specification of the 3 embryonic germ layers.

The embryonic axis is derived from dorsal mesoderm, the formation of which is directed by maternal factors present at fertilization in *Xenopus laevis* embryos. These maternal factors are members of the TGF-β and canonical Wnt signaling pathways. The intersection of these two pathways defines the Nieuwkoop centre in dorsal-vegetal cells, which induces the formation of the Spemann Organizer in overlying dorsal-equatorial cells (*i.e.* dorsal mesoderm) (Figure 1.1) (Nishita et al. 2000). The Spemann Organizer then directs the formation and patterning of the dorsal-anterior body axis.

Xenopus embryos are triploblastic (*i.e.* composed of 3 primary germ layers: ectoderm, mesoderm and endoderm). The mesodermal germ layer is formed from the overlying ectoderm by inductive signals emanating from the endoderm at gastrulation (Nieuwkoop 1973; Nakamura and Takasaki 1970). These germ layers are patterned along the dorsal-ventral axis, established by fertilization. Fertilization of the embryo induces the rotation of the dense, outer, cortical cytoplasm (*i.e.* the cortex). Cortical rotation displaces maternal factors from the vegetal pole to a more equatorial position, opposite the sperm entry site, that locally stimulate canonical Wnt signaling (Larabell et al. 1997; Darras et al. 1997; Marikawa et al. 1997; Marikawa and Elinson 1999; Schneider et al. 1996).

Figure 1.1 Establishment of the embryonic body plan.

An overview of the early embryonic processes that generate the embryonic axes and lead to the specification of the embryonic body plan. Top row: The fertilizing sperm initiates the rotation of the egg cortex and displacement of maternal determinants (shown in purple) that induce nuclear accumulation of β-catenin protein (shown in green) thus specifying dorsal cell fate. Bottom row: The dorsal endodermal region of active canonical Wnt signaling is known as the Nieuwkoop Centre (NC) and induces the formation of the Spemann Organizer (SO) in the overlying dorsal marginal zone cells. Superimposition of the dorsal-ventral axis upon the primary germ layers can be used to visualize the embryo body plan and identify the embryonic primordia of organ systems.

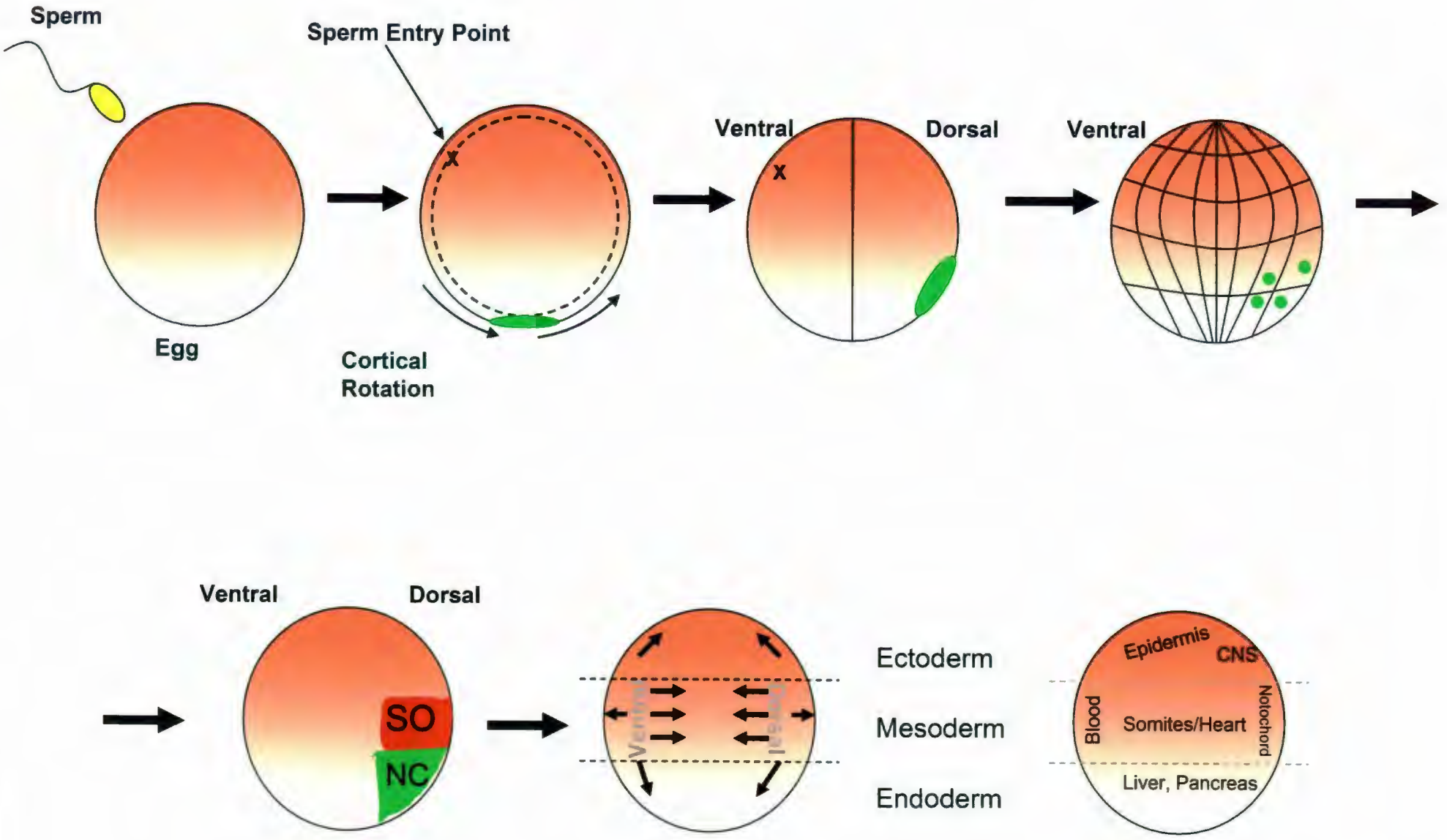
Sperm
Sperm Entry Point
Egg
Cortical
Rotation
Ventral
Dorsal
X
Ventral
Ventral
Dorsal
SO
NC
Ectoderm
Mesoderm
Endoderm
Epidermis
CNS
Blood
Notochord
Somites/Heart
Liver, Pancreas

This molecular asymmetry establishes dorsal-ventral polarity in cleavage stage embryos.

In *Xenopus laevis*, the 3 embryonic germ layers are specified during late blastula stages. However, the zygotic genome is largely transcriptionally silent during the first 4.5-5 hours (at ~23°C) of embryogenesis. Large scale zygotic transcription commences at the mid-blastula transition stage (MBT) when the frog embryo is composed of ~4000 cells. The active pre-MBT transcription of *Xnr5* and Xnr6 are the only known exceptions in *Xenopus* (Yang et al. 2000). Hence, maternal factors primarily regulate the transcription of zygotic genes that mediate germ layer specification (Heasman 1997; Heasman 2006). In mouse, *Nodal*, a TGF-β subfamily, was first identified as an essential gene for the involution of ectodermal cells into the primitive streak where they form mesoderm (Zhou et al. 1993). In *Xenopus*, Nodal-related proteins (Xnrs), form the endogenous mesoderm inducing signal and is regulated by both *VegT* and *β-catenin* activity in endodermal (vegetal) cells (Agius et al. 2000; Hashimoto-Partyka et al. 2003; Heasman 2006; Jones et al. 1995). However, the activity of ectodermally derived factors such as *Ectodermin* (Dupont et al. 2005), *Xdpcp* (Cheong et al. 2009), *Foxi1e* (Mir et al. 2007; Suri et al. 2005), *XRel3* (Kennedy et al. 2007) and maternal B1-type SOX's (Zhang et al. 2004a) inhibit mesoderm formation by multiple mechanisms that function to negatively regulate Xnr signaling. Hence, the mesodermal domain is defined by the action of endodermally and ectodermally derived factors, which activate or attenuate Xnr signaling, respectively. However, the timing and intensity of the Xnr signal imparts pattern to the mesoderm itself. Early/high levels of Xnr signaling require the cooperative activity of VegT/Vg1 and β-catenin and lower levels are induced by VegT/Vg1 alone

(Agius et al. 2000). In this way, dorsal mesodermal cell fate is established by an Xnr morphogen gradient created by the asymmetric stimulation of canonical Wnt signaling on a uniform VegT background.

I will next give a detailed explanation of the processes that establish dorsal-ventral polarity and regulate germ layer formation.

1.1.4 Dorsal-Ventral Polarization

1.1.4.1 Overview

The *Xenopus* egg is a radially symmetric cell that has a darkly pigmented animal hemisphere and a lightly pigmented, yolk laden vegetal hemisphere. The thin layer of cytoplasm associated with the egg plasma membrane is called the egg cortex, which surrounds the yolk-rich core. Fertilization initiates a process called cortical rotation, in which the cytoplasmic yolky core is displaced relative to the cortex (Gerhart et al. 1984; Vincent et al. 1987; Vincent et al. 1986). Cortical rotation is effected by the assembly of a parallel array of polarized microtubules (Elinson and Rowning 1988), organized from the sperm aster (Houliston and Elinson 1991; Ubbels et al. 1983), that extend into the vegetal cortex, rotating it ~30°C in the direction opposite the sperm entry point (SEP) (Vincent et al. 1986). The displacement of the vegetal pole cortex to a subequatorial position establishes dorsal-ventral polarity (Figure 1.1).

Formation of the dorsoventral axis is dependent upon cortical rotation since inhibition of cortical rotation causes embryos to develop devoid of any identifiable body axis. They do not form dorsoanterior structures such as heads, eyes or cement glands and

are said to be 'ventralized' (Vincent and Gerhart 1987). Cortical rotation can be inhibited by destabilizing the parallel array of microtubules by ultra-violet (UV)-irradiation of the vegetal pole or by the use of chemical agents such as nocodazole. As well, exposure of frog embryos to cold temperatures or high pressure causes ventralized phenotypes (Scharf and Gerhart 1983; Malacinski et al. 1978). Normal development in these embryos can be rescued by oblique tilting which seems to use gravity to mimic the rotation (Scharf and Gerhart 1980). Additionally, tilting the embryo orthogonal to the animal-vegetal axis early during the first cell cycle ensures dorsalization of the side of the embryo facing up and can rescue normal development of a ventralized embryo (Scharf and Gerhart 1980). The period of sensitivity of embryos to any such treatments is limited to approximately the first 30-40 minutes (~30%) of the first cell cycle, concomitant with the normal timing of cortical rotation (Vincent et al. 1986).

These results led to the realization that maternal determinants capable of dorsalizing cells were localized to the vegetal pole and were displaced to an equatorial position by cortical rotation. This hypothesis was further supported by studies whereby the transplantation of dorsal vegetal cells or injection of dorsal cytoplasm from 16-64 cell stage embryos to the equatorial region of either UV-irradiated or to the ventral equatorial region of normal recipient embryos rescued dorsal axis formation or induced axial duplication, respectively (Fujisue et al. 1993; Gimlich and Gerhart 1984; Gimlich 1986; Kageura 1990; Yuge et al. 1990; Holowacz and Elinson 1993). Also, injection of vegetal pole cytoplasm from embryos prior, but not after cortical rotation could induce the formation of a second dorsal axis (Fujisue et al. 1993). Since it was well known that the

Spemann Organizer is formed from dorsal equatorial cells and contains the dorsal axis promoting activity, it became clear that the process of cortical rotation was necessary to form the Spemann Organizer itself.

1.1.4.3 Cortical Rotation regulates spatial activation of the Canonical Wnt pathway

The first indication of the identity of the molecular nature of the dorsal determinants came from the landmark study by McMahon and Moon (1989). At this time it had become apparent that the *wingless* (*wg*) pathway was important for patterning processes during *Drosophila* development but its involvement during vertebrate embryogenesis was unknown. To determine a role for *wg* signaling in vertebrate embryogenesis they ectopically expressed *int-1* mRNA encoding a mouse orthologue of the fly glycoprotein wingless (wg), in *Xenopus* embryos. As a result of this experiment, they discovered that int-1 protein was capable of inducing the formation of a complete supernumerary axis (*i.e.* conjoined twins) (McMahon and Moon 1989). This also suggested for the first time that in *Xenopus*, the *wg/int-1* (*i.e. Wnt*) pathway could induce an ectopic Spemann Organizer by utilizing endogenous mechanisms. These results were further supported by the isolation of orthologous *Xenopus* Wnt genes such as *Wnt8* that could induce the formation of a dorsal axis (Christian et al. 1991; Sokol et al. 1991). However, neither the molecular components that transmit the Wnt signal, nor its target gene(s), were known.

Subsequently, it was discovered that the cadherin binding protein, β-catenin, also played a role in cell signaling and was essential for the formation of dorsal axial

structures (Heasman et al. 1994; Funayama et al. 1995; McCrea et al. 1993). This was demonstrated in three ways. First, McCrea et al. (1993) injected purified anti-β-catenin Fab fragments, ventrally into *Xenopus* embryos resulting in conjoined embryos and could also rescue axis formation in UV ventralized embryos. As will become clearer in Section 1.1.4.4, the Fab fragments presumably stabilized β-catenin protein, which was then able to activate transcription of target genes independently of an extracellular signal such as Wnt. Secondly, Heasman et al. (1994) depleted maternal stores of β-catenin mRNA and protein by injecting antisense oligonucleotides into mature oocytes (*i.e.* unfertilized eggs). These eggs were then fertilized by the host transfer technique and developed without dorsal axial structures, indicating an essential requirement of β-catenin for axis formation. Thirdly, the ventral overexpression of β-catenin mRNA in *Xenopus* embryos induced the formation of a secondary axis with a full complement of dorsal, anterior structures (Funayama et al. 1995).

Additional evidence implicating β-catenin as a key modulator of axis development came from observations on its expression in embryos in which the axis was altered. For instance, while β-catenin was found to be preferentially expressed in dorsal mesendodermal nuclei (*i.e.* Nieuwkoop Centre and Spemann Organizer regions; see Figure 1.1) of blastula stage embryos (Schneider et al. 1996), UV irradiation of embryos abolished this protein expression pattern. On the other hand, hyperdorsalization of embryos, achieved by overexpressing *Wnt8* mRNA or with lithium (Li^+) ions, presented exaggerated nuclear β-catenin accumulation throughout the entire embryo (Schneider et al. 1996). This result was extended by the observation that β-catenin protein becomes

enriched dorsally during the first few cell cycles and is detectable in dorsal nuclei by the 16-32 cell stage (Larabell et al. 1997). Taken together, these observations firmly established β-catenin as a key factor in dorsal axis formation and demonstrated that its nuclear accumulation was dependent upon cortical rotation.

The search for molecular markers that were uniquely expressed in the Spemann Organizer led to the discovery of the zygotic homeobox genes *siamois* (Lemaire et al. 1995), *twin* (Laurent et al. 1997) and *goosecoid* (Cho et al. 1991) and the TGF-β subfamily member, *Xnr3* (Smith et al. 1995). The mRNA expression of all three of these genes is restricted to the Spemann Organizer although *Xnr3* is only found in the superficial 'epithelial' layer (Smith et al. 1995). The ectopic expression of any of these genes can induce axial duplications and/or rescue dorsal axis formation in UV-irradiated embryos.

Determination of the expression of these zygotic molecular markers suggested they could be regulated downstream of a maternal canonical Wnt pathway, itself dependent on cortical rotation. Since it was well known that maternal dorsalizing determinants were localized to the vegetal cortical cytoplasm (VCC) of unfertilized eggs, Darras et al. (1997) injected VCC into the animal pole of embryos and discovered that these determinants could locally induce the zygotic expression of the Spemann Organizer genes, *siamois* and *Xnr3*. Furthermore, In UV-irradiated embryos, *siamois* and *Xnr3* were expressed at the vegetal pole (Darras et al. 1997; Marikawa et al. 1997; Marikawa and Elinson 1999). These observations confirmed that VCC contains cytoplasmic factors

capable of activating Spemann Organizer gene expression and led to the notion that the proper spatial expression of *siamois* and *Xnr3* is dependent on cortical rotation.

Since Spemann Organizer genes are zygotically expressed, *siamois* and *Xnr3* were suggested to be downstream of the dorsal nuclear accumulation of β-catenin. These results were further confirmed by the determination that injection of β-catenin mRNA into animal cap explants was sufficient to induce the expression of *siamois*, *Xnr3* and *goosecoid* and that their correct spatial expression was dependent on cortical rotation (Medina et al. 1997). However, the regulation of *goosecoid* expression appeared more complicated as the transcription of *siamois* and *Xnr3* was still induced in UV-irradiated embryos at almost control levels while *goosecoid* levels were barely detected (Medina et al. 1997).

Thus, cortical rotation establishes the dorsal-ventral axis by redistributing maternal factors that are required to initiate canonical Wnt signaling. All these maternal factors function to stabilize β-catenin to activate Wnt target gene transcription. Before proceeding, it is necessary to give a detailed biochemical description of the canonical Wnt signaling pathway and its core components in order to understand the significance of the regulated distribution of dorsalizing factors by cortical rotation.

1.1.4.4 The Canonical Wnt Signaling Pathway

There are multiple branches of the Wnt signaling pathway, all of which play important roles in various cellular processes that are categorized as either canonical or

non-canonical Wnt pathways. There is only one canonical but several non-canonical pathways. Non-canonical pathways include the planar cell polarity (PCP) and Wnt/Ca^{2+} pathways. The PCP pathway regulates cytoskeletal rearrangements by mediating Rho and Rac proteins, thus controlling cell shape and movement (Habas and Dawid 2005; Huelsken and Behrens 2002). The Wnt/Ca^{2+} pathway regulates Protein Kinase C (PKC) and Camodulin-dependent kinase II (CamKII) that are also involved in cell adhesion and cell movements (Kohn and Moon 2005).

Canonical Wnt signaling is required for cellular differentiation. The defining characteristic of canonical Wnt signaling is non-membrane associated (*i.e.* soluble) β-catenin protein (MacDonald et al. 2009; Mosimann et al. 2009). My thesis is focused on the regulation of β-catenin activity, therefore non-canonical Wnt pathways will not be discussed herein.

Canonical Wnt signaling is characterized by the stabilization of cytoplasmic β-catenin and its subsequent transposition to target gene promoters. In the absence of pathway stimulation, cytoplasmic β-catenin is bound in a large destruction complex that targets it for proteolytic degradation by the 26S proteasome (MacDonald et al. 2009; Aberle et al. 1997). The current model (Figure 1.2) depicts β-catenin bound by the scaffolding protein, Axin and the encoded protein of the tumor suppressor gene, *adenomatous polyposis coli (APC)* (Kishida et al. 1998; Hart et al. 1998). The binding of β-catenin by Axin and APC transforms β-catenin into a substrate for the 'dual-kinase mechanism' regulated by Casein Kinase Iα/ε (CKIα/ε) and Glycogen Synthase Kinase 3β

(GSK-3β) (Liu et al. 2002), which hyperphosphorylates the N-terminus of β-catenin. CKIα/ε acts as a priming kinase that phosphorylates the Serine 45 residue of β-catenin (Amit et al. 2002; Sakanaka 2002). Subsequently, β-catenin is phosphorylated by GSK-3β at Threonine 41, Serine 37 and Serine 33 (Orford et al. 1997; Yost et al. 1996). GSK-3β also phosphorylates Axin and APC which is suggested to strengthen their affinity for β-catenin, reinforcing their inhibitory function (Ikeda et al. 1998; Huang and He 2008). Hyperphosphorylated β-catenin is then ubiquitinated by the E3 Ubiquitin ligase, SLimb/β-transducin repeat containing protein (β-TrCP) (Jiang and Struhl 1998; Marikawa and Elinson 1998), marking it for proteasomal degradation (Aberle et al. 1997).

Activation of the Wnt pathway by the binding of extracellular Wnt ligands to their cognate receptors, results in the inhibition of the destruction complex thus stabilizing β-catenin and leading to its translocation to nuclei and activation of target gene transcription. Wnt ligands are glycoproteins that interact with the seven-pass, Frizzled (Fz) family of membrane co-receptor proteins. The interaction of Wnt with Fz is enhanced extracellularly by Heparan Sulfate Proteoglycans (HSPG's).
Pathway activation through Fz also requires the Low Density Lipoprotein 5/6 co-receptors (LRP 5/6). Ligand-stimulated pathway activation causes the phosphorylation of PPPSPxS sequences in the cytoplasmic domain of LRP5/6 by GSK-3β and CK1α (Ranganathan et al. 2004; Swiatek et al. 2006; Wu et al. 2009a). Phosphorylated Dishevelled (Dsh) then recruits Axin to phosphorylated LRP5/6 at the plasma membrane (Cliffe et al. 2003; Gonzalez-Sancho et al. 2004; Mao et al. 2001; Tolwinski et al. 2003);

Figure 1.2 Schematic representation of the canonical Wnt pathway.

Left panel: In the absence of pathway stimulation, cytoplasmic β-catenin is sequestered and chemically modified, marking it for proteasomal degradation and down-regulating target gene expression. Right panel: Ligand-stimulation of the pathway stabilizes cytoplasmic β-catenin by inhibiting the phosphorylating, ubiquitinating destruction complex. This allows β-catenin to accumulate in the nucleus where it associates with a number of co-transcriptional activators to induce the expression of target genes.

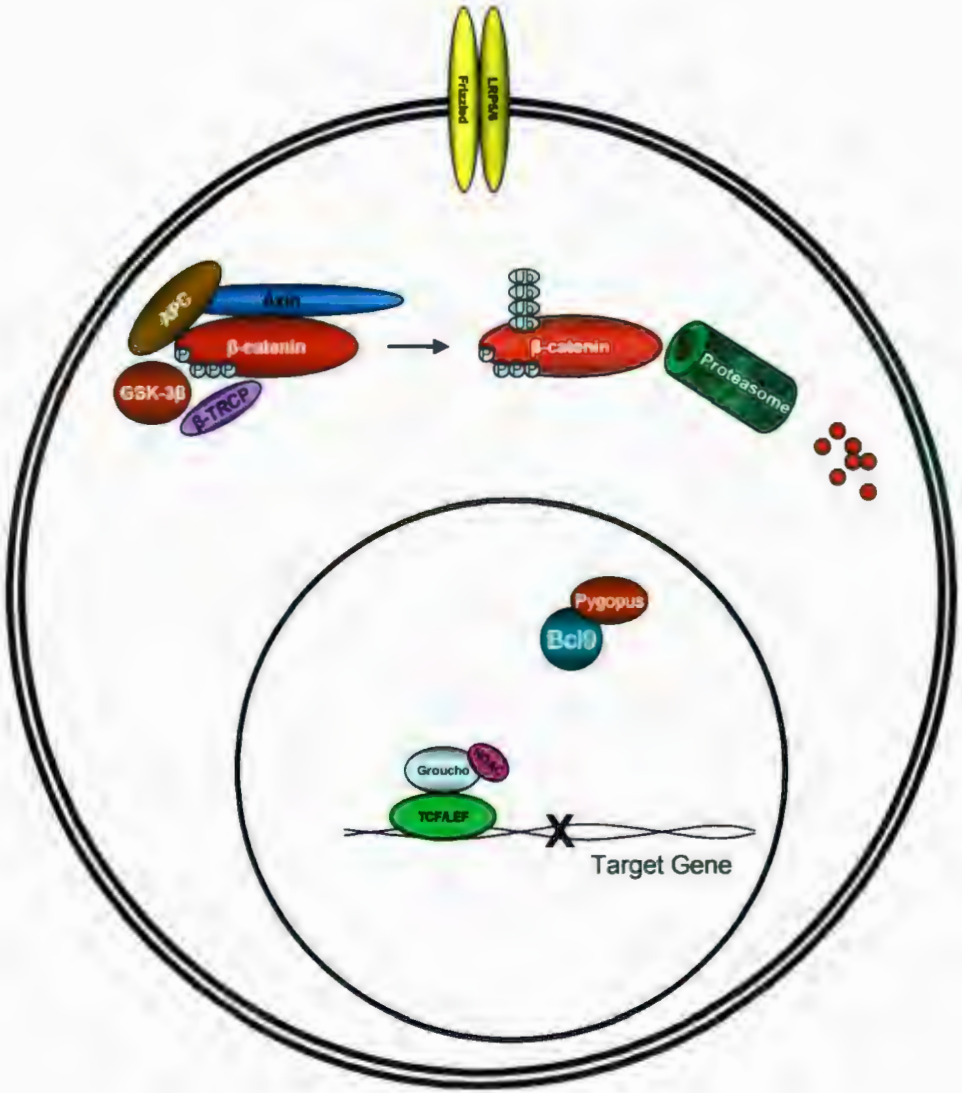

Pathway: OFF

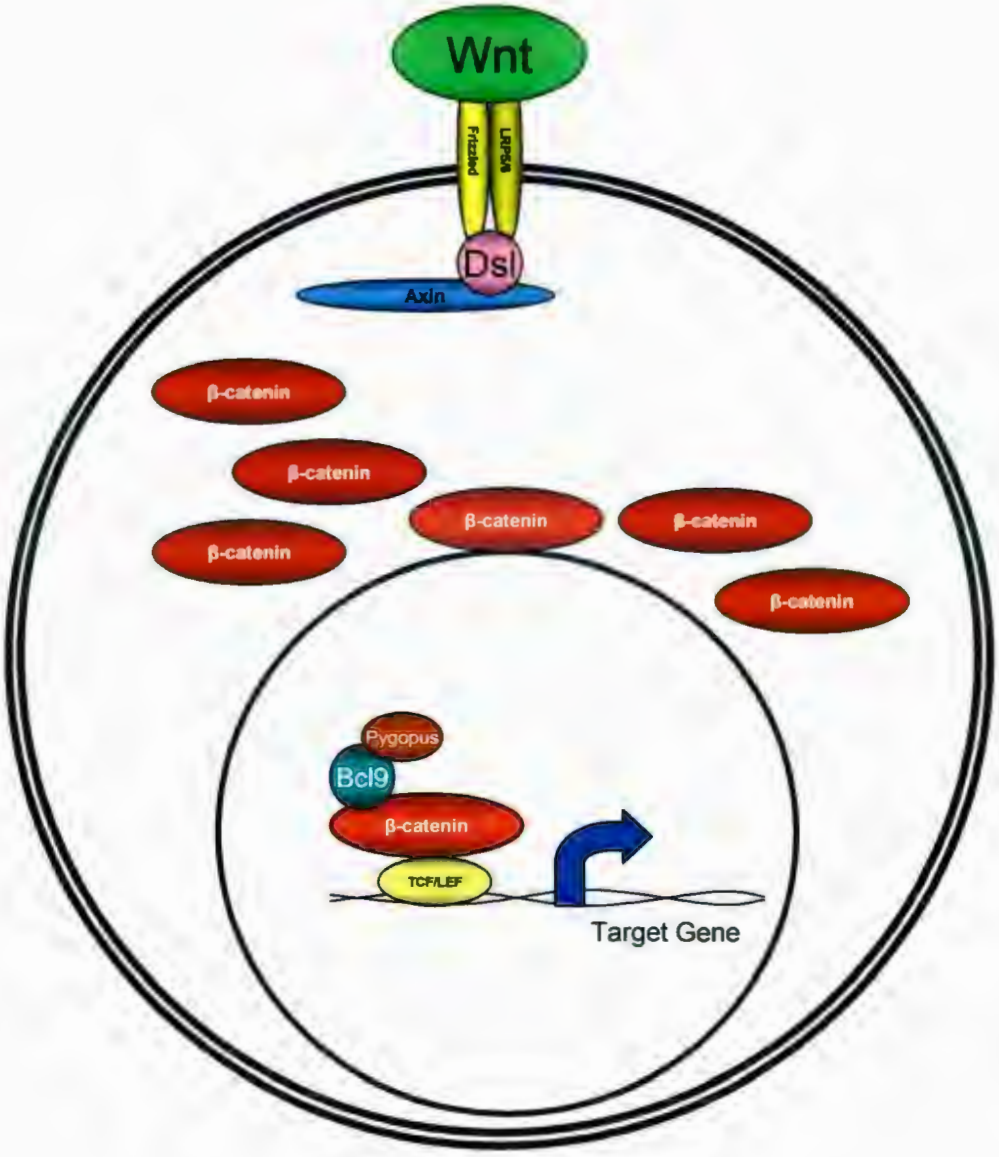

Pathway: ON

As well, phosphorylated PPPSPxS sequesters GSK-3β at the membrane (Piao et al. 2008).

These observations imply that the sequestration of Axin and GSK-3β allows β-catenin to evade the phosphorylation-ubiquitination cascade. Co-incidently, phosphorylation of β-catenin by Casein Kinase II (CKII) on Threonine 393 decreases its affinity for Axin (Dominguez et al. 2004; Dominguez et al. 2005; Song et al. 2003; Wu et al. 2009b). In this way β-catenin is stabilized and can be recruited to the nucleus.

In the nucleus, β-catenin is assembled into a multipartite transcription activating complex. β-catenin binds the T-Cell Factor/Lymphoid Enhancing factor (TCF/LEF) high mobility group (HMG) box family of DNA-binding proteins (Molenaar et al. 1996), which are constitutively localized on Wnt target gene promoters. In the absence of β-catenin, TCF/LEF proteins are directly repressed by Groucho/TLE (Brantjes et al. 2001; Roose et al. 1998) and Histone Deacetylase (HDAC) factors (Billin et al. 2000). Nuclear β-catenin displaces Groucho/TLE repressors by binding TCF/LEF and activates transcription in a complex with other proteins that locally recruit the basal transcriptional machinery (Fisher and Caudy 1998; Daniels and Weis 2005).

Activation of β-catenin-induced transcription requires the chromatin modifying enzyme CREB Binding Protein (CBP)/p300 (Takemaru and Moon 2000). CBP/p300 acetylates Histones, thus promoting transcriptional activation through chromatin remodeling (Ogryzko et al. 1996). Additionally, Legless/B-Cell Lymphoma 9 (Lgs/Bcl9) directly interacts with the N-terminus of β-catenin and acts as a bridging protein to Pygopus (Pygo) (Kramps et al. 2002; Thompson et al. 2002). Pygo associates with the

'mediator complex' via its Med12 and Med13 components which in turn recruits RNA Polymerase (Pol) II to activate gene transcription (Carrera et al. 2008). Bcl9-Pygo dimers may also regulate access to Wnt target gene promoters by interpreting the Histone methylation code and/or cooperative acetylation of Histones with CBP/p300 (Andrews et al. 2009; Fiedler et al. 2008). Furthermore, the transcriptional potency of β-catenin is dependent upon the association of Parafibromin/Hyrax with the C-terminus of β-catenin (Mosimann et al. 2006). Interestingly, in *Drosophila*, Parafibromin/Hyrax also requires Bcl9-Pygo for its transcriptional activity though not for its interaction with β-catenin (Mosimann et al. 2006).

1.1.4.5 Canonical Wnt signaling is regulated by cortical rotation

The canonical Wnt pathway consists of many intracellular components, not limited to those core components described above that regulate target gene transcription. Hence, how cortical rotation efficiently stimulates this biochemical cascade to direct dorsal gene expression is of prime interest.

In addition to β-catenin, several activating components of the canonical Wnt pathway are asymmetrically expressed by cortical rotation. These include GSK-3β binding protein (GBP) (Weaver et al. 2003), Dishevelled (Dsh) (Miller et al. 1999) and Wnt11 (Ku and Melton 1993). Conversely, cortical rotation leads to decreased dorsal GSK-3β levels (Dominguez and Green 2000). GBP was identified as a Dsh binding protein that also interacted with GSK-3β (Li et al. 1999). In this way, GBP-Dsh was proposed to activate canonical Wnt signaling by depleting GSK-3β in dorsally fated cells

(Dominguez and Green 2000). GBP also interacts with kinesin light chain (KLC), a component of the microtubule motor kinesin protein complex and is transported along the microtubules during cortical rotation (Weaver et al. 2003). Interestingly, KLC competitively interacted with the GSK-3β binding domain of GBP (Weaver et al. 2003), which suggests that the KLC-GBP interaction is transient and ends with cortical rotation (Dominguez and Green 2000).

Dsh is associated with small vesicle-like organelles in the vegetal cortex and is enriched dorsally by cortical rotation (Miller et al. 1999; Rowning et al. 1997). Wnt11 mRNA is expressed in the vegetal cortex of unfertilized eggs and is also translocated to the dorsal region by cortical rotation (Ku and Melton 1993; Kloc and Etkin 1995; Tao et al. 2005). Recently, maternally expressed Wnt11 and Wnt5a were shown to dimerize and co-function as the activating ligand for dorsal axis formation (Tao et al. 2005; Cha et al. 2008).

Cortical rotation has been suggested to be regulated by the localization of the maternal transcript, *trim36*, to the germ plasm associated with the vegetal cortex (Cuykendall and Houston 2009). Trim36 is a member of the tripartite motif-containing protein family, Trim (a.k.a. RBCC) (Meroni and Diez-Roux 2005) that contains an N-terminal RING finger domain with ubiquitin ligase activity. *Xenopus* embryos devoid of maternal *trim36* were ventralized as a result of impaired microtubule polymerization following fertilization (Cuykendall and Houston 2009). As a result, the re-positioning of dorsal determinants that activate canonical Wnt signaling was inhibited.

Previously, it was unclear whether dorsal activation of canonical Wnt signaling occurred by extracellular signaling since many of the intracellular components capable of activating the pathway were dorsally enriched by cortical rotation (Moon and Kimelman 1998). However, the landmark paper by Tao et al. (2005) clearly demonstrates that Wnt11 ligand-mediated activation of maternal canonical Wnt signaling regulates the formation of the dorsal axis and required the extracellular Heparin sulfate proteoglycan (HSPG), Exostosin1 (X.EXT1), and the extracellular EGF-CFC family protein, FRL1 (Tao et al. 2005). However, it is unknown whether Wnt11 stimulation of the dorsal axis is dependent on cortical rotation.

Thus, the burden of evidence indicates that cortical rotation regulates canonical Wnt signaling on two levels. First it creates a dorsal gradient of Wnt ligand(s) that stimulates the pathway. Second, the asymmetric expression of intracellular activating components ensures transduction of the Wnt signal leading to stabilized β-catenin protein. This explanation however is somewhat unsatisfying since the 'dogma of molecular signaling' would insist that activation of the pathway should be sufficient to direct all necessary intracellular interactions that lead to the stabilization of β-catenin protein.

Why are *intracellular* pathway components, therefore, re-distributed by cortical rotation? One possibility is that the dorsally enriched intracellular canonical Wnt pathway components are not 'active' but are competent to instruction from a Wnt signal. It also suggests that they are not sufficient for pathway activation. For example, it appears that Dsh recruits Axin to the membrane upon pathway activation in *Drosophila* and

Zebrafish. However, in *Xenopus* oocytes and during early cleavage stages, Wnt signaling through LRP6 co-receptors negatively regulates Axin protein levels (Kofron et al. 2007). As well, it has been suggested that Dsh has a nuclear function necessary for canonical Wnt signaling in *Xenopus* and mammalian cells (Itoh et al. 2005). Hence it is possible that Dsh is dorsally enriched but either regulates axin and/or accumulates in the nucleus only in response to the maternal Wnt signal. Furthermore, dorsal enrichment of GBP by cortical rotation is necessary for down regulating GSK-3β levels (Dominguez and Green 2000). Hence, GBP and Dsh may need to be functionally activated by a Wnt signal.

Thus, while the roles of many of the components of the canonical Wnt pathway required for dorsal-ventral asymmetry have been described, there remain gaps in our understanding of how cells that have been specified to become dorsal by this pathway are instructed to terminally differentiate into the dorsal lineage.

1.1.5 Mesoderm formation

1.1.5.1 Maternal factors regulate zygotic expression of mesoderm inducing and patterning factors

Equally important to the establishment of the dorsal-ventral body axis is the formation of the three primary germ layers, which in *Xenopus* occurs in conjunction with, but in a roughly orthogonal direction to the dorsoventral body axis. The mesodermal germ layer gives rise to many cell types including those that form the head mesenchyme, notochord, muscle, pronephros, and blood. Mesoderm forms at the embryo equator by inductive signals produced in the endoderm. In the seminal experiments of Nakamura and

Takasaki (1970) and Nieuwkoop (1973), it was demonstrated that vegetal pole explants (endoderm) could convert animal pole explants (ectoderm) (*i.e.* Nieuwkoop recombinants) into mesoderm. This result suggested that mesoderm-inducing signals originate in the endoderm and instruct the overlying equatorial ectoderm to differentiate into mesoderm.

The '3 Signal Model' was subsequently proposed to explain mesoderm induction and patterning. Two inducing signals were proposed to originate in the endoderm and the third from the Spemann Organizer region. J.M. Slack and colleagues put forth this model with evidence demonstrating that dorsal endoderm induced dorsal mesoderm (signal 1) and ventral endoderm induced ventral mesoderm (signal 2) (Dale and Slack 1987). The combination of dorsal and ventral mesoderm induced ventral mesoderm to form intermediate mesoderm (signal 3) without affecting the dorsal mesoderm graft (Dale et al. 1985). Hence, the combination of 3 inductive signals was sufficient to form and pattern the mesodermal germ layer. Furthermore, the vegetal mesoderm inducing signals were demonstrated to be maternally regulated since heterochronic Nieuwkoop recombinants using 16-cell stage vegetal masses, could induce mesoderm formation in late blastula/early gastrula animal caps (Jones and Woodland 1987).

Further evidence of the dorsalizing signal came from studies using Li^+ (Kao et al. 1986). Injection of Li^+ ions into the vegetal-most cells at the 32 cell stage embryo could efficiently rescue axis formation in UV irradiated embryos suggesting it could mimic or stimulate the endogenous dorsal mesoderm inducing factor(s) (Kao and Elinson 1989). As well, Li^+ could re-specify ventral mesoderm to form Spemann Organizer tissue

(dorsal mesoderm) (Kao et al. 1986; Kao and Elinson 1988; Kao and Elinson 1989). The Li^+ phenomenon was later discovered to be a result of aberrant activation of the canonical Wnt pathway by direct inhibition of GSK-3β (Klein and Melton 1996).

1.1.5.2 VegT releases mesoderm inducing signals

Since the discovery of mesoderm induction, many zygotic factors have been identified which can induce and/or pattern the mesoderm. Candidate inducers include members of the TGF-β (Xnr and Bone Morphogenetic Protein (BMP)), Fibroblastic Growth Factor (FGF) and Wnt signaling families (Kimelman 2006). While it is clear that members of these pathways are necessary for mesoderm maintenance and patterning, the primary inducers are likely to be Xnr mediated signals (Agius et al. 2000), as elaborated below.

Zygotic Xnr signaling is regulated by maternal VegT and β-catenin (Xanthos et al. 2001; Zhang et al. 1998; Hashimoto-Partyka et al. 2003). VegT is a T-box transcription factor localized to the vegetal cortex during oogenesis (Zhang and King 1996) and is the master regulator of endoderm formation required to regulate the zygotic transcription of multiple TGF-β factors necessary for mesoderm induction (Kofron et al. 1999; Clements et al. 1999). Depletion of maternal stores of *VegT* from oocytes by injecting VegT mRNA-specific antisense oligonucleotides, prevents endoderm formation as well as the release of mesoderm inducing factors, although interestingly, some mesoderm does form near the vegetal pole in these *VegT* null embryos (Zhang et al.

1998). These TGF-β-like mesoderm inducing factors include the *nodal*-related genes *Xnr1*, *Xnr2* (Jones et al. 1995), *Xnr4* (Joseph and Melton 1997), *Xnr5*, *Xnr6* (Takahashi et al. 2000), *Vg1* (Dale et al. 1993; Thomsen and Melton 1993), *derrière* (Sun et al. 1999) and *Activin* (Asashima et al. 1990; Smith et al. 1990).

To dissect the involvement of the various classes of mesoderm inducing factors, Agius et al. (2000) used a mutant form of Cerberus, Cerberus-short (Cer-S), that specifically inhibits Xnrs without affecting Wnt, Activin B, derrière or Vg1 (Piccolo et al. 1999). Cerberus is a Spemann Organizer secreted protein that promotes ectopic head, liver and heart formation in *Xenopus* embryos (Bouwmeester et al. 1996) that functions as a local inhibitor of Wnt, Xnr and BMP ligands in the extracellular matrix (Piccolo et al. 1999). Remarkably, the ectopic expression of Cer-S mRNA inhibited mesoderm formation in embryos and blocked mesoderm induction in Nieuwkoop recombinants (Agius et al. 2000). Because Cer-S does not interfere with Wnt, derrière, Vg1 or Activin, this experiment demonstrated that Xnrs are likely the primary inducers of mesoderm formation in *Xenopus*.

The spatial distribution of Xnr proteins underscores their importance as signaling molecules which direct mesoderm differentiation and patterning. Xnrs are expressed in endodermal cells in a dorsal-ventral gradient. This gradient is created by the synergistic activation of Xnr transcription by VegT and Vg1 with β-catenin (Agius et al. 2000). Both VegT and Vg1 but not β-catenin activates Xnr1 transcription in animal cap explants but the co-expression of either VegT or Vg1 with β-catenin, however, synergistically induces even higher levels of Xnr1 messages (Agius et al. 2000). Interestingly, this result

Figure 1.3 Mesoderm Induction and patterning.

A central theme of mesoderm formation is the spatiotemporal regulation of Xnr expression and activity. A) Left: Vegetally localized maternal VegT and Vg1 are required to activate the expression of all Xnrs, with the exception of Xnr3. Center: A dorsal-ventral gradient of β-catenin is required to activate multiple signaling pathways as well as to control the timing and dorsal amplification of Xnr expression. Right: Animally localized maternal factor preserve ectoderm formation by limiting the domain of Xnr expression and activity. B) A simplified view of the genetic network control of mesoderm formation.

A

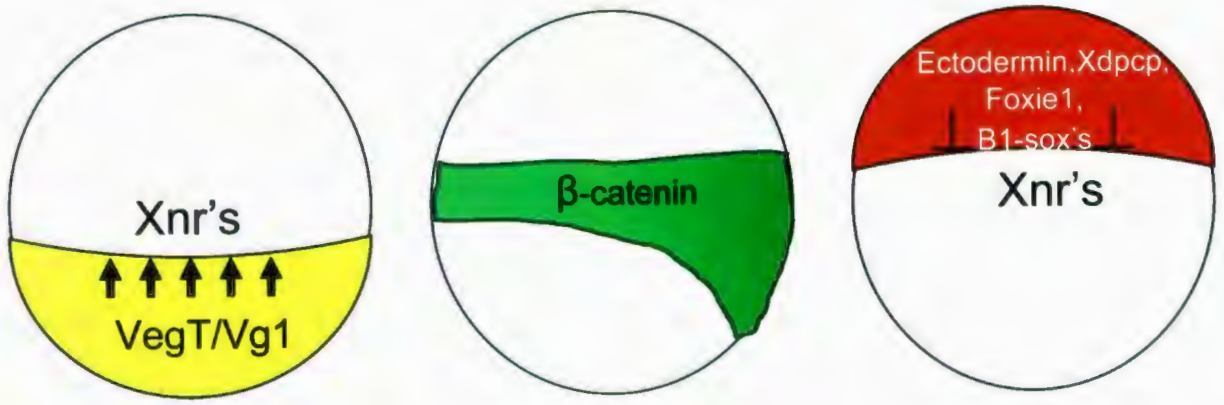
Xnr's
VegT/Vg1
β-catenin
Ectodermin,Xdpcp,
Foxie1,
B1-sox's
Xnr's

B

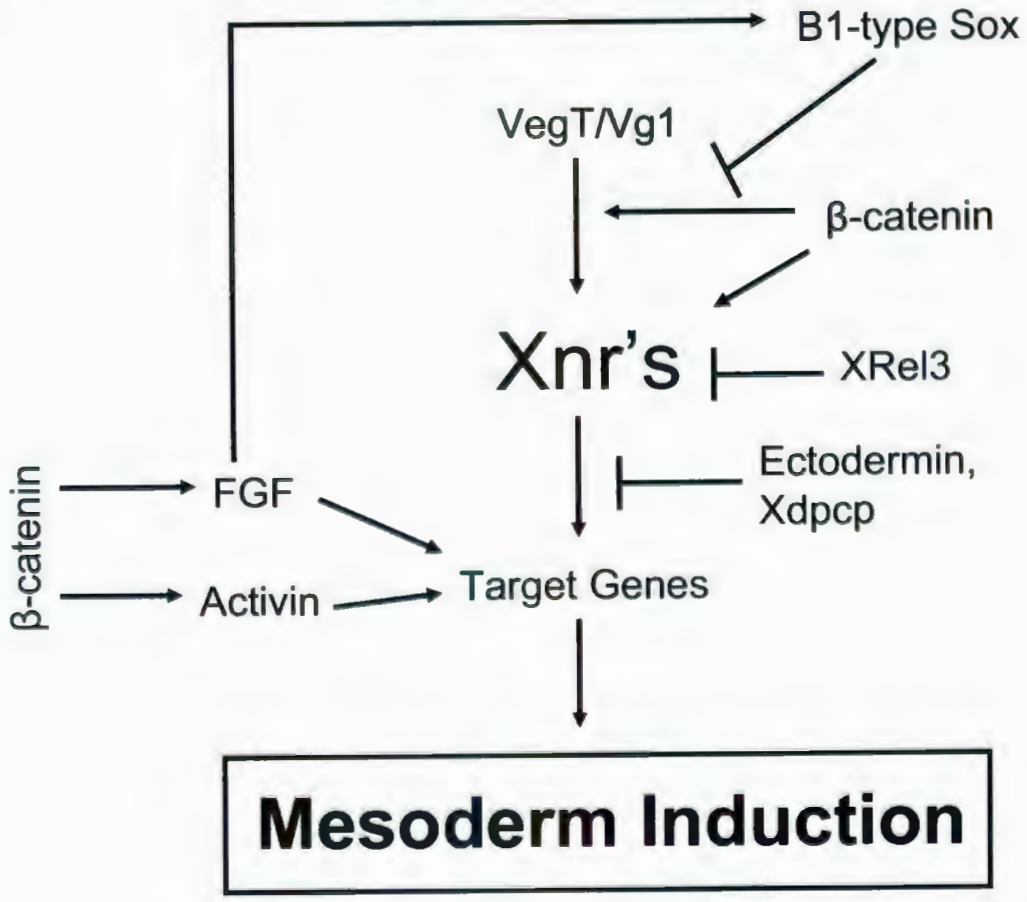
B1-type Sox
VegT/Vg1
β-catenin
Xnr's
XRel3
Ectodermin,
Xdpcp
β-catenin
FGF
Activin
Target Genes
Mesoderm Induction

was substantiated and extended by Hashimoto-Partyka et al. (2003) who demonstrated that maternal, endogenous factors activate an Xnr reporter construct in the absence of β-catenin. However, the levels and timing of Xnr transcriptional activation in dorsal cells was dependent on β-catenin (Hashimoto-Partyka et al. 2003). Importantly, BMPs and FGFs are unlikely to function as endogenous mesoderm *inducers* since mesoderm formation was not blocked by injection of Follistatin mRNA (BMP antagonist) or bFGF blocking antibodies (Slack 1991). However, both pathways do play important roles in mesoderm *formation*.

BMPs, for example, are necessary for dorsal-ventral mesoderm patterning (De Robertis and Kuroda 2004; De Robertis 2009). Inhibition of various BMP growth factors in several genetic animal models, leads to excessive dorsalization, indicating a requirement in ventral cell fate. Complementary to this, the inhibition of BMP antagonists reduces dorsal mesoderm formation with concomitant ventral mesoderm expansion. Several BMP antagonists are targets of the Wnt pathway, including *Chordin* and *Noggin*. The protein products of both these genes are secreted from the Spemann organizer and bind to BMPs in the extracellular space thus preventing them from interacting with cognate membrane receptors (De Robertis 2009; Piccolo et al. 1996; Zimmerman et al. 1996). As such, a ventral-dorsal gradient of BMP signaling is necessary for proper mesoderm patterning.

FGF signaling also has an indispensible role during mesoderm formation and patterning. Originally, FGFs were identified as mesoderm inducers in *Xenopus* (Kimelman et al. 1988; Kimelman and Kirschner 1987; Paterno et al. 1989; Slack et al.

1989). However, expression analysis of multiple FGFs determined they were expressed in the animal hemisphere and that only *basic* (*b*)*FGF*, *FGF9* and *embryonic* (*e*)*FGF* are maternally expressed. As a result FGFs were effectively eliminated as potential maternal endogenous mesoderm inducer(s) which were clearly determined to be of vegetal origin (Jones and Woodland 1987; Nakamura and Takasaki 1970; Nieuwkoop 1973).

Subsequently, FGFs were proposed to act as competence factors necessary for animal cells to respond to mesoderm induction stimuli (Slack et al. 1990; Gillespie et al. 1989; Isaacs 1997; Isaacs et al. 1994; Cornell et al. 1995). For example, although Li^{+} can dorsalize ventral mesoderm, it requires FGF signaling to induce muscle (dorsal mesoderm derivative) in animal caps (Slack et al. 1988). Likewise, Activin induces dorsal mesoderm formation in animal cap explants, however, the injection of a dominant negative FGF receptor (XFD) antagonizes Activin induction suggesting Activin acts upstream of FGF signaling (Amaya et al. 1993; Cornell and Kimelman 1994; Kimelman and Kirschner 1987).

FGF signaling activates the MAP kinase pathway and is essential for the expression the pan-mesodermal marker, *XBra* (LaBonne et al. 1995; Isaacs et al. 1994) and other early markers of mesoderm formation (Teplitsky et al. 2003; Paterno et al. 1997). The activation of *Xbra* expression initiates an autocatalytic feedback loop with zygotic *FGF4* that functions to maintain mesoderm gene expression during gastrulation (Isaacs et al. 1994). More recently, determination of the FGF regulated transcriptome revealed 73 genes either positively or negatively regulated by FGF (Branney et al. 2009).

Lastly, FGF signaling was shown to be required for the activation of VegT mesodermal target genes (Fletcher and Harland 2008).

All in all, these findings suggested a revision of the original '3 Signal Hypothesis' to a '2 Signal Hypothesis', whereby the 2 endoderm emitted signals could be reduced to a single, Xnr inducing stimulus that initiates FGF-sensitized mesoderm induction and generates dorsal and ventral identity by an Xnr gradient patterned by maternal Wnt signaling (Agius et al. 2000; Hashimoto-Partyka et al. 2003).

1.1.5.3 A role for maternal canonical Wnt signaling in mesoderm formation

Additional evidence suggests that maternal canonical Wnt signaling plays a role in early mesoderm induction. First, β-catenin was found to regulate the patterns of phosphorylation of key intracellular regulators of the 3 signaling pathways that regulate mesoderm formation: MAPK (int-2/FGF3)*)*, Smad1 (BMP) and Smad2 (Nodal/Activin/Vg1), thus suggesting it functioned upstream of all 3 pathways (Schohl and Fagotto 2002). Secondly, analysis of the spatiotemporal expression pattern of maternal β-catenin protein identified it as being localized to dorsal nuclei at or before MBT, consistent with previous studies (Larabell et al. 1997; Schneider et al. 1996), but also in a ring around the equator by late blastula (Schohl and Fagotto 2003; Figure 1.3). This previously, unrecognized pattern of β-catenin protein expression was suggested to be a result of maternally localized transcripts/protein separate from β-catenin protein stabilized by cortical rotation. However, depletion of maternal β-catenin using antisense

oligonucleotides (Heasman et al. 1994) or antisense morpholinos (Heasman et al. 2000) prevented only dorsal mesoderm without affecting the expression of ventral or general mesoderm markers (Heasman et al. 1994).

Schohl and Fagotto (2003) demonstrated that β-catenin regulated the expression of *FGF3* which in turn induced the phosphorylation of MAPK, a necessary step in FGF-mediated mesoderm formation (Christen and Slack 1999; LaBonne et al. 1995; LaBonne and Whitman 1997; Whitman and Melton 1992). As well, β-catenin was required for the expression of the mesodermal markers, *Xbra*, *Goosecoid* and *Eomesodermin* (Schohl and Fagotto 2003). This observation suggests a role for canonical Wnt signaling upstream of FGF-mediated mesoderm formation in addition to regulating the endodermal pattern of Xnr expression, as described above.

1.1.5.4 Restricting mesoderm formation to the marginal zone

Why does mesoderm only form at the marginal zone? The answer to this question has at least 2 parts. Firstly, as described in sections 1.1.4.1 and 1.1.4.2, Xnr signals are secreted mesoderm inducers. Hence their ability to diffuse through the extracellular space likely dictates their range of activity. In fact Xnrs have been shown to have short range function whereas Activin has been suggested to act over relatively large distances (Hashimoto-Partyka et al. 2003; Jones et al. 1996).

Secondly it has recently been shown that several maternal factors are expressed in the ectoderm capable of enforcing the mesectodermal boundary. *Ectodermin* was the first

reported molecule capable of promoting ectoderm formation by directly inhibiting mesoderm formation in the animal pole. Ectodermin is an E3 ubiquitin ligase that specifically targets Smad4 thus abrogating Xnr signaling (Dupont et al. 2005). Additionally, *foxie1/Xema*, a foxi subclass winged-helix transcription factor, inhibits mesoderm formation and controls animal cell position in blastulae, though the precise molecular mechanism is unclear (Mir et al. 2007; Suri et al. 2005). Xdpcp is a phosphotyrosine binding protein that inhibits Activin/Nodal signaling by binding to Alk4, a type I Activin/Nodal receptor, and inhibits the phosphorylation and nuclear translocation of Smad2 (Cheong et al. 2009). As well, the maternal B1-type SOXs (*i.e. SOX1, SOX2* and *SOX3*) (Zhang et al. 2004a) and XRel3 (Kennedy et al. 2007) were also demonstrated to inhibit mesoderm formation though negative regulation of nodal signaling (Kennedy et al. 2007; Zhang et al. 2004a) The B1-type SOXs were shown to repress nodal expression by inhibiting VegT and β-catenin (Zhang et al. 2004a) but the mechanism by which XRel3, a Dorsal/Rel/NF-κB orthologue, attenuates Xnr signaling is unclear.

1.1.5.5 Dorsal/Rel/NF-κB regulates mesoderm formation

Dorsal/Rel/NF-κB factors regulate transcription during immune and inflammatory responses and are important regulators of cell survival and differentiation during embryogenesis. In *Drosophila melanogaster*, the Rel/NF-κB orthologue, Dorsal (Dl), establishes dorsal-ventral polarity in the egg during fly oogenesis. Dl accumulates

specifically in ventral nuclei creating a ventral-dorsal gradient. Mutant flies that lack Dl have an increased number of cells committed to dorsal lineages. Rel/NF-κB is also important for notochord (a mesoderm derivative) formation in the ascidian, *Ciona intestinalis* (Kawai et al. 2005). Genetic studies of all the Rel/NF-κB factors have been analyzed either individually or in various combinations in mice. However, the defects are most commonly associated with impaired lymphoid cell development (*NF-κB1*$^{-/-}$, *NF-κB2*$^{-/-}$, *RelA*$^{-/-}$, *c-Rel*$^{-/-}$, and *RelB*$^{-/-}$) (Gerondakis et al. 2006). Others have epidermal defects (*RelA*$^{-/-}$ and *RelA*$^{-/-}$*/c-Rel*$^{-/-}$*/TNF*$^{-/-}$) (Gugasyan et al. 2004; Zhang et al. 2004b) or craniofacial defects (*NF-κB1*$^{-/-}$*/NF-κB2*$^{-/-}$) (Franzoso et al. 1997; Iotsova et al. 1997). Of particular interest, NF-κB$^{-/-}$/RelA$^{-/-}$ and RelA$^{-/-}$/c-Rel$^{-/-}$ double knockout mice die at embryonic stage (E) 13 due to defective hematopoietic systems, a ventral mesoderm derivative (Gerondakis et al. 2006).

In *Xenopus laevis*, 4 Rel/NF-κB factors have been identified: *XRelA* (Kao and Hopwood 1991), *XRel2* (Tannahill and Wardle 1995), X*RelB* and *NF-κB1* (Suzuki et al. 1995; Suzuki et al. 1998) and *XRel3* (Yang et al. 1998). XRelA, XRel2 and XRel3 have all been implicated in mesoderm and axis formation of the *Xenopus* embryo (Beck et al. 1998; Tannahill and Wardle 1995; Kao and Lockwood 1996; Kennedy et al. 2007). Ectopic expression of XRelA mRNA inhibited endogenous axis formation and prevented axial duplications when co-injected with a dominant negative GSK-3β (Kao and Lockwood 1996). Furthermore, XRelA mRNA injected into animal cells could inhibit bFGF and Activin induced mesoderm formation in animal cap explant assays (Beck et al. 1998), while injection of synthetic XRel2 mRNA into *Xenopus* embryos disrupted axis

formation and inhibited the expression of the mesodermal markers *Goosecoid*, *XBra*, *Wnt8*, and *Snail* (Tannahill and Wardle 1995). XRelA and XRel3 have been implicated in mesoderm formation through feedback regulatory circuits of *Twist* and *Slug* (Zhang et al. 2006; Zhang and Klymkowsky 2009). More recently, it has been demonstrated that XRel3 is important in establishing the mesoderm-ectoderm boundary by suppressing Xnr signaling in animal cells (Kennedy et al. 2007).

1.1.5.6 Overview of the Rel/NF-κB signaling cascade

The Rel/NF-κB signaling pathway is an important regulator of embryonic development and disease. Founding members of this biochemical cascade were shown to encode proteins that bind to sequence specific elements of immunoglobulin promoters in lymphoid cells (Staudt et al. 1986; Singh et al. 1986; Sen and Baltimore 1986b). Since this discovery, intense research on the Rel/NF-κB pathway has shown it to regulate the transcription of more than 200 genes (Pereira and Oakley 2008) and more than 750 natural and synthetic inhibitors have been identified (Gilmore 2006).

There are 5 Rel/NF-κB proteins that share structural homology with the avian retroviral oncogene *Reticuloendotheliosis* (v-Rel). Rel/NF-κB proteins are intracellular proteins that share a conserved N-terminal region termed the Rel homology domain (RHD). The RHD mediates the ability of Rel/NF-κB proteins to dimerize, to localize to nuclei, and to bind target DNA sequences. The C-terminal region contains a

transactivation domain in RelA (p65), RelB and c-Rel, though not in NF-κB1 (p50) and NF-κB2 (p52) (Gilmore 2006; Pereira and Oakley 2008; Perkins 2007).

Many cytokines and growth factors activate Rel/NF-κB to mediate a variety of physiological processes such as inflammation, cell growth and cell survival, such as Interleukin-1 (IL-1), Tumor necrosis factor-α (TNF-α) (Krasnow et al. 1991; Osborn et al. 1989; Israel et al. 1989) and bacterial lipopolysaccharide (LPS) (Sen and Baltimore 1986a). In the absence of pathway stimulation, Rel/NF-κB dimers are cytoplasmically sequestered by Inhibitor κ B proteins (IκB) by masking the nuclear localization sequence (NLS) (Figure 1.4A) found within the RHD (Beg et al. 1992; Haskill et al. 1991) .

Pathway stimulation results in the phosphorylation of two IκB N-terminal serine residues that target it for ubiquitination and proteasomal degradation, thus resulting in the release of Rel/NF-κB factors. IκB is phosphorylated by a complex of 3 IκB kinases (IKK)s: IKK-α, IKK-β and NEMO (IKK-γ) (Figure 1.4B) (DiDonato et al. 1997; Zandi et al. 1997; Mercurio et al. 1997). Rel/NF-κB dimers then translocate to target gene promoters in the nucleus, and in association with co-activators or co-repressors, regulate gene expression.

1.1.6 The embryonic body axis

1.1.6.1 At the nexus of dorsal-ventral polarity and mesoderm formation

The earliest events that pattern the embryo are still incompletely understood. Formation of the primary body axis is, however, dependent on elaborate spatiotemporal

Figure 1.4 Overview of the Rel/NF-κB signaling cascade.

A) In the absence of pathway activation, Rel/NF-κB dimers are inactivated by sequestration in the cytoplasm. B) Ligand (*e.g.* TNF-α, IL-1 or LPS) stimulated activation initiates a series of kinases that induce the release of Rel/NF-κB proteins to manage gene expression.

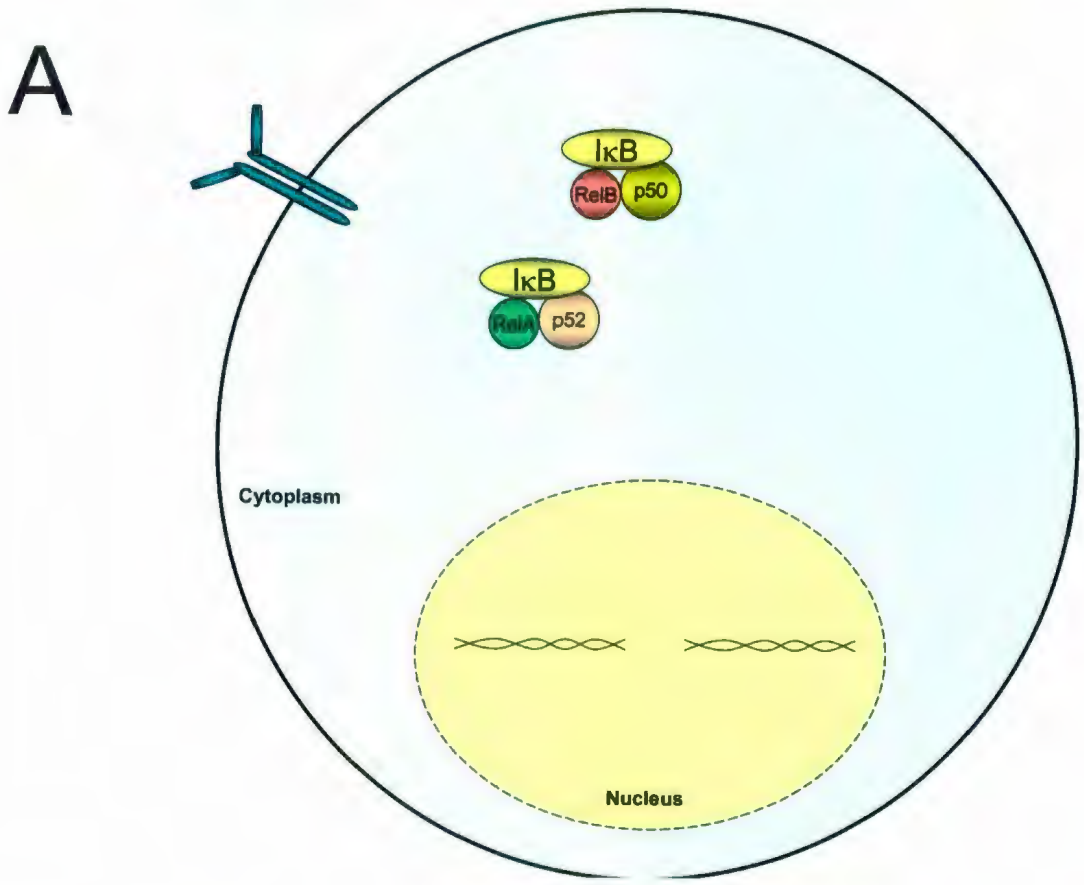
A
IκB
RelB
p50
IκB
RelA
p52
Cytoplasm
Nucleus

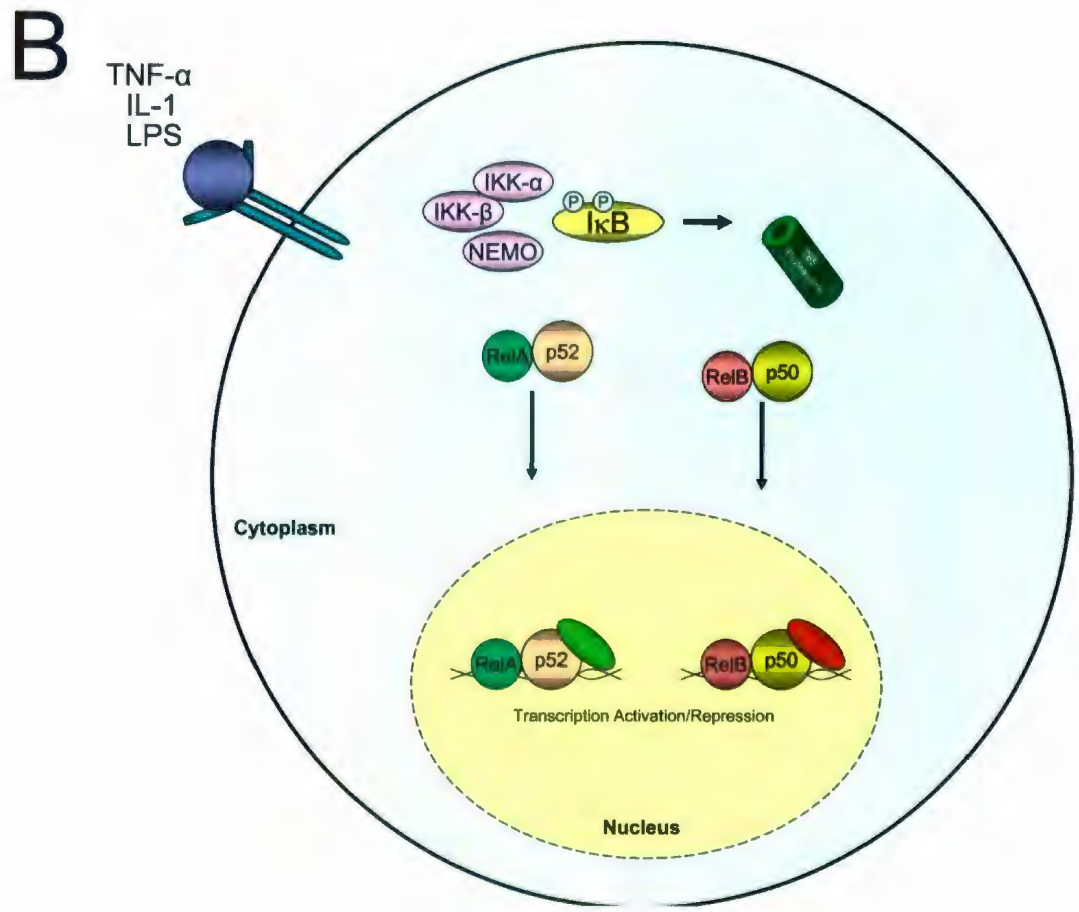
B
TNF-α
IL-1
LPS
IKK-α
IKK-β
NEMO
P
P
IκB
RelA
p52
RelB
p50
Cytoplasm
RelA
p52
RelB
p50
Transcription Activation/Repression
Nucleus

regulation of gene expression that establishes dorsal-ventral asymmetry and formation of the mesoderm germ layer.

The goal of my thesis was to study how the regulation of transcription during embryonic development controls cell fate, thus regionalizing the embryo into an organized body plan. I have focused on two signal transduction pathways, the Rel/NF-kB signaling pathway, which regulates gene expression required for formation of mesoderm, and the canonical Wnt pathway, which is required to activate expression of many genes required for genes that determine dorsal body structures.

There are 3 main objectives to my thesis.

1.1.6.2 Objective 1: Mechanism of XRel3/XRelA mediated Xnr signaling

The morphogenetic field of mesoderm formation is limited, in part, by negative regulators expressed in the animal half of the embryo. In chapter 2, I describe experiments that address the molecular mechanism by which XRel3 and to a lesser extent XRelA, regulate mesoderm formation. This project began with the observation that the ectopic expression of XRel3 or XRelA mRNA into the marginal region of *Xenopus* embryos caused abnormal axial development. In conjunction with former lab members, I analyzed the expression of mesoderm inducers and markers in embryos over-expressing XRel3. Using this approach I determined that XRel3 was an inhibitor of endogenous mesoderm inducers (Xnrs). I hypothesized that XRel3 carried out this function by regulating the canonical Wnt signaling pathway, a known activator of Xnr expression.

My results demonstrate that in gain-of-function assays, XRelA and XRel3 can attenuate β-catenin activity, likely through a direct interaction between XRel3 and β-catenin proteins. These results suggest that XRel3 and/or XRelA may function to negatively regulate canonical Wnt target gene expression during early development.

1.1.6.3 Objective 2: Identification of an orthologous β-catenin regulating protein in Xenopus

Dorsal mesoderm formation requires activation of the canonical Wnt pathway. However, because activation of the pathway appears to be labile from fertilization until the mid-blastula, it is not clear what are the determining factors that commit Wnt activated cells to the dorsal lineage. I hypothesized that although Wnt signaling is required to specify the dorsal cells of the blastula stage embryo, the mobilization and recruitment of components downstream of the signal transduction event are essential for determination of the dorsal phenotype. To this end, I isolated *XBcl9*, a *Xenopus* orthologue to Lgs/Bcl9. Lgs/Bcl9 was identified as a core component of the canonical Wnt transcriptional complex and its recruitment to the transcription complex is thought, along with its binding partner, Pygopus, to represent a determinative step in Wnt signal transduction. My experiments in Chapter 3 address the hypothesis that recruitment of Lgs/xBcl9 represents a determinative step in dorsal differentiation. I characterized the developmental expression of XBcl9 and its conserved biochemical interactions. I further asked if XBcl9 was required for body axis formation and used gain- and loss-of-function experiments to address this question. My results demonstrate that XBcl9's interaction with β-catenin and Pygopus is conserved in *Xenopus* embryos. I also determined that

XBcl9 accumulates in dorsal cell nuclei after MBT, corresponding to the activation of Wnt target gene expression. Furthermore, gain-of-function assays suggested that XBcl9 requires Pygopus to ectopically stimulate dorsal gene expression and loss-of-function experiments determined that maternal XBcl9 is required for dorsal axis formation. Hence XBcl9 is a necessary component of the canonical Wnt signal transduction pathway, dependent upon Pygopus, and acts as a determinative factor of dorsal cell fate.

1.1.6.4 Objective 3: Analysis of the post-transcriptional regulation of XBcl9

The establishment of XBcl9 as a determinative component in dorsal differentiation suggests that its regulation is important for the formation of the embryonic body plan. The expression analysis of XBcl9 mRNA and protein derived from Objective 2 suggested that XBcl9 mRNA was post-transcriptionally regulated. To this end, in Chapter 4, I report the identification of XBcl9 regulation at the level of translation. I mapped a minimal repression element to the 5'UTR of XBcl9 mRNA that inhibited translation in embryos and human cells. Furthermore, I determined that this repression element was relatively well conserved in the 5'UTR of several orthologous Bcl9 sequences and is predicted to form a stable secondary structure. These results suggest that the 5'UTR of XBcl9 mRNA may regulate its translation in embryos, thus conferring a novel mechanism governing XBcl9-dependent transcription during embryogenesis.

Chapter 2: Molecular crosstalk between Rel/NF-κB and β-catenin proteins regulates dorsal mesoderm formation

2.1 Introduction

Establishment of the dorsal-ventral axis is an essential step for primary body axis formation. In fly embryos, a nuclear-cytoplasmic gradient of the Rel/NF-κB orthologue, Dorsal (Dl), in ventral cells establishes the dorsal-ventral axis and specifies the presumptive mesoderm (Moussian and Roth 2005). In vertebrates, the canonical Wnt pathway establishes dorsal-ventral polarity and regulates dorsal mesoderm formation in early development (Croce and McClay 2006; Heasman 2006; Marikawa 2006).

Interestingly, components of the *Drosophila* spätzle/Toll pathway that positively regulate Dl protein expression, have dorsalizing activity when expressed in vertebrate (frog) embryos suggesting that Dl can function via evolutionarily conserved mechanism(s) (Armstrong et al. 1998). On the contrary, during *Xenopus* embryogenesis, the orthologous Dl proteins XRelA, XRel2 and XRel3 negatively regulate mesoderm induction and inhibit formation of the dorsoanterior axis (Beck et al. 1998; Kao and Lockwood 1996; Kennedy et al. 2007; Tannahill and Wardle 1995). These results suggest that *Dorsal* and *Rel/NF-κB* genes are paralogous homologs that have evolved divergent functions between frogs and flies.

Rel/NF-κB proteins are pleiotropic transcription factors that are involved in myriad processes such as cellular differentiation, cell survival, immune and inflammatory responses and possibly memory formation (Papa et al. 2006; Pereira and Oakley 2008; Perkins 2007). There are five Rel/NF-κB transcription factors: NF-κB1 (p50), NF-κB2 (p52), RelA (p65), RelB and c-Rel (Pereira and Oakley 2008; Perkins 2007). Rel/NF-kB

proteins are DNA-binding proteins that function as hetero- or homo-dimers and may activate or repress transcriptional targets in a cell context dependent manner.

In the absence of Rel/NF-κB pathway stimulation, Rel/NF-κB dimers are inactivated and sequestered in the cytoplasm by inhibitor-κB (IκB) proteins. In addition to ligands which interact with Toll-like receptors (TLR), the Rel/NF-κB pathway can be activated by stimuli such as cytokines or bacterial lipopolysaccharide (LPS). Pathway stimulation induces the phosphorylation of IκB by IκB kinases (IKK), thus releasing Rel/NF-κB dimers which then translocate to nuclei to regulate transcription (Perkins 2007).

In *Xenopus*, activation of the maternal canonical Wnt pathway regulates Xnr signaling, which is required for dorsal mesoderm formation in the marginal zone (Wylie et al. 1996; Agius et al. 2000; Hashimoto-Partyka et al. 2003). Maternal canonical Wnt signaling also regulates ventrolateral mesoderm formation by activating *FGF3* expression with subsequent activation of MAPK, and concomitant Smad1 and Smad2 phosphorylation (Schohl and Fagotto 2002; Schohl and Fagotto 2003). Thus, elucidating the mechanisms that regulate the canonical Wnt pathway is paramount to understanding how it regulates biological processes such as dorsal axis formation.

One mechanism that regulates the canonical Wnt pathway is molecular crosstalk with the Rel/NF-κB signaling pathway. However, typical of Rel/NF-κB transcription factors, Rel/NF-κB proteins can both co-activate and repress transcription of canonical Wnt target genes in various human cancer cell lines, making interpretation of results sometimes difficult (Cho et al. 2008). More recently, an interdependency of Rel/NF-κB

and canonical Wnt signaling pathways for induction of hair follicle primordia has been reported (Zhang et al. 2009).

Ectopic expression of XRelA, XRel2 or XRel3 mRNA in *Xenopus* embryos negatively affects axis formation, a canonical Wnt dependent event (Beck et al. 1998; Kao and Lockwood 1996; Tannahill and Wardle 1995). Therefore, I hypothesized that Rel/NF-κB signaling negatively regulates canonical Wnt dependent transcription in early *Xenopus* development.

In this chapter I confirmed that ectopic expression of XRelA or XRel3 mRNA in dorsal marginal zones prevented formation of the endogenous body axis and suppressed axial duplication when co-expressed with wildtype Xβ-catenin or β-catenin^{S37A} mRNA. I re-examined the effect of ectopic XRel3 mRNA on β-catenin regulated gene expression, which suggested that XRel3 may enforce the boundary of mesoderm formation by inhibiting post-MBT *Xnr* transcription (Kennedy et al. 2007). Lastly, I determined that XRel3 but not XRelA directly interacted with β-catenin, *in vitro*, suggesting a possible mechanism by which Rel/NF-κB signaling negatively regulates canonical Wnt dependent target gene transcription in *Xenopus* embryos.

2.2 Materials and Methods

2.2.1 Embryo collection and manipulation

Wild type embryos were obtained from female *Xenopus laevis* using standard techniques as described (Kao and Lockwood 1996; Lake et al. 2001). Fertilized eggs were injected in 50% Normal Amphibian Medium (NAM) supplemented with 2-4% Ficoll and cultured in 5% NAM. Embryos were staged according to Nieuwkoop and Faber (1994). Embryos were fixed and stored in MEMFA (100mM MOPS, 0.1mM $MgSO_4$, 2mM EGTA, 3.7% Formaldehyde) at room temperature. Embryos were photographed for phenotype analysis using a Leica MZ FLIII microdissection microscope fitted with 'Cool Snap' camera and software.

2.2.2 Plasmids and RNA synthesis

pCS2+/XRelA was constructed by PCR amplification of the XRelA coding region using the p64T/XRelA plasmid (Kao and Hopwood 1991) as template, restriction digested and inserted into pCS2+ EcoRI and XhoI restriction sites. XRelA primer sequences: forward primer 5'-CGGATTTCTTGAACATGGATGGATTC-3'; reverse primer 5'-GCCTCGAGCATGCTTAGTCTTATTGC-3' (restriction sites included in the primers are underlined). pCS2+/XRel3 was previously described (Lake et al. 2001). pGEX4T-3/XRel3 was constructed by subcloning the XRel3 coding region from pCS2+/XRel3 into the pGEX4T-3 BamHI/NotI restriction sites. pCS2+/β-catenin^{S37A} was previously described (Popadiuk et al. 2006). pCS2+/Xβ-catenin and pGEX4T-1/Xβ-

catenin were constructed as described in chapter 3 (Kennedy et al. 2009). pCS2+ and pCS2+/β-galactosidase, pCS2+/Axin and the pSia-Luciferase reporter vector were kind gifts from Dr. Dave Turner, Dr. Peter Klein and Dr. Segei Sokol, respectively.

In vitro transcription of all mRNAs used in this chapter, except β-catenin^{S37A} mRNA, was carried out using the SP6 mMessage mMachine RNA syntheis kit, as per manufacturer's protocol (Ambion). β-catenin^{S37A} mRNA was transcribed using Sp6 Ribomax kit (Promega).

2.2.3 GST-Pullown Assay

GST pulldowns were performed as per manufacturers protocol (Stratagene). GST-fusion protein was expressed in BL 21 RP competent cells, extracted and purified using Glutathione Sepharose 4B beads (GE Healthcare). Approximately 1 μg of total GST fusion protein was used in each pulldown reaction. Approximately 1μl of XRelA, 2μl of XRel3 and 0.5μl of Axin *in vitro* translated, radiolabelled (^{35}S-[Met] (Perkin Elmer)) proteins, made in cell-free rabbit reticulocyte lysate (Promega) as per manufacturer's protocol, were used per GST-pulldown. Proteins were resolved using 10% acrylaminde SDS-PAGE gels. Gels were subsequently stained in Coomassie for 1hour and destained overnight (74%H_20, 6% Glacial Acetic Acid, 20% Methanol) at room temperature. Interacting radiolabelled protein was detected by exposure to film (X-OMAT LS, Kodak) overnight at room temperature.

2.2.4 β–galactosidase and Luciferase Assays

All embryos used for luciferase assays were co-injected with 50pg each of pSia-Luciferase plasmid and β-galactosidase (β-gal) mRNA in addition to XRelA/3 and Xβ-catenin/β-catenin^{S37A} mRNA for each experiment. β-gal assays were performed as per manufacturer's protocol (Clontech). Total protein was extracted from 3 pools of 5 embryos from 3 independent batches of embryos. Approximately 10µl of whole embryo protein extracts were incubated in 200µl of Z-buffer (60mM $Na_2HPO_4•7H_2O$, 40mM $NaH_2PO_4•H_2O$, 10mM KCl, 1mM $MgSO_4•7H_2O$, pH 7.0) with 4g/L ONPG (2-Nitrophenyl β-D-galactopyranoside) (SIGMA) and β-Mercaptoethanol (0.27%) at 37°C until yellow color develops. Reactions were then stopped by the addition of an equal volume of 1M Tris (pH 11) and colour intensity was measured using a BioRad 3550 microplate reader.

Luciferase assays were performed as per manufacturer's protocol. Approximately 10µl of total protein extracts were used per luciferase reaction. Samples were read in Monolight 2010 Luminometer.

2.2.5 RNA Isolation and Real-Time PCR

Total RNA was extracted from 10-12 embryos using the Nucleospin II RNA Extraction Kit (Clontech). Reverse transcription of ~1µg of total RNA to cDNA was performed using MMLV-RT (Invitrogen) as per manufacturer's protocol. cDNA was

then diluted 1:10 and 2 μl was used per quantitative Real-Time PCR (qPCR) reaction. Marker expression was analyzed by SYBR Green (Applied Biosystems) incorporation detected using the ABI Prism 7000 Detection System (Applied Biosystems). Results were analyzed using the comparative Ct method (*i.e.* $2^{-\Delta\Delta Ct}$) (Livak and Schmittgen 2001; Schmittgen and Livak 2008a). Total cDNA was normalized to Histone H4 levels. Reverse transcription reactions did not give any/specific products. Dissociation curves (*i.e.* melting curves) confirmed a single PCR amplicon in all reactions. All qPCR primer sequences are listed Table 2.1.

2.3 Results

2.3.1 Ectopic XRelA or XRel3 expression disrupts axis formation

In *Drosophila*, the dorsoventral axis is defined by the nuclear accumulation of the transcription factor 'Dorsal' in ventrally-fated cells (Roth et al. 1989; Roth 2003; Hong et al. 2008). Dorsal is closely related to Rel/NF-κB proteins in vertebrates (Armstrong et al. 1998; Prothmann et al. 2006). In *Xenopus*, *RelA* and *Rel3* transcripts are expressed in the animal hemisphere including the dorsal marginal zone of cleavage stage embryos (Kao and Hopwood 1991; Yang et al. 1998). Therefore, I was interested in determining whether Rel/NF-κB proteins, specifically XRelA and XRel3 were functionally conserved during *Xenopus* development.

Previously, *XRelA* was shown to negatively regulate dorsal patterning due to its ability to attenuate Activin and FGF-stimulated convergent extension movements in animal cap explants (Beck et al. 1998). It could also inhibit dorsoanterior development or ectopic body axes induced by ventral co-injection of synthetic mRNA encoding dominant negative GSK3β (R85) (Kao and Lockwood 1996). R85 is a kinase-dead GSK3β mutant (K85R residue substitution) incapable of phosphorylating β-catenin. Overexpression of R85 activates canonical Wnt signaling, presumably by interfering with endogenous GSK3β function (Dominguez et al. 1995).

While ectopic expression of XRel3 mRNA into animal or vegetal pole cells induced epidermal tumor formation in tadpoles, overexpression of the synthetic wildtype or DNA-binding deficient XRel3Δ58 variant (*i*.e. dominant negative XRel3) into the

prospective mesoderm region, or marginal zone, impaired dorsal-anterior development (Yang et al. 1998; Lake et al. 2001; Kennedy et al. 2007). To confirm these results I injected 250pg of either synthetic XRelA or XRel3 mRNA into the presumptive dorsal marginal zone of 2-cell stage embryos. The dorsal side of embryos was identified primarily based on pigmentation, size differences in dorsal and ventral cells and the sperm entry point (SEP). Ectopic expression of XRelA (n= 15) or XRel3 (n=15) mRNA in the dorsal marginal zone severely perturbed body axis development with no identifiable dorsoanterior structures (Figure 2.1 and Table 2.2). For comparison, injection of 500pg of Axin mRNA, encoding a known inhibitor of dorsal axis formation (Ikeda et al. 1998; Itoh et al. 1998), into the dorsal marginal zone impaired normal axis development (Figure 2.1D). These embryos displayed similar phenotypes caused by ectopic *XRelA* and *XRel3* expression. These results are consistent with previous reports (Kao and Lockwood 1996; Kennedy et al. 2007). Since the body axis is derived from the mesodermal germ layer, these results suggest a role for XRelA and XRel3 in inhibiting dorsal mesoderm formation.

2.3.2 XRel3 inhibits mesoderm formation

Ectopic expression of XRel3 in animal cells caused the formation of embryonic tumors with elevated levels of anterior neural patterning genes such as *Gli*, *Shh*, and *Otx* (Lake et al. 2001; Yang et al. 1998), thus suggesting a role in promoting ectodermal cell

Figure 2.1 Ectopic expression of XRelA or XRel3 mRNA inhibits axis formation.

A) Uninjected control embryos. B) Embryos injected with 250pg XRel3 mRNA or C) with 250pg XRelA mRNA into the equatorial region. D) Injection of 500pg Axin mRNA into the dorsal equatorial region. Injected embryos failed to develop the elongated dorsal axis and heads. Scale bar is 1mm.

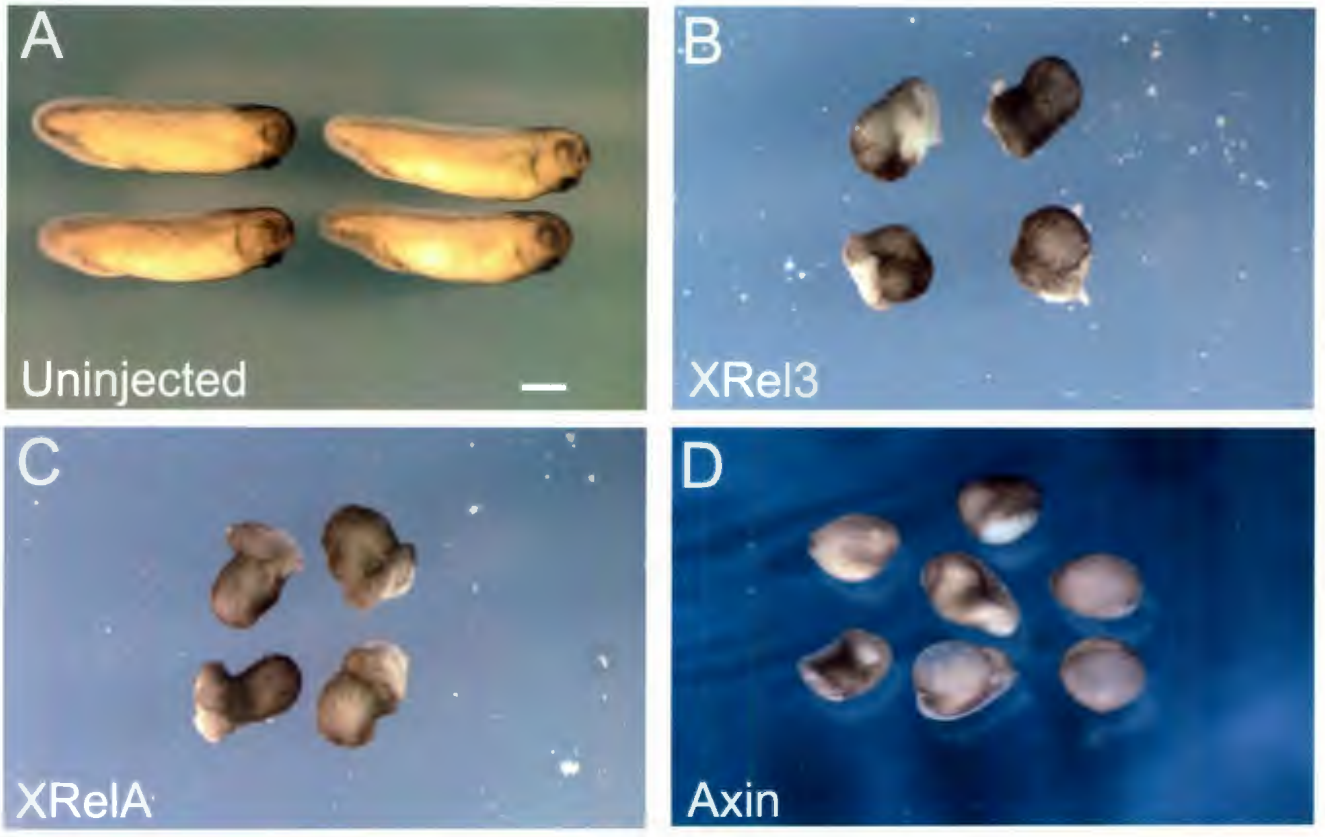
A
Uninjected
B
XRel3
C
XRelA
D
Axin

fate. Based on the injection site-specific ability of XRel3 to either promote ectodermal cell lineages (animal pole) or to inhibit mesodermal cell lineages (marginal zone) I hypothesized that endogenous XRel3 may be necessary for formation of the ectoderm and/or restriction of the mesoderm boundary during germ layer specification.

In collaboration with other lab members we addressed this question in two ways. First, I injected increasing dosages of synthetic XRel3 mRNA into both cells at the animal-vegetal pigment boundary (marginal zone) of 2 cell stage embryos. I then assayed the effect of elevated *XRel3* levels on mesoderm-specific gene expression in stage 10 embryos using qPCR. To confirm that synthetic XRel*3* mRNA was not degraded upon injection, I initially assayed the overall levels of XRel*3* messages in injected embryos compared with uninjected controls. Figure 2.2A shows a representative experiment where injection of 250pg of XRel3 mRNA increased total *XRel3* messages by ~3.4 fold, 500pg by ~4 fold and 1000pg by 10.2 fold relative to uninjected control levels.

Next I assayed the response of 6 mesoderm-specific markers to *XRel3* overexpression. All 6 markers were reduced in a dose dependent manner. At the highest dosage (1000pg) of *XRel3* mRNA the pan-mesodermal marker *Xbra*, and the mesendodermal marker *mix2* were reduced by ~80% and ~75%, respectively. The ventral mesodermal markers *vent1*, *vent2* and *derrière*, were each reduced by ~60% and the dorsal mesodermal *goosecoid* (*gsd*) was reduced by ~55% (Figure 2.2B). These results clearly show that XRel3 can suppress mesoderm-specific gene expression in the marginal zone of *Xenopus* embryos.

Table 2.1 Primers used for qPCR analysis.

Primer Name	Sequence (5'—3')	Reference
Histone (H4)	U-CGGGATAACATTCAGGGTATCACT D-ATCCATGGCGGTAACTGTCTT	Lake et al. 2001
Xrel3	U-CAAGAGAGACGTGAACCAATTCC D-GGCGCTGCTGTTGGTGCTGTGC	New
Xbra	U-GGATCGTTATCACCTCTG D-GTGTAGTCTGTAGCAGCA	New
Xnr1	U-GTAGGAGAGTGGACATGATTGTGG D-TTAACTGCACCCACATTCCTCTACAATC	New
Xnr2	U-CGCCATTGCCTCCCTTATGC D-CAGATTCTTGCAGGACGGG	New
Xnr5	U-CCAGAACAGCATCATAAGAAGCGG D-GGCTTGAAGTTCTCATCCAGTGG	New
Xnr6	U-CCACACCAAAGACCGTCACGAG D-CCAACATGACTCTCTCCGCAAC	New
mix2	U-TGCAAGCCATCATTATTCTAGC D-AGGAACCTCTGCCTCGAGACAT	New
Goosecoid	U-GTGCTGATTCCACCAGTGCCTCACC D-CAACTGTCAGAGTCCAGGTCAG	New
Derrière	U-CATCTCCACTTACCTTCCAGG D-CCTTGATCTCGATATGAGCGGAC	New
Vent1	U-GCTTGGTTCCTCCTCCCGTC D-CATGGTGGTGGAGTGGCTGG	New
Vent2	U-CCATCCCTGCCTTCCTGGAAC D-CCTGTGTAGCAATCCATTGTCTCC	New

Figure 2.2 Ectopically expressed XRel3 mRNA inhibits mesodermal marker expression.

A) qPCR detection of increasing amounts of XRel3 transcripts in XRel3 mRNA injected embryos. B-C) qPCR analysis of mesodermal markers (B) and inducers (C) assayed at stage 10 indicating reduced mesoderm formation by attenuated induction. Relative fold change was calculated using the 2-ΔΔCt method using H4 as the reference gene and uninjected embryos as normal expression. All experiments were performed three times. A representative experiment is shown in this figure.

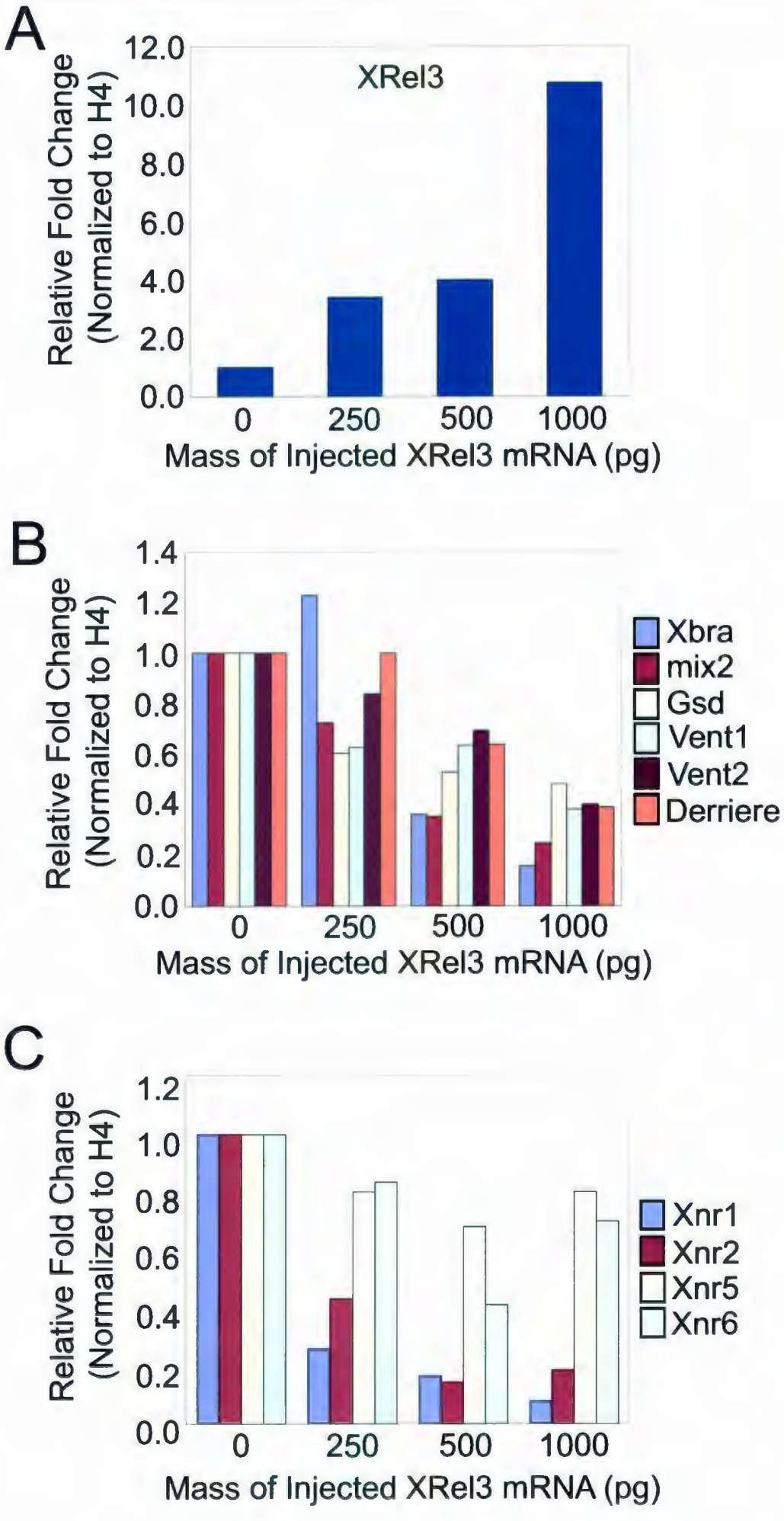
A
XRel3
Relative Fold Change (Normalized to H4)
12.0
10.0
8.0
6.0
4.0
2.0
0.0
0
250
500
1000
Mass of Injected XRel3 mRNA (pg)
B
Relative Fold Change (Normalized to H4)
1.4
1.2
1.0
0.8
0.6
0.4
0.2
0.0
Xbra
mix2
Gsd
Vent1
Vent2
Derriere
0
250
500
1000
Mass of Injected XRel3 mRNA (pg)
C
Relative Fold Change (Normalized to H4)
1.2
1.0
0.8
0.6
0.4
0.2
0.0
Xnr1
Xnr2
Xnr5
Xnr6
0
250
500
1000
Mass of Injected XRel3 mRNA (pg)

Signals emanating from the endoderm have been shown to induce the overlying ectoderm to form mesoderm, thus establishing all three germ layers. These endogenous signals are suggested to be members of the Nodal (Xnr in *Xenopus)* signaling pathway (Agius et al. 2000; Jones et al. 1995). I asked, therefore, whether ectopic *XRel3* expression could inhibit Xnr expression. As above, increasing amounts of *XRel3* mRNA were injected into the marginal zone of 2-celled embryos and cohorts of 10-12 embryos were collected at stage 10. The relative levels of 4 Xnr family members were assayed by real-time PCR. The expression of *Xnr1*, *Xnr2*, *Xnr5*, and *Xnr6* were all reduced by the overexpression of *XRel3* in a dose dependent manner (Figure. 2.2C). Injection of the highest dosage of *XRel3* mRNA (1000pg) reduced *Xnr1* and *Xnr2* by ~90% and ~80% compared to uninjected control levels, respectively (Figure 2.2C). In comparison, *Xnr5* and *Xnr6* were reduced by ~20% and ~30%, respectively (Figure 2.2C). Secondly, other findings from colleagues indicated that XRel3 specific antisense morpholinos which inhibit zygotic XRel3 expression, also expands the domain of the pan-mesodermal marker *Xbra* towards the animal pole and that co-injection of synthetic Xnr2 mRNA with XRel3 mRNA rescues normal development in a dose dependent manner (Kennedy et al. 2007). Taken together, these results suggested that XRel3 may limit the domain of mesoderm formation through negative regulation of Xnr transcription.

2.3.3 XRelA and XRel3 inhibit canonical Wnt signaling

In *Xenopus*, canonical Wnt signaling has been demonstrated to be important for mesoderm formation (Schohl and Fagotto 2003; Heasman et al. 2000) and shown to regulate the expression of *Xnr1*, *Xnr2*, *Xnr5* and *Xnr6* (Agius et al. 2000; Hashimoto-Partyka et al. 2003; Takahashi et al. 2000). As previously mentioned, injection of XRelA mRNA neutralized the induction of a second body axis in response to R85-stimulated canonical Wnt signaling (Kao and Lockwood 1996). To determine if ectopic *XRelA* or *XRel3* expression can inhibit β-catenin induced transcription I co-injected 50pg, 100pg, 250pg or 500pg of XRelA or XRel3 mRNA with 400pg of Xβ-catenin mRNA and 50pg of the pSia-Luciferase (pSia-Luc) reporter plasmid into the marginal zone at the 2 cell stage; this dosage of Xβ-catenin mRNA was empirically determined as the optimal dosage to induce formation of a supernumerary axis. pSia-Luc contains a portion of the *siamois* promoter sequence that is specifically responsive to β-catenin induced transcription, fused with the firefly *Luciferase* gene (Brannon et al. 1997; Fan et al. 1998). Substrate-specific *Luciferase* activity was measured to infer the degree to which β-catenin stimulated the expression of the reporter. Luciferase activity was measured at stage 10. Each experiment was performed 2-4 times on independent batches of embryos and assayed in triplicate.

Injection of 400pg β-catenin mRNA alone induced the levels of reporter transcription between 52-120 fold above the level of endogenous activation (Figure 2.3A-B). The co-injection of β-catenin with XRelA or XRel3 mRNA reduced the level of reporter transcription in a dose-dependent manner (Figure 2.3A-B). Injection of 50pg of

Figure 2.3 XRelA and XRel3 inhibits β-catenin induced transcriptional activation.

A) Co-injection of XRelA mRNA or B) XRel3 mRNA represses β-catenin induced transcriptional activation of the pSia-Luc reporter construct in a dose-dependent manner. C) Ectopically expressed XRelA or XRel3 inhibits endogenous activation of the pSia-Luc reporter construct. D) XRelA and E) XRel3 inhibits transcriptional stimulation by a constitutively active β-catenin mutant (Xβ-catenin^{S37A}). All transcription assays were performed 2-4 times in triplicate.

A

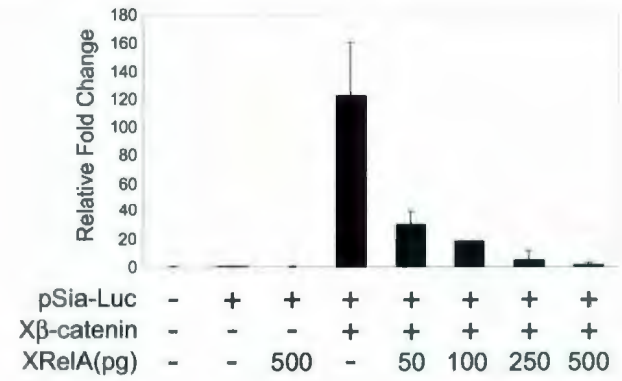
Relative Fold Change
180
160
140
120
100
80
60
40
20
0
pSia-Luc - + + + + + + +
Xβ-catenin - - - + + + + +
XRelA(pg) - - 500 - 50 100 250 500

B

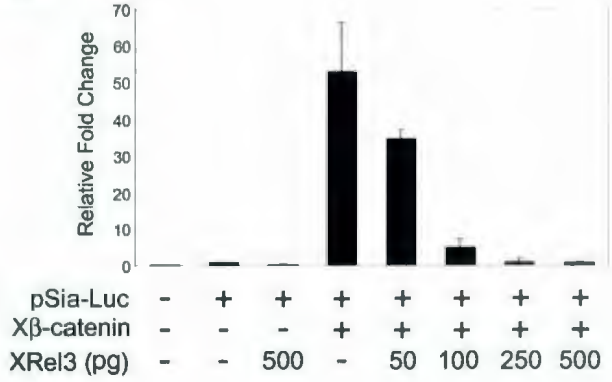
Relative Fold Change
70
60
50
40
30
20
10
0
pSia-Luc - + + + + + + +
Xβ-catenin - - - + + + + +
XRel3 (pg) - - 500 - 50 100 250 500

C

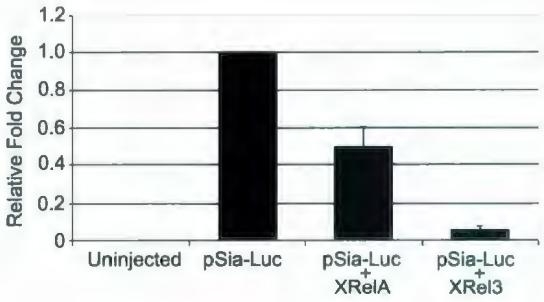
Relative Fold Change
1.2
1.0
0.8
0.6
0.4
0.2
0
Uninjected
pSia-Luc
pSia-Luc + XRelA
pSia-Luc + XRel3

D

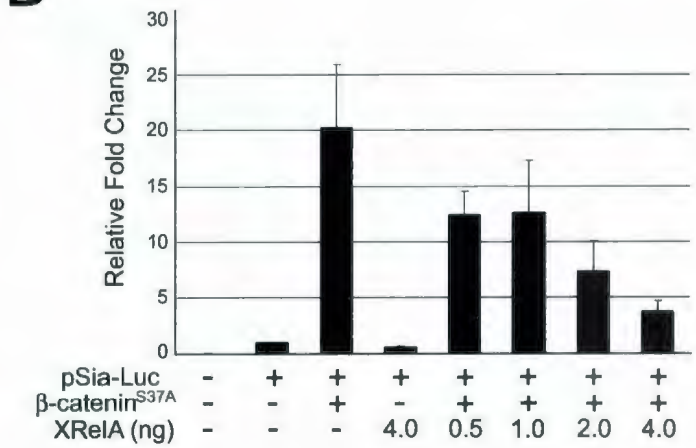
Relative Fold Change
30
25
20
15
10
5
0
pSia-Luc - + + + + + + +
β-catenin S37A - - + - + + + +
XRelA (ng) - - - 4.0 0.5 1.0 2.0 4.0

E

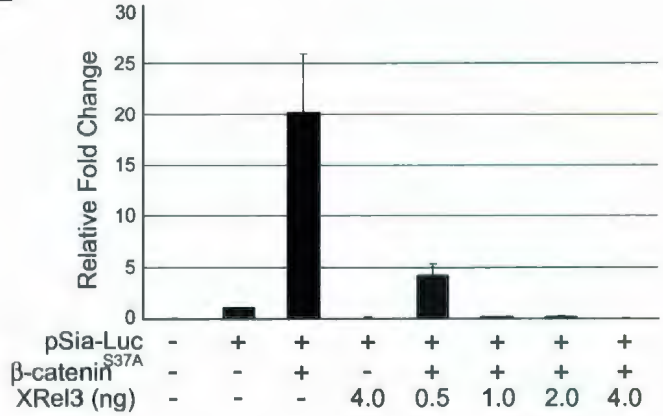
Relative Fold Change
30
25
20
15
10
5
0
pSia-Luc - + + + + + + +
β-catenin S37A - - + - + + + +
XRel3 (ng) - - - 4.0 0.5 1.0 2.0 4.0

XRelA mRNA reduced pSia-Luc reporter transcription from ~120 fold to about ~30 fold compared to endogenous activation (Figure 2.3A). At 500pg XRelA mRNA, reporter activation was reduced to approximately the same levels determined when 50pg of pSia-Luc was injected alone (Figure 2.3A). Similarly, injection of 250pg of XRel3 mRNA reduced the levels of reporter activation to endogenously activated levels (Figure 2.3B). It should also be noted that since the pSia-Luc reporter was stimulated by endogenous proteins, I co-injected 50pg of the reporter with 500pg of XRelA mRNA or 2000pg XRel3 mRNA without exogenous β-catenin. As expected, since the overexpression of either XRelA or XRel3 mRNA prevents mesoderm formation (Figure 2.2B-C; Kennedy et al. 2007), endogenous activation of the pSia-Luc reporter was also suppressed by 50% or 95%, respectively (Figure 2.3C), suggesting that both Rel/NF-κB proteins could interact with endogenous proteins to regulate/attenuate transcription.

Based on the observation that injection of XRelA mRNA could rescue normal development in embryos co-injected with R85 mRNA (Kao and Lockwood 1996), I next asked if XRelA and/or XRel3 negatively regulates β-catenin at the level of GSK3β or downstream of β-catenin stabilization. GSK3β phosphorylates serine residues 33 and 37 and Threonine 41 in the N-terminus of β-catenin, signaling the protein for ubiquitination and subsequent proteosomal destruction (Orford et al. 1997; Yost et al. 1996). Alanine substitution of either of these residues stabilizes β-catenin protein and aberrantly stimulates Wnt target gene transcription. Overexpression of the constitutively 'active' human β-catenin^{S37A} mutant, isolated from the TOV-112D, ovarian epithelial cancer cell line (Popadiuk et al. 2006), in ventral marginal cells induced the formation of a complete

secondary axis in *Xenopus* embryos (Table 2.2) and stimulated transcription from the pSia-Luc reporter plasmid (described above) ~20 fold above endogenously activated levels (Figure 2.3D-E).

To determine if XRelA/XRel3 could attenuate TCF-dependent transcription in the presence of the constitutively active β-catenin, I co-injected β-catenin^{S37A} mRNA and 50pg of pSia-Luc reporter plasmid with 0ng, 0.5ng, 1ng, 2ng or 4ng of XRelA or XRel3 mRNA into the ventral marginal region of both cells at 2 cell stage. Both XRelA and XRel3 inhibited pSia-Luc transcription induced by β-catenin^{S37A} in a dose dependent manner (Figure 2.3D-E). Interestingly XRel3 inhibited reporter activation more strongly at all equivalent XRelA dosages. These results suggested that exogenously expressed XRelA and XRel3 can inhibit β-catenin mediated transcription independently of its phosphorylation status.

Ventral expression of (wild type) β-catenin^{WT} or β-catenin^{S37A} mRNA injected into the marginal zone of 2-cell stage *Xenopus* embryos efficiently induced the formation of a complete secondary axis in 62/78 (80%) and 29/33 (88%) embryos, respectively (Table 2.2). Co-injection of 100pg or 250pg of either XRelA or XRel3 mRNA with β-catenin^{WT} mRNA completely inhibited supernumerary axis formation (Figure 2.4D-E, 2.3.5D-E, Table 2.2) and caused axis deficient phenotypes in 21-36% of injected embryos (Figure 2.4F, 2.5F and Table 2.2). Furthermore, co-injection of 500pg of XRelA or XRel3 mRNA with 2000pg β-catenin^{S37A} reduced the frequency of conjoined embryos from 29/33(88%) induced by β-catenin^{S37A} alone to 2/10(20%) and 3/12(25%),

Figure 2.4 XRelA inhibits β-catenin induced axial duplication.

A) Uninjected control embryos. B) Ventral-marginal injection of synthetic Xβ-catenin mRNA causes twinning. C) Ectopic ventral-marginal expression of XRelA mRNA does not inhibit formation of the body axis. However at dosages of 250pg, embryos did exhibit slight defects with blastopore closure, possibly due to reduced ventral mesoderm formation. D-E) Co-injection of 100pg of XRelA mRNA with Xβ-catenin into ventral-marginal regions inhibited axial duplication. F) In a few co-injected embryos, XRelA inhibited formation of ectopic and endogenous body axis formation, possibly due to off-target injection. **NB.** Black arrow heads indicate twinned embryos with duplicated heads. Scale bar is 1mm.

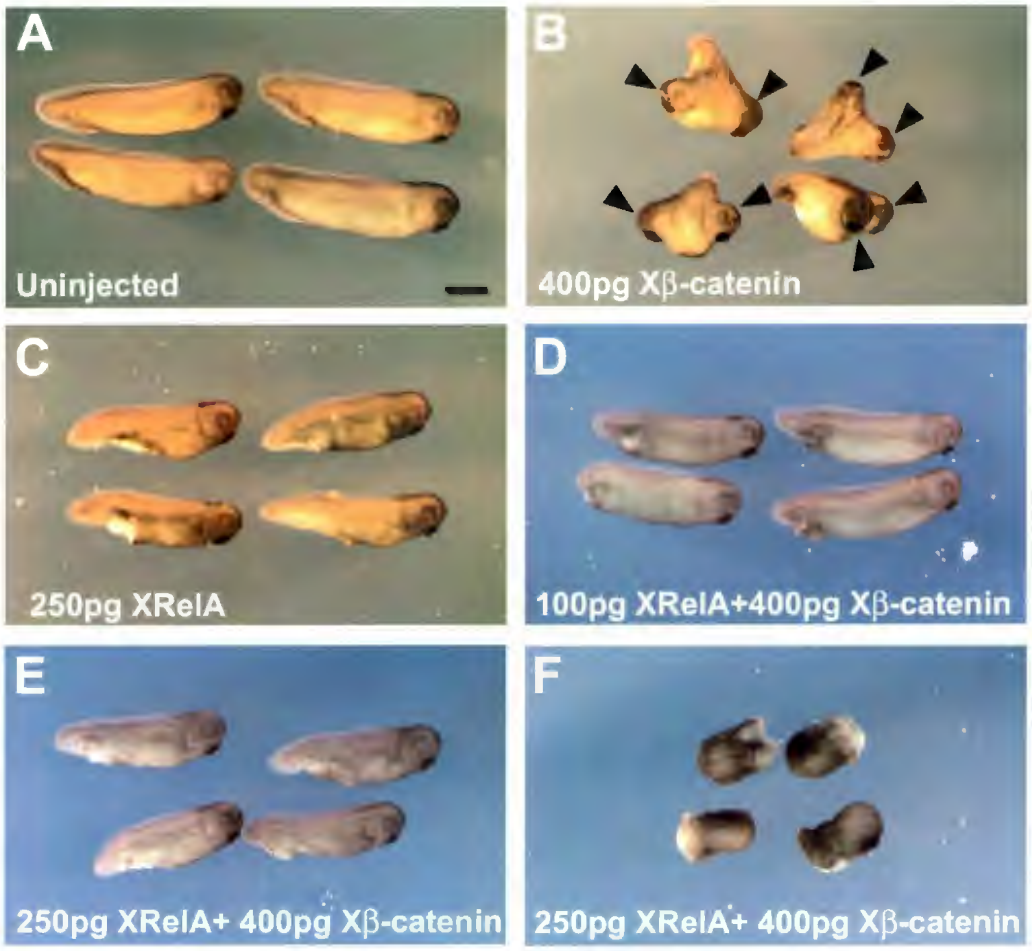
A
Uninjected
B
400pg Xβ-catenin
C
250pg XRelA
D
100pg XRelA+400pg Xβ-catenin
E
250pg XRelA+ 400pg Xβ-catenin
F
250pg XRelA+ 400pg Xβ-catenin

Figure 2.5 Co-injection of XRel3 inhibits β-catenin induced axial duplication.

A) Uninjected control embryos. B) Ventral-marginal injection of synthetic Xβ-catenin mRNA induces twinning. C) Ectopic ventral-marginal expression of XRel3 mRNA does not inhibit formation of the body axis. However at dosages of 250pg, embryos did exhibit slight defects with blastopore closure, possibly due to reduced ventral mesoderm formation. D-E) Co-injection of as little as 100pg of XRel3 mRNA with Xβ-catenin into ventral-marginal regions inhibited axial duplication. F) In some co-injected embryos, XRel3 inhibited formation of ectopic and endogenous body axis formation, possibly due to off-target injections. Black arrow heads indicate twinned embryos with duplicated heads. Scale bar is 1mm.


A
Uninjected
B
400pg Xβ-catenin
C
250pg XRel3
D
100pg XRel3 + 400pg Xβ-catenin
E
250pg XRel3 + 400pg Xβ-catenin
F
250pg XRel3 + 400pg Xβ-catenin

Table 2.2. Phenotype analysis of β-catenin co-injected with and without XRelA and XRel3 mRNA

Injected mRNA's					Scored Phenotypes (%)			
Xβ-catenin (pg)	S37A (pg)	XRel3 (pg)	XRelA (pg)	Total Number of Embryos	Single axis	Full 2° axis	Partial 2° axis	Axis Deficient
0	0	0	0	239	238 (99.5)	0 (0)	1 (0.5)	0 (0)
400	0	0	0	78	16 (20)	62(80)	0 (0)	0 (0)
0	0	250	0	39	31 (79)	0 (0)	0 (0)	8 (21)
400	0	100	0	40	30 (75)	0 (0)	0 (0)	10(25)
400	0	250	0	39	25 (64)	0 (0)	0 (0)	14(36)
0	0	0	250	40	26 (65)	0 (0)	0 (0)	14(35)
400	0	0	100	41	25 (61)	0 (0)	2 (5)	14(34)
400	0	0	250	39	26 (67)	0 (0)	0 (0)	13(33)
0	2000	0	0	33	4 (12)	29(88)	0 (0)	0 (0)
0	2000	500	0	10	8 (80)	2 (20)	0 (0)	0 (0)
0	2000	0	500	12	9 (75)	3 (25)	0 (0)	0 (0)

respectively (Table 2.2). These results confirm the ability of Rel/NF-κB to modulate β-catenin activity observed with the artificial pSia-Luc reporter.

2.3.4 XRel3 directly interacts with β-catenin, in vitro

Crosstalk between NF-κB and canonical Wnt signaling pathways has been suggested from various studies in cancer cell lines. However, diverse observations have been reported, ranging from NF-κB attenuating Wnt signaling in colon cancer cells (Cho et al. 2005), to Wnt signaling inhibiting NF-κB signaling in colon and breast cancer cells (Deng et al. 2002) to Wnt and NF-κB stimulating and regulating each other during development of hair follicle primordia (Zhang et al. 2009). Exogenously expressed RelA (p65) and NF-κB1 (p50) both interact in a complex with endogenous β-catenin protein on synthetic NF-κB-binding probes (Deng et al. 2002). Therefore, we tested the possibility that XRelA and/or XRel3 protein may interact with Xβ-catenin.

To determine whether XRelA and/or XRel3 interacted with β-catenin, I fused the β-catenin coding region with the glutathione s-transferase (GST) gene. Bacterially expressed GST-Xβ-catenin fusion protein was purified and incubated with approximately equal amounts of radiolabelled, *in vitro* translated XRelA, XRel3 or Axin protein. Axin was used as a known binding protein control in the GST-pulldown assay. Although mammalian RelA has been shown to interact with β-catenin *in vivo*, the orthologous *Xenopus* protein did not interact, *in vitro* (Figure 2.6A). However, GST-Xβ-catenin did

Figure 2.6 Identification of the *in vitro* interaction between XRel3 and Xβ-catenin.

A) GST-pulldown demonstrating that XRel3 but not XRelA interacts with Xβ-catenin. Axin was used as an *in vitro* binding control. B) XRel3 forms homodimers (XRel3-XRel3) and heterodimers with XRelA, *in vitro*. Input lanes indicate the migratory endpoint of *in vitro* translated (IVT) proteins on the denaturing gel. Lanes containing GST protein indicate the level of background/non-specific binding of IVT proteins. Bottom panel of coomassie stained gels show equal amounts of total GST-tagged proteins were used for each pulldown. This experiment was performed 5 times.

A

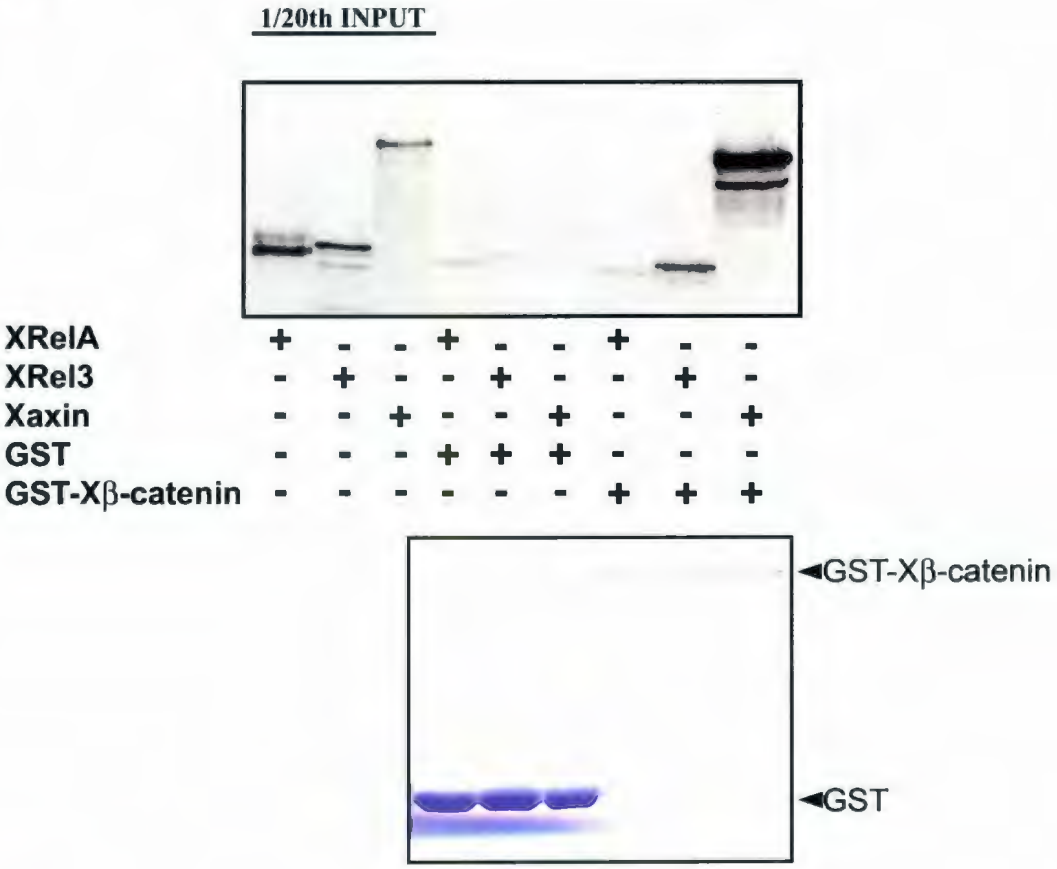
1/20th INPUT
XRelA + - - + - - + - -
XRel3 - + - - + - - + -
Xaxin - - + - - + - - +
GST - - - + + + - - -
GST-Xβ-catenin - - - - - - + + +
GST-Xβ-catenin
GST

B

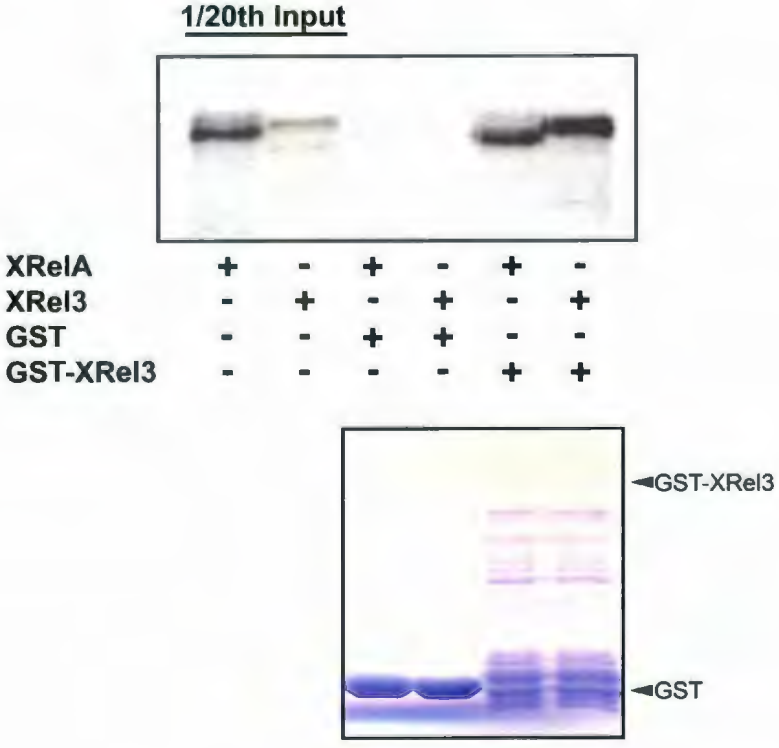
1/20th Input
XRelA + - + - + -
XRel3 - + - + - +
GST - - + + - -
GST-XRel3 - - - - + +
GST-XRel3
GST

interact with XRel3 protein, *in vitro* (Figure 2.6A) suggesting a level of specificity for Rel/NF-κB and β-catenin interactions in *Xenopus* embryos.

Rel/NF-κB proteins are known to function as homo- and hetero-dimers (Pereira and Oakley 2008). Based on the observations that exogenous expression of either XRelA or XRel3 mRNA alone can inhibit Xβ-catenin activity in embryos (Figure 2.4, 2.5 and Table 2.2) but only XRel3 directly interacts with Xβ-catenin, immediately suggested that XRelA+XRel3 heterodimers and/or XRel3 homodimers mediated the repressive effect on Wnt target gene transcription. Therefore, I determined, *in vitro*, whether such dimerization patterns were possible. Using GST-XRel3 fusion proteins, I detected the formation of both GST-XRel3+XRel3 and GST-XRel3+XRelA protein dimers (Figure 2.6B). These results indicated the existence of a mechanism whereby endogenous Xβ-catenin transcriptional activity may be suppressed by XRelA-XRel3 and XRel3-XRel3 protein complexes.

2.4 Discussion

2.4.1 Opposing Rel/NF-κB and Canonical Wnt signals regulate mesoderm formation

Rel/NF-κB and canonical Wnt signaling pathways have opposing roles in *Xenopus* mesoderm development. Various Rel/NF-κB factors have been demonstrated to antagonize FGF and TGF-β mediated mesoderm development, whereas canonical Wnt signaling directly activates transcription of FGF and TGF-β factors to promote mesoderm induction and patterning. In this chapter I have extended previously published findings (Kennedy et al. 2007) with evidence suggesting that the mechanism by which Rel/NF-κB signaling inhibits mesoderm formation is possibly through direct inhibition of β-catenin-mediated transcription (Figure 2.7).

Gain- and loss-of-function studies aimed at determining the role of XRelA and XRel3 in Xenopus development identified them as important regulators of mesoderm formation (Kao and Lockwood 1998; Kennedy et al. 2007; Zhang et al. 2006; Zhang and Klymkowsky 2009). However, the mode of action of Rel/NF-κB transcription factors is unclear. Recently, investigators reported a feedback regulatory circuit through which XRelA/XRel3 activates the expression of the mesoderm markers, twist and Snail1/2 (slug) resulting in the inhibition of Cerberus and the up-regulation of the Xnr target Smad2 (Zhang et al. 2006; Zhang and Klymkowsky 2009). These findings were inconsistent with my observations demonstrating the inhibition of mesoderm formation by ectopic XRel3 mRNA expression and expanded mesoderm formation in XRel3 depleted embryos (Kennedy et al. 2007). As well, several studies have confirmed that

Figure 2.7 Xrel3 inhibits β-catenin to restrict Xnr expression during mesoderm formation.

Left to Right: Maternal expression of *VegT*, *β-catenin* and *XRel3*. Maternal *VegT* is required to activate zygotic Xnr expression, which function as the endogenous mesoderm inducers. Maternal β-catenin activity regulates the timing and level of *Xnr* expression, primarily in dorsally fated cells. XRel3 and possibly XRelA activity, preserves the domain of ectoderm formation by inhibiting *Xnr* expression by antagonizing β-catenin-dependent transcription. Dorsal is oriented to the right.

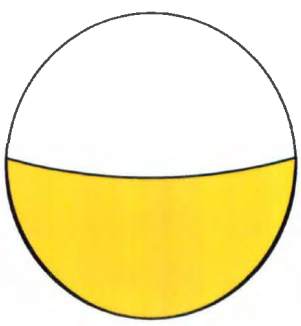

VegT/Vg1

β-catenin

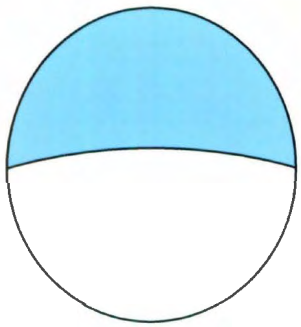

XRel3

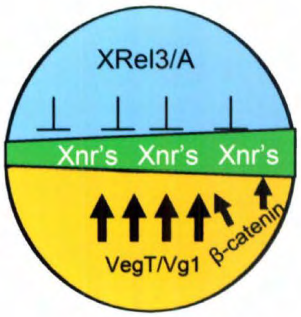

ectopically expressed XRelA mRNA perturbs dorsal axis formation and suppresses the expression of Xbra, Goosecoid, snail, twist, cardiac actin and XlhBox*1* (Kao and Lockwood 1996; Kennedy et al. 2007; Tannahill and Wardle 1995). The discrepancy between the two studies implying that XRelA/XRel3 activates mesoderm gene expression versus the many previous studies to the contrary may be related to cell-specific effects. It is possible that the studies demonstrating inhibition may be events occurring in the early embryo, in cells that are multipotent and relatively undifferentiated, whereas the study in which activation occurred may have been performed in cells from a later stage when other factors affecting RelA/Rel3 may be active.

My evidence of a molecular mechanism through which XRel3 directly interacts with Xβ-catenin is in support of a role for XRelA and XRel3 transcription factors as inhibitors of early mesoderm formation. Furthermore, since Rel/NF-κB proteins function as homo- and hetero-dimers our results suggest the formation of XRel3-XRel3 and/or XRel3-XRelA dimers may mediate β-catenin activity. The effect of XRelA on β-catenin-directed transcription suggests it is capable of associating with endogenous XRel3 or other Rel/NF-κB proteins. This hypothesis is supported by the observation in mammalian cells where RelA (p65) alone could not directly interact with β-catenin in GST-pulldown assays, but required the addition of cell lysate to promote their association (Masui et al. 2002).

Both XRelA and XRel3 are maternal factors present at fertilization and capable of regulating zygotic gene expression. Rel/NF-κB proteins are pleiotropic transcription factors whose function is cell type and context dependent. For example, in *Xenopus*,

ectopic expression of XRel3 in animal pole or vegetal pole regions induces tumor formation with concomitant epidermal and neural marker activation (Lake et al. 2001; Yang et al. 1998). However, injection of synthetic XRelA or XRel3 mRNA into the marginal zone disrupts mesoderm morphogenesis. In combination with previous results, (Kennedy et al. 2007) my observations suggest that the domain of mesoderm formation is, in part, defined by the opposing activity of Rel factors and Xnr family members.

In embryos, the highest proportion of XRelA and XRel3 transcripts were detected in equatorial explants with lower amounts detected in animal and vegetal pole explants. Since, β-catenin was reported to pattern cell autonomous Xnr expression, the local enrichment of Rel proteins possibly attenuates β-catenin-mediated transcription to regulate Xnr expression in the equatorial region. In turn, since Xnrs have been suggested to act as short-range morphogens, such a mechanism would limit the field of Xnr activity. This is further supported by the observation that morpholino mediated repression of XRel3 expression in the equatorial region expanded the domain of mesoderm formation towards the animal pole (Kennedy et al. 2007). The new mesectodermal boundary was then possibly defined only by the maximal range of VegT/Vg1 and β-catenin activated Xnr transcription.

How XRel3/XRelA inhibits the functional activity of β-catenin is unclear. One possibility that was suggested in endometrial carcinoma cell lines was the ability of RelA to sequester CBP/p300, a co-factor required for β-catenin-dependent transcription (Saegusa et al. 2007). In *Drosophila* embryos, Dl recruits Groucho, to repress transcription (Dubnicoff et al. 1997; Ratnaparkhi et al. 2006). Hence, the possibility

exists that in vertebrates Rel may also recruit Groucho/TLE homologs when bound to β-catenin to repress transcription. Since β-catenin binds to TCF/LEF proteins with higher affinity than does Groucho/TLE proteins, any cooperative mechanism of transcriptional repression likely interferes with β-catenin's association with transcriptional co-activators. A key experiment, to this end, would be to demonstrate the formation of a TCF/LEF-β-catenin-Rel-Groucho/TLE complex on target gene promoters by chromatin immunoprecipitation analysis and determine if transcriptional co-activators such as Bcl9 and Pygopus are still present.

XRelA and XRel3 transcripts and protein are expressed primarily in the animal hemisphere (Bearer 1994; Kao and Hopwood 1991; Yang et al. 1998). However, the soluble fraction of β-catenin protein is enriched from animal pole to vegetal pole on the dorsal side of the embryo (Larabell et al. 1997). Interestingly, ectopic expression of β-catenin in animal cells can induce the formation of a secondary axis, albeit at a low frequency compared to vegetal and marginal cells. However, the primary body axis does not form from animal pole cells so it is likely that negative regulators, such as Rel/NF-κB proteins, may also repress β-catenin activity in these regions thus creating a spatial boundary that defines the dorsal mesoderm territory.

Chapter 3: A Co-dependent requirement of XBcl9 and XPygo2 for embryonic body axis formation in *Xenopus*

3.1 Introduction

In the previous chapter, I demonstrated the role of the Rel/NF-κB family in regulation of the Wnt pathway, which was necessary for formation of the primary body axis. In this chapter, I will explore the role of a positive intracellular effector/regulator of the Wnt pathway.

3.1.1 Canonical Wnt mediated dorsal axis formation in Xenopus

The unfertilized radially symmetric *Xenopus* egg consists of a pigmented animal hemisphere and a yolk-laden vegetal hemisphere. The egg cortex is a thin outer layer of egg cytoplasm associated with the plasma membrane. Breaking of radial symmetry is precipitated by the fertilizing sperm, which causes the cortex to rotate with respect to the inner egg cytoplasmic mantle (Vincent et al. 1986; Vincent et al. 1987). The rotational shift displaces cortical components originally concentrated at the vegetal pole to a location opposite the sperm entry site (Weaver and Kimelman 2004; Holowacz and Elinson 1995; Rowning et al. 1997; Tao et al. 2005; Marikawa et al. 1997; Marikawa and Elinson 1999). These components activate canonical Wnt signaling in cells so that they differentiate into dorsal, anterior structures to produce an elongated body axis (Rowning et al. 1997; Tao et al. 2005; Marikawa et al. 1997; Marikawa and Elinson 1999). In the absence of the rotation, or when the Wnt pathway is inhibited, the embryo fails to develop a body plan (Vincent and Gerhart 1987).

Canonical Wnt signaling activates an elaborate network of transducers that stabilize soluble/cytoplasmic β-catenin, which then translocates to the nucleus. In the nucleus, β-catenin is assembled into a transcriptional activation complex that promotes expression of genes required for axis development (Cadigan 2008; Huang and He 2008). The essential components of the transcriptional activation complex includes the adapter protein Pygopus (Pygo) (Hoffmans et al. 2005; Kramps et al. 2002; Thompson et al. 2002; Belenkaya et al. 2002; Hoffmans and Basler 2004; Vincent and Gerhart 1987). Pygo links the basal transcription machinery to β-catenin (Carrera et al. 2008), by its association with legless (Lgs).

Structurally, Pygo is composed of an N-terminal NHD motif with transactivating potential connected to a C-terminal plant homeodomain (PHD), also known as a Leukemia associated protein (LAP) domain, by a proline-rich linker region (Kramps et al. 2002; Thompson et al. 2002). In flies, Lgs is a 1464 amino acid protein with no commonly conserved structural motifs. However, the Lgs N-terminus does contain 3 stretches of ~30 amino acids, referred to as homology domains (HD), and are numbered sequentially from HD1 to HD3 (Kramps et al. 2002). The HD1 interacts with the PHD of Pygo and the HD2 with armadillo repeat 1 of fly β-catenin (Arm) (Hoffmans and Basler 2004; Kramps et al. 2002; Thompson et al. 2002; Sampietro et al. 2006; Townsley et al. 2004a). Both *lgs* and *Pygo* were considered to be essential for the fly *wingless* (wg/Wnt) pathway because mutant alleles of both genes phenocopied *wg* and *arm* mutants (Kramps et al. 2002; Thompson 2004). Furthermore, development of *lgs* mutants could not be

rescued by constitutively active Arm protein indicating that it was critically dependent on Lgs for activity (Kramps et al. 2002).

A variety of studies have demonstrated that Pygo is necessary for vertebrate development. In Xenopus, antisense depletion of maternal Pygo resulted in inhibition of body axis development similar to that caused by β-catenin depletion (Belenkaya et al. 2002; Heasman et al. 2000) while zygotic depletion of Pygo using antisense morpholinos caused defects in head and eye development (Lake and Kao 2003b). Surprisingly, restoration of expression of a variety of head-specific genes in these Pygo-deficient embryos was achieved by expression of Pygo proteins that lacked the ability to participate in Wnt-dependent transcription (Lake and Kao 2003b). In mouse, targeted deletion of *mpygo2* resulted in a variety of developmental defects, most of which were related to canonical Wnt signaling, but also for non-Wnt function, such as lens development (Jonckheere et al. 2008; Li et al. 2007; Song et al. 2007). These studies suggested that Pygo has functions required for development in vertebrates that are broader than those dependent on, or dedicated to canonical Wnt signaling.

Because of its apparent multifunctional roles, an important question that we ask is: what regulates the participation in vertebrate development of Pygo in canonical Wnt cellular functions? In this study, we have addressed this question by examining legless/Bcl9, a Pygo binding protein, in *Xenopus* development. We report the identification and biochemical characterization of the *Xenopus* orthologue of Bcl9 (XBcl9), its embryonic expression patterns and its dorsalizing activity in early embryos. In particular, our data indicate that XBcl9 protein accumulates initially in the dorsal side

of the marginal zone of early blastula stage embryos and we provide evidence of a co-dependency of XBcl9 and XPygo2 on nuclear localization, which is required to promote dorsal gene expression and axis formation. Furthermore, we provide evidence of the requirement of maternal XBcl9 for body axis formation.

3.2 Materials and Methods

3.2.1 In silico identification of XBcl9

A *Xenopus laevis* I.M.A.G.E. clone, Accession Number BC070813, with homology to mammalian Bcl9 protein sequences was identified by *in silico* analysis (http://blast.ncbi.nlm.nih.gov/Blast.cgi).

3.2.2 Plasmids and RNA synthesis

XBcl9 coding region cDNA was PCR amplified from stage 1 *Xenopus* cDNA, and cloned into pCS2+ ClaI and XhoI restriction sites (forward primer: 5'-CGATCGAT**ATG**CTGGAGCTGCAGGAGG-3'; reverse primer: 5'-CGCTCGAGGCAGCTTAAAACATCATGTTCCCG-3'; Annealing temperature 60°C). All XBcl9 primers were based on the BC070813 sequence (Restriction sites are underlined).

pCS2+/EGFP and pCS2+/mRFP expression plasmids were constructed by PCR amplification of coding regions (lacking stop codons) and inserted after restriction digestion into BamHI/ClaI sites in pCS2+. pEGFP-C2 and pcDNA/mRFP (Addgene) were used as templates for mRFP and EGFP DNA. EGFP and/or mRFP tagged constructs were then made by PCR amplification of XBcl9 or Xβ-catenin coding regions from embryonic cDNA and inserted after restriction digestion, downstream of the fluorescent tags (Cla1/XhoI restriction sites). The pCS2+/XTcf3 expression plasmid was constructed by PCR amplification of XTcf3 coding region from embryonic cDNA and after

restriction digestion, inserted into pCS2+ (XhoI/XbaI restrictions sites). pCS2+/XPygo2α/β was previously described (Lake and Kao 2003b). pCS2+/XPygo2β was used as template to PCR clone the XPygo2β coding region into pCS3+MT (EcoRI/XhoI restriction sites) containing an N-terminal Myc tag. GST tagged XBcl9(HD1-3), XPygo2β and Xβ-catenin coding regions were also PCR cloned, restriction digested and inserted into pGEX4T-1: XBcl9(HD1-3) and XPygo2β using EcoRI/Xho1 sites and Xβ-catenin using BamHI/EcoRI sites. XBcl9^{H417A,R418A} and Xβ-catenin^{D164A} or Xβ-catenin^{D162A,D164A} point mutations were made by Quick Change Site-Directed Mutagenesis (Stratagene). XBcl9^{H417A,R418A} primers (5-CTTTCTCAAGAGCA ACTGGAGGCCGCAGAACGCTCTTTGCAAACCCT-3 and the reverse compliment), Xβ-catenin^{D164A} primers (5-CTGCTTAATGAC GAGGCCCAGGTTGTAGTTAAC-3 and the reverse compliment) and Xβ-catenin^{D162A,D164A} primers (5-CTGCTTAATGACG AGGCCCAGGTTGTAGTTAAC-3 and the reverse compliment) were all PAGE purified (IDT DNA). pCS2+MT-XAxin was a kind gift from Dr. Peter Klein and pYX-Asc/mBcl9-2 was purchased from Open Biosystems.

In vitro transcription of all RNAs used in this paper was performed using Sp6 mMessage mMachine RNA synthesis kit, as per manufacturer's protocol (Ambion).

3.2.3 Embryo collection and manipulation

Wild type embryos were obtained from female *Xenopus laevis* using standard techniques as described (Kao and Lockwood 1996), maintained in 1/20 Normal

Amphibian Medium (NAM) and staged according to Nieuwkoop and Faber (1994). Embryos were tilted and immobilized in wells of an agarose coated Petri dish in 4% Ficoll in 1/2xNAM until completion of first cell division to establish the position of the dorsal-ventral axis. Animal caps were excised from blastula stage embryos as described (Kennedy et al. 2007), cultured for 1 hour in 50% NAM and fixed in MEMFA for 30' at room temperature and dehydrated and stored in 100% Methanol at -20°C until needed. Dorsoanterior development was semi-quantitatively measured using the DAI scale (Kao and Elinson, 1988). Both the median and average DAI are reported to better represent the central tendency since the average may not properly reflect the data if the distribution of the data values are skewed.

3.2.4 Host-transfer

Maternal XBcl9 mRNA was depleted from stage VI oocytes as described (Mir and Heasman 2008) using phosphothioated antisense oligonucleotides (IDT DNA). XBcl9 antisense: 5' G*G*G*TCACGATACAGCAGTGCTC*A*T*C 3' (asterisk indicates phosphothioate bonds). Stage VI oocytes were manually defolliculated and maintained in oocyte culture medium (OCM) (Leibovitz medium (L-15) supplemented with L-glutamine, Penicillin/Streptomycin and 0.4% bovine serum albumin (BSA), pH 7.6-7.8). Antisense injected oocytes were cultured for 2 days prior to progesterone-induced maturation. Oocytes were stained with vital dyes (Neutral Red, Nile Blue B, and Bismarck Brown) prior to transfer into the body cavity of a laying female to distinguish them from host eggs.

3.2.5 RNA Analysis: Northern Blotting and qPCR

Total RNA was extracted from staged embryos using the Nucleospin RNA II Kit (Clontech Laboratories, Inc.) and analyzed by northern blotting essentially as described (Kao and Hopwood 1991). Probes were generated by PCR amplification of a fragment of Histone 4 (Lake and Kao 2003b) or *XBcl9* coding region (485-1019bp). XBcl9 primers: forward - 5' ATGCATTCCAGTAACCCCAAAGTG '3; reverse - 5' AGTAGAGAAGA CATACACCACTT '3). PCR products were gel purified (Ultrafree-DA, Millipore Corp.) and end-labeled (Prime-a-Gene, Promega) with ^{32}P-γ (Perkin-Elmer). Radiolabelled probes were hybridized at 58-60°C and visualized by autoradiography.

qPCR analysis on total RNA extracted from stage 10 embryos injected with XBcl9 and/or XPygo2β was performed as described (Kennedy et al. 2007). Isolation of total RNA from oocytes and embryos from the host transfer experiment was performed as described (Tao et al. 2005). First strand cDNA synthesis was performed using M-MLV Reverse Transcriptase as per manufacturers protocol (Invitrogen). Synthetic cDNA was diluted 1:10 and 2ul was used per qPCR reaction. Relative gene expression was analyzed by SYBR Green (Applied Biosystems) incorporation detected using the ABI Prism 7000 Detection System (Applied Biosystems). Results were analyzed using the comparative Ct method (*i.e.* $2^{-\Delta\Delta Ct}$) (Livak and Schmittgen 2001; Schmittgen and Livak 2008). Relative levels were normalized to ornithine decarboxylase (ODC) levels. All qPCR primer sequences are listed in Table 3.2.

3.2.6 Co-immunoprecipitation and Western Blotting

Co-immunoprecipitation (Co-IP) was performed by injecting 40-50 embryos with *in vitro* synthesized RNA at the 2-cell stage. Total protein was extracted by homogenization in 1XTm (10mM Tris (pH 7.5), 1% Triton-X 100, 10 mM EDTA, 0.02% NaN_3) with protease inhibitors, and incubated on ice, 30min. Homogenate was then passed through a 1cc syringe 8-10 times and centrifuged at ~ 14000 rpm at 4°C, 10 minutes to pellet cellular debris. Equal amount of total protein lysate (as determined by Bradford Assay, BioRad) was used for each IP. Final volumes were equalized with 1XTm. Anti-GFP (Abcam) (dilution 1:250) was used for IP at 4°C rotating overnight. Protein A beads (GE Healthcare) were pre-washed with IP buffer and 30ul of 50% bead slurry was added to each IP for 1hr at 4°C, with rotation. Beads were washed 4 times with 1xTm and twice with 1XPBS (pH 7.5). Co-IP'd proteins were analyzed by Western blotting as described below. Antibodies used and dilutions: anti-Myc (dilution 1:2000) (9E10, Developmental Studies Hybridoma Bank), anti-GFP (dilution 1:3000) and anti-RFP (1:1000) (Abcam), anti-β-tubulin (dilution 1:3000) (Developmental Studies Hybridoma Bank).

Bcl9 antiserum was generated by injection of GST fused human Bcl9 fragment (amino acids 697- 1294) into New Zealand White rabbits. Cross-reacting antiserum was affinity purified by passing whole antiserum 5 times over GST protein covalently linked to Glutathione Sepharose 4B beads (GE Healthcare) packed into protein purification columns (Econo-Column, BioRad) using a peristaltic pump (2232 Microperplex S, LKB Bromma). Flow-through was then passed 5 times through a second column packed with

beads covalently cross-linked to GST-XBcl9 using peristalsis. XBcl9 specific antibodies were eluted from the beads using Glycine-HCl (pH 2.0). The pH was neutralized using 2M Tris, pH8. Buffer exchange using 1XTBS (25mM Tris, pH 7.5; 150mM NaCl) was then performed by successive dilution-concentration cycles using Amicon Ultra-15 tubes (Millipore). Ten percent glycerol was added to final concentrated XBcl9 antibody fraction. XBcl9 Membranes were probed using affinity purified XBcl9 antiserum (dilution 1:750), β-tubulin antibody (Developmental Studies Hybridoma Bank,) (dilution 1:3000), β-catenin (monoclonal) antibody (Santa Cruz) (1:1000 dilution) and GSK3β (Cell Signal) (1:500 dilution). HRP-conjugated secondary antibodies (Amersham) were detected using the ECL-Plus and ECL (GE Healthcare) western detection systems, respectively.

3.2.7 GST Pulldowns

GST-pulldowns were performed as per manufacturer's protocol. GST-fusion protein was expressed in BL 21 RP competent cells, extracted and purified using Glutathione Sepharose 4B beads (GE Healthcare). Approximately 1 μg of total GST fusion protein was used in each reaction. Approximately 2μl XPygo2α/β, 5μl Xβ-catenin, 3μl XTcf3, 1μl XAxin, and 1μl XBcl9 (wildtype) or XBcl9^{H417A,R418A} *in vitro* translated, radiolabelled proteins, made in cell-free rabbit reticulolysate (Promega) as per manufacturer's protocol, were used per GST-pulldown. Gels were stained in Coomassie

for 1hour at and destained overnight (74%H_20, 6% Glacial Acetic Acid, 20% Methanol) at room temperature.

3.2.8 Immunofluorescent Staining and Imaging

Stored embryos/animal caps fixed in MEMFA/MeOH were re-hydrated in a graded methanol series and blocked in PBT (1XPBS, 2mg/ml BSA, 0.2% TritonX-100) for at least 1 hour at room temperature. Samples were then incubated in primary antibody diluted in PBT overnight at 4°C; whole Bcl9 antiserum (and pre-immune serum controls) was used at 1:350 dilution and anti Myc (Developmental Studies Hybridoma Bank) at 1:250 dilution. Embryos were washed 5x20' in PBT with agitation, and incubated 1.5-2 hours with fluorescently labeled secondary antibody diluted 1:250 in PBT at room temperature (secondary antibodies: anti-Rabbit-FITC, BD Biosciences; anti-mouse-Cy5, Cedarlane), followed by washing 5x20' in PBT. Nuclei were stained using DAPI (4'-6-Diamidino-2-phenylindole, diluted to 200ng/ml). Stained embryos/animal caps were mounted in 10% Glycerol/1XPBS and visualized using Confocal Laser Scanning Microscopy (Olympus) and Fluoview software. Pre-immune controls were visualized using the same PMT settings as well as the same thickness and number of optical sections scanned. EGFP fluorescence was detected without antibody staining.

3.3 Results

3.3.1 Identification of XBcl9, the Xenopus orthologue of Lgs/Bcl-9

A candidate Xenopus orthologue of *lgs/Bcl9* with accession number BC070813 (Klein et al. 2002), was identified by 'Blast'ing (www.pubmed.com) known fly, mouse and human Lgs/Bcl9 cDNA and protein sequences against all Genbank *Xenopus laevis* sequences. BC070813 has 2 tandemly arranged opening reading frames (ORFs); a 2586bp N-terminal ORF and a 1893bp C-terminal ORF. Conceptual translation of the N-terminal ORF predicted a protein with significant similarity (66%) to the N-terminal half of fly, mouse and human Lgs/Bcl9. The second ORF predicted a protein containing sequences that had significant similarity (78%) with vertebrate Bcl9 sequences only. These two out-of-frame ORFs are separated by a single nucleotide, which may likely have been introduced during cloning of BC070813, but this does not strictly rule out the possibility of BC070813 representing an expressed pseudo allele of a Xenopus *lgs/Bcl9* orthologue. I therefore PCR amplified a single cDNA clone, named XBC01, with an uninterrupted ORF spanning both BC070813 ORFs from cDNA of stage 1 (Nieuwkoop and Faber) embryos that when translated *in vitro*, produced a single protein of approximately 160-170 kD (Figure 3.2A).

The XBC01 cDNA (NCBI accession no. GQ891057) encoded a predicted 1473 amino acid protein similar to Lgs/Bcl9 (theoretical mass ~156kDa), with 65 amino acid residues at the N-terminus not found in other Lgs/Bcl9 sequences. The predicted protein has the 6 domains conserved in the Bcl9 family (HD1 to HD6) (Katoh and Katoh 2003).

Figure 3.1 Identification of the Xenopus Bcl9 orthologue.

A) Alignment of the evolutionarily conserved homology domains (HD1-3) of XBcl9 with other selected Lgs/Bcl9 family members. Identical residues are shaded. B) Phylogram based on the amino acid sequences of all known and predicted Bcl9 and Bcl9-2 proteins available from NCBI with accession numbers for each protein included in parentheses. The percent identity of full length XBcl9 amino acid sequences with selected orthologous Bcl9 proteins.

A

HD1:

dLgs	318	I	F	V	F	S	T	Q	L	A	N	K	G	A	E	S	V	L	S	G	Q	F	Q	T	I	I	A	Y	H
hBcl9	177	V	Y	V	F	S	T	E	M	A	N	K	A	A	E	A	V	L	K	G	Q	V	E	T	I	V	S	F	H
XBcl9	238	V	Y	V	F	S	T	E	M	A	N	K	A	A	E	A	V	L	K	G	Q	A	E	S	I	V	L	F	H
hBcl9-2	235	V	Y	V	F	T	T	H	L	A	N	T	A	A	E	A	V	L	Q	G	R	A	D	S	I	L	A	Y	H

HD2:

dLgs	515	E	N	L	T	P	Q	Q	R	Q	H	R	E	E	Q	L	A	K	I	K	K	M	N	Q	F	L	F	P	E
hBcl9	349	D	G	L	S	Q	E	Q	L	E	H	R	E	R	S	L	Q	T	L	R	D	I	Q	R	M	L	F	P	D
XBcl9	408	D	G	L	S	Q	E	Q	L	E	H	R	E	R	S	L	Q	T	L	R	D	I	Q	R	M	L	F	P	D
hBcl9-2	392	E	G	L	S	K	E	Q	L	E	H	R	E	R	S	L	Q	T	L	R	D	I	E	R	L	L	L	R	S

HD3:

dLgs	706	Q	M	E	W	S	K	I	Q	H	Q	F	F	E	E	R
hBcl9	469	Q	I	A	W	L	K	L	Q	Q	E	F	Y	E	E	K
XBcl9	528	Q	V	A	W	L	K	M	Q	Q	E	F	Y	E	E	K
hBcl9-2	512	Q	V	A	W	R	K	L	Q	E	E	Y	Y	E	E	K

B

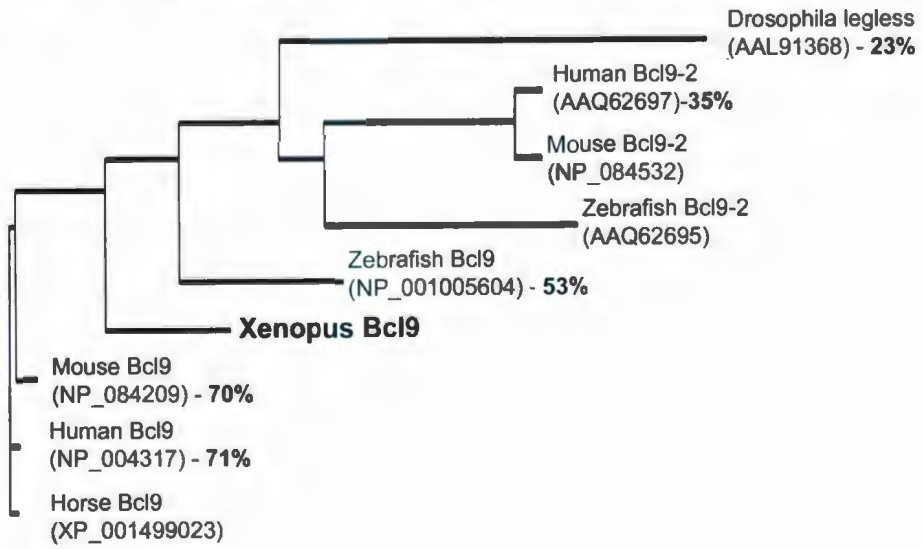

HD1-3 are present in the N-terminal half (Figure 3.1A) and HD4-6 in the C-terminal half (data not shown). Phylogenetic analysis (ClustalW2) of the protein sequences of all known and predicted Bcl9 and Bcl9-2 proteins suggests that XBC01 encodes either XBcl9 or XBcl9-2 (Figure 3.1B). Based on protein sequence, however, XBC01 predicts a protein more closely related to Bcl9 than Bcl9-2. It is ~70-71% identical to murine and human Bcl9 as compared to Bcl9-2, which has ~35% identity with the predicted XBC01 protein but is only ~23% identical to *Drosophila* Lgs (Figure 3.1B), where only HD1-3 is conserved. Because it is most similar to the mammalian Bcl9 proteins, I have named the gene encoding this predicted protein, *XBcl9*.

3.3.2 Biochemical characterization of XBcl9

XBcl9 encodes a protein with biochemical characteristics indicative of its role as a Lgs/Bcl9 orthologue. In *Drosophila*, Lgs/Bcl9 interacts directly with Pygo2 via the HD1 domain and β-catenin via the HD2 domain to mediate transcriptional activation of Wnt reporter constructs and target genes (Parker et al. 2008; Parker et al. 2002; Thompson et al. 2002). Consistent with these previous observations, *in vitro* GST-Pulldown assays demonstrated that XBcl9 interacts with Xβ-catenin and both isoforms of XPygo2. The *in vitro* GST-XBcl9-Xβ-catenin interaction was specific but weaker than the interaction between GST-XBcl9 and XPygo2α/β (Figure 3.2B).

Mutation of the aspartate residues at positions 162 or 164, within armadillo repeat 1 of β-catenin to alanines was sufficient to reduce the transcriptional activity of β-catenin

Figure 3.2 Identification and biochemical characterization of XBcl9 protein by GST pulldown analysis.

A) *In vitro* translated, radiolabelled proteins from BC070813, XBcl9 (HD1-3) (*i.e.* the N-terminal ORF from BC070813) and full length embryonically derived XBcl9 cDNAs B) XBcl9 (HD1-3) interacts with both isoforms of XPygopus2 (XPygo2) and Xβ-catenin. C) Residues D162 and D164 of Xβ-catenin mediate its interaction with XBcl9, *in vitro*. XAxin and XTcf3 were used as known binding protein controls to show specificity of the point mutations. D) GST-pulldown demonstrating residues H417 and R418 of XBcl9 specifically disrupt its interaction with Xβ-catenin without affecting its ability to bind XPygo2, *in vitro*. **NB.** Bottom panel of Coomassie stained GST proteins shows equal amounts of proteins were used for each pulldown.

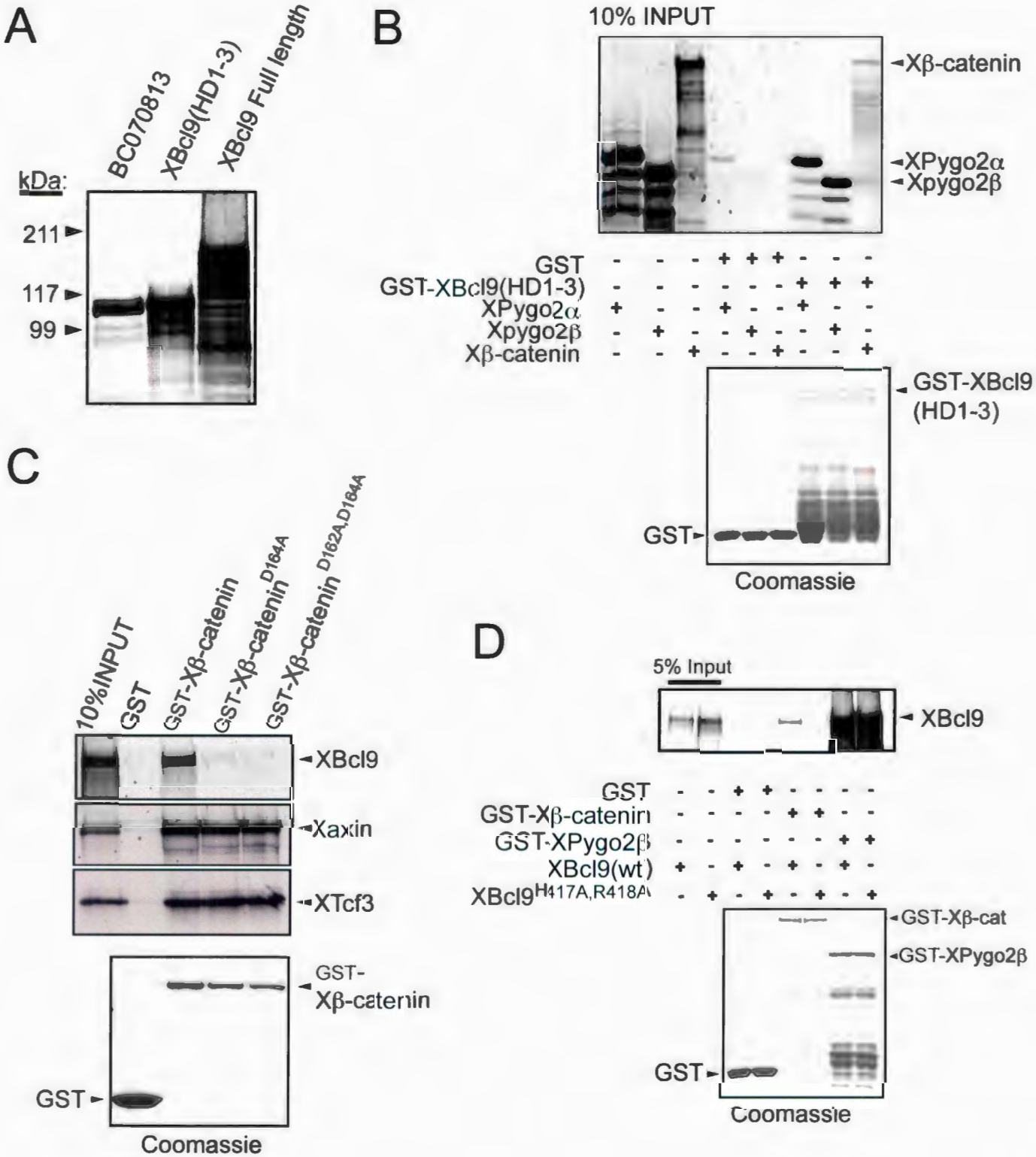
A
BC070813
XBcl9(HD1-3)
XBcl9 Full length
kDa:
211
117
99
B
10% INPUT
Xβ-catenin
XPygo2α
Xpygo2β
GST
GST-XBcl9(HD1-3)
XPygo2α
Xpygo2β
Xβ-catenin
GST-XBcl9 (HD1-3)
GST
Coomassie
C
10%INPUT
GST
GST-Xβ-catenin
GST-Xβ-catenin D164A
GST-Xβ-catenin D162A,D164A
XBcl9
Xaxin
XTcf3
GST-Xβ-catenin
GST
Coomassie
D
5% Input
XBcl9
GST
GST-Xβ-catenin
GST-XPygo2β
XBcl9(wt)
XBcl9 H417A,R418A
GST-Xβ-cat
GST-XPygo2β
GST
Coomassie

(Hoffmans and Basler 2004). Subsequent analysis of the crystal structure of the HD2–β-catenin-Tcf4 complex confirmed that Bcl9 interacts with the so-called 'acidic knob' centered at D162 and D164 of β-catenin while residues H417 and R418 of Bcl9 were important for its interaction with β-catenin (Sampietro et al. 2006). I therefore generated two mutant forms of Xβ-catenin, one in which D164 was altered to an alanine (Xβ-catenin^{D164A}) and one in which both D162 and D164 were altered to alanines (Xβ-catenin^{D162A,D164A}) (Figure 3.2C). Similarly, H417 and R418 of the HD2 of XBcl9 were both mutated (Figure 3.2D) to alanines to generate XBcl9$^{H417A, R418A}$. These mutant proteins were then used to determine if the indicated residues were important for interaction of their respective proteins in *Xenopus*.

Mutation of the above mentioned residues in Xβ-catenin significantly reduced but did not completely eliminate its ability to interact with XBcl9, *in vitro* (Fig. 2C) as compared to wild-type Xβ-catenin. Both, however, were able to interact with XAxin or XTcf3 (Figure 3.2C). Likewise, XBcl9^{H417A,R418A} interacted strongly with GST-XPygo2β but not with GST-Xβ-catenin (Figure 3.2D). These data indicated that the predicted protein interactions of XBcl9, and the critical residues associated with those interactions, are conserved between *Xenopus* and other species.

3.3.3 Xβ-catenin^{D162A,D164A} inefficiently rescues Xβ-catenin depleted embryos

The interaction between Xβ-catenin and XBcl9 is also required to promote axis formation. The Dorsoanterior index (DAI) scale was used to quantitatively measure dorsal axis formation. DAI = 5 represents normal phenotype; DAI > 5 is dorsalized; DAI

Table 3.1 Xβ-catenin^{D162A,D164A} inefficiently rescues body plan formation as compared to wild type Xβ-catenin.

Sample	DAI 1	2	3	4	5	6-10	n	Ave DAI	Median DAI
Uninjected			2	1	84	1 (DAI 8)	88	4.98	5
Xβ-cat MO	43	6	13	9			71	0.83	0
Xβ-cat MO +200pg D162A,D164A	11	3	3	4	1		22	1.27	0.5
Xβ-cat MO +400pg D162A,D164A	33	5	16	8	3		65	1.12	0
Xβ-cat MO +800pg D162A,D164A	5	2	10	2	21	3	43	2.95	4
Xβ-cat MO +200pg WT	14	1	8	10	4	1	38	1.79	2
Xβ-cat MO +400pg WT	5	5	15	10	10	10	55	2.82	3
Xβ-cat MO +800pg WT	2	1	10	11	17	8	49	3.31	4

< 5 is ventralized (Kao and Elinson 1988). As previously shown (Heasman et al. 2000), antisense morpholinos complementary to Xβ-catenin caused complete elimination of the body axis when injected into 2-celled embryos resulting in an average DAI score of 0.83 (n=71) (Table 3.1). As expected, wildtype Xβ-catenin mRNA rescued axis development in a dose-dependent manner raising the average DAI to 1.79 at 200pg and 2.82 at 400pg (Figure 3.3D, F, H; Table 3.1). Xβ-catenin^{D162A,D164A} mRNA, however, was less effective at rescuing axis development (Figure 3.3C, E; Table 3.1) raising the average DAI to 1.27 at 200pg and 1.12 at 400pg.

At 800 pg dosage, both the wild-type and mutant Xβ-catenin mRNAs rescued development to an equivalent amount suggesting that XBcl9 can still weakly interact with Xβ-catenin^{D62A,D164A} as indicated in Figure 3.2C with mutant Xβ-catenin. Alternatively, these mutant Xβ-catenin proteins may act in an alternate manner by displacing endogenous wildtype Xβ-catenin from the plasma membrane similar to "localization" mutants described previously in Xenopus (Miller and Moon 1997) and as suggested for a Lgs binding defective armadillo (arm$^{S10\text{-}D164A}$) mutant of Drosophila (Hoffmans and Basler 2004).

3.3.4 XBcl9 mRNA and Protein Expression

The embryonic expression of *XBcl9* is consistent with a potential role for this gene in axial patterning. Northern blot analysis of total RNA extracted from staged embryos (Nieuwkoop and Faber, 1994) detected a single, ~5.4kb band at all stages

Figure 3.3 Mutations of residues required for Xβ-catenin to interact with XBcl9 reduce its ability to rescue Xβ-catenin-depleted embryos.

A) Uninjected control embryos. B) 15ng Xβ-catenin morpholino (MO) was injected into the dorsal-vegetal region of 2 cell stage embryos to inhibit dorsal axis formation. Increasing amounts of either wild-type (WT) Xβ-catenin (Fig 3D, F, H) mRNA or Xβ-catenin^{D162A,D164A} mutant mRNA (Fig 3C, E, G) were co-injected with Xβ-catenin MO to rescue morphant phenotypes.

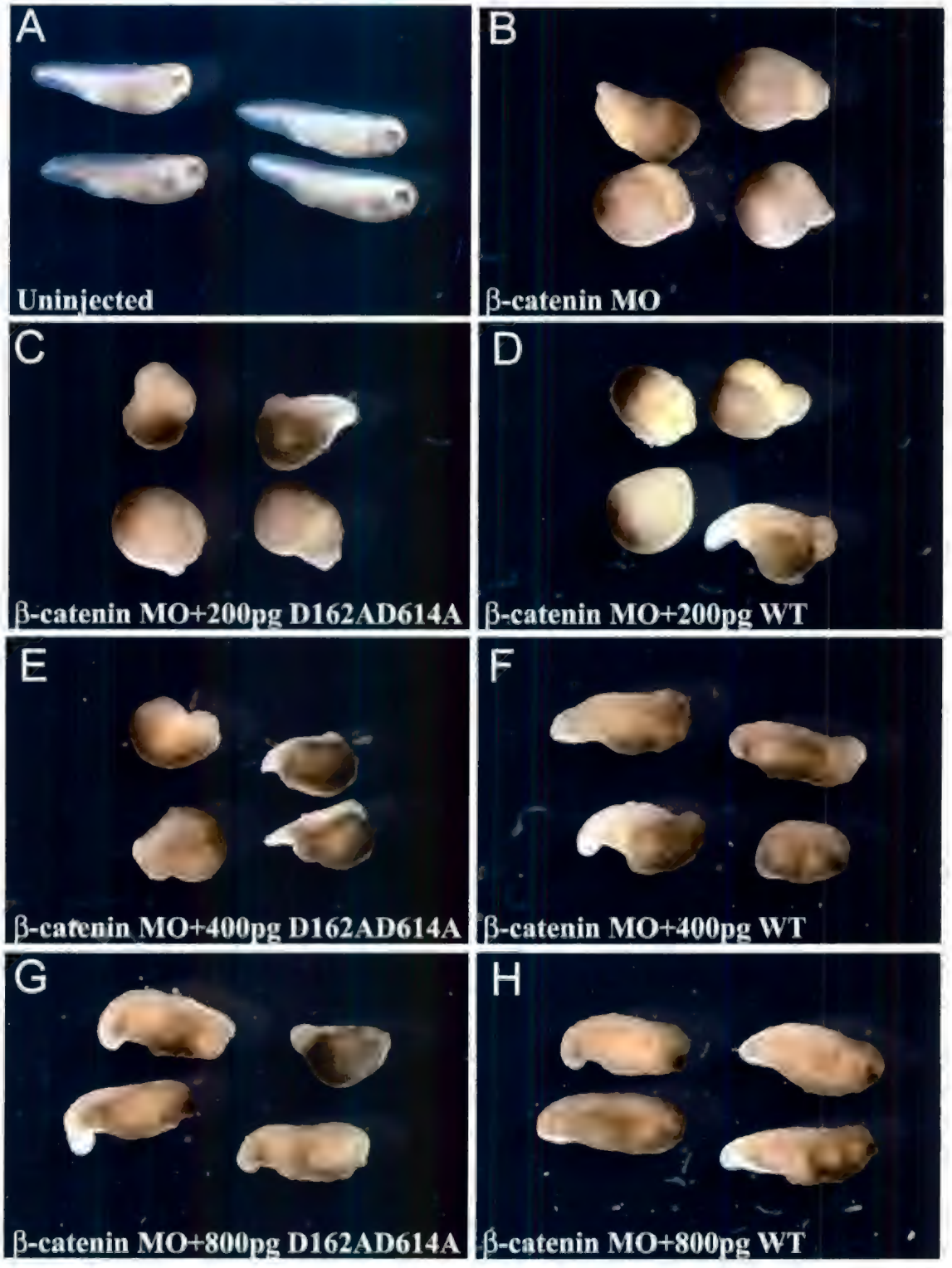
A
Uninjected
B
β-catenin MO
C
β-catenin MO+200pg D162AD614A
D
β-catenin MO+200pg WT
E
β-catenin MO+400pg D162AD614A
F
β-catenin MO+400pg WT
G
β-catenin MO+800pg D162AD614A
H
β-catenin MO+800pg WT

corresponding to the XBcl9 transcript. The highest levels of XBcl9 mRNA were present during cleavage and blastula stages (NF stages 1-8). By gastrulation (Stage 10) XBcl9 mRNA decreased to very low but detectable levels that persisted throughout embryonic development (Figure 3.5A). These XBcl9 levels mirrored the temporal expression pattern of XPygo2β (Lake and Kao 2003b). Western blotting using affinity purified polyclonal rabbit antiserum (Figure 3.4) to detect XBcl9 protein extracted from staged embryos indicated that in early development, XBcl9 was expressed in a reciprocal pattern to that of its mRNA. Protein expression was at low levels throughout cleavage and blastula stages but plateaued at St.10 until early tailbud stages after which it became undetectable (Figure 3.5B).

3.3.5 Subcellular XBcl9 expression and XBcl9 levels correlate with dorsal development

The marked increase in XBcl9 expression in embryos between St.8 and St.10 was mainly attributed to accumulation of protein in their marginal zones observed at St.9 (Figure 3.5C). Since Bcl9 is a predominantly nuclear protein required for Wnt target gene transcription (Krieghoff et al. 2006; Thompson et al. 2002; Thompson 2004; Townsley et al. 2004a), and both known XBcl9 binding proteins, Xβ-catenin and XPygo2, are required for dorsal axis formation (Heasman *et al.*, 2000; Belenkaya *et al.*, 2002), we

Figure 3.4 Generation and affinity purification of XBcl9 antiserum.

A) Immunoprecipitation (IP) of radiolabelled, *in vitro* translated XBcl9 using hBcl9 antiserum demonstrated species cross-reactivity of antiserum. Lanes 1 and 2 are 5% input volumes of XBcl9 and Myc-tagged (MT) XBcl9 proteins, respectively. Lane 3 is an IP of MT-XBcl9 using anti-Myc as a positive IP control; Lane 4 is an IP of XBcl9 using Myc antibody as a negative antibody control. Lanes 5 and 6 are IP's of XBcl9 using a 1:200 dilution hBcl9 antiserum generated from two different rabbits. Lane 5 suggests that antiserum from this rabbit contained a significant fraction of XBcl9 cross-reacting antibodies. The XBcl9 specific antiserum was affinity purified. B) XBcl9 protein was specifically detected in *in vitro* translated protein lysates (TNT), whole *Xenopus* embryo protein extract and human cell line (ES-2; clear cell ovarian carcinoma) total protein extract by the affinity purified XBcl9 antiserum. Importantly, the antibody did not detect *in vitro* translated mouse Bcl9-2 protein further confirming its high specificity for XBcl9. See Figure 3.1B for XBcl9 percent similarity to other Bcl9 and Bcl9-2 orthologues.

A

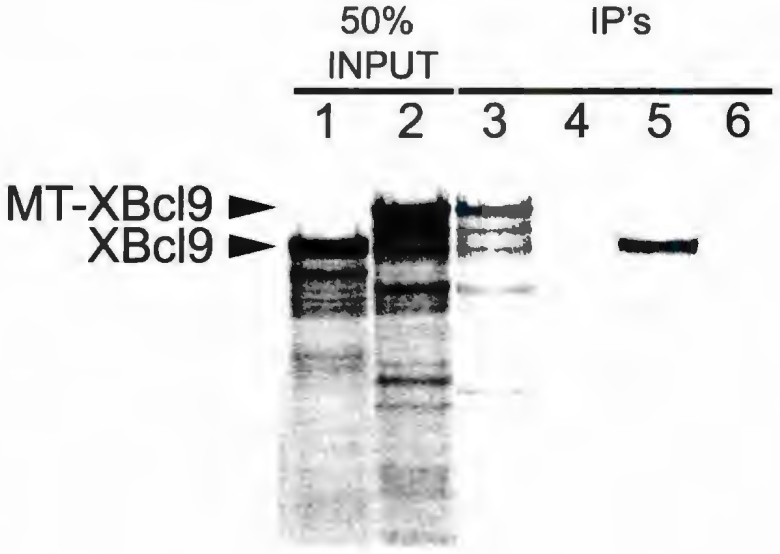
50%
INPUT
IP's
1 2 3 4 5 6
MT-XBcl9
XBcl9

B

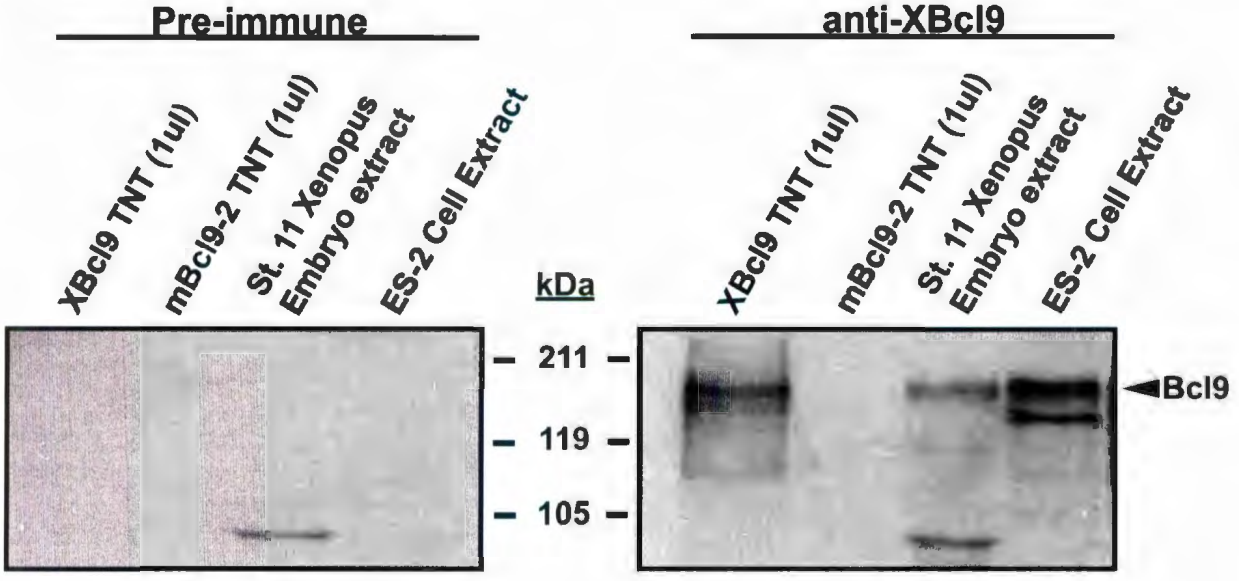
Pre-immune
anti-XBcl9
XBcl9 TNT (1ul)
mBcl9-2 TNT (1ul)
St. 11 Xenopus Embryo extract
ES-2 Cell Extract
kDa
211
119
105
Bcl9

Figure 3.5 Analysis of the developmental expression of XBcl9 mRNA and protein.

A) Northern blot analysis for XBcl9 mRNA. The 28s and 18s ribosomal RNAs are indicated. Total RNA was extracted from staged embryos (Nieuwkoop and Faber, 1994) and normalized to Histone 4 (H4) levels. B) Western blot analysis of XBcl9 protein from total protein extracts of staged embryos (Nieuwkoop and Faber 1994). Total protein was standardized using β-tubulin as the loading control. C) Schematic representation of XBcl9 mRNA (blue) and protein (red) embryonic expression profiles. D) Western blot analysis of XBcl9 protein distribution along the animal-vegetal axis in St. 9 embryos. Total protein levels were normalized to β-tubulin as a loading control.

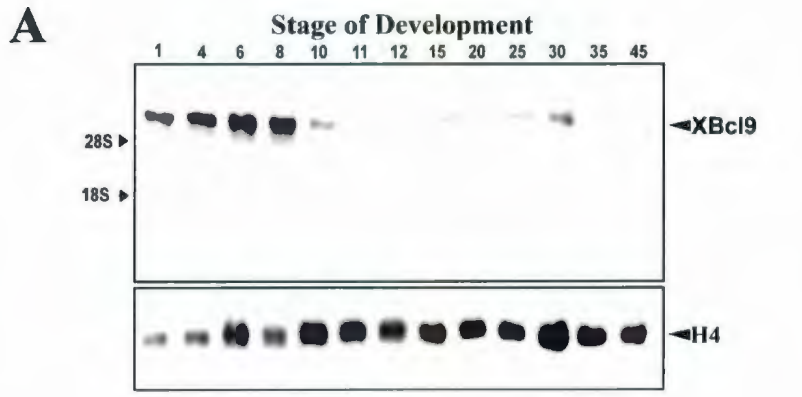
A
Stage of Development
1 4 6 8 10 11 12 15 20 25 30 35 45
28S
18S
XBcl9
H4

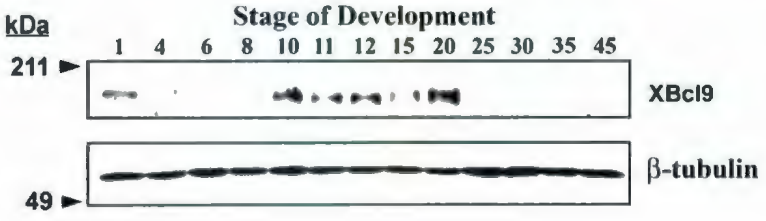
B
kDa
Stage of Development
1 4 6 8 10 11 12 15 20 25 30 35 45
211
XBcl9
β-tubulin
49

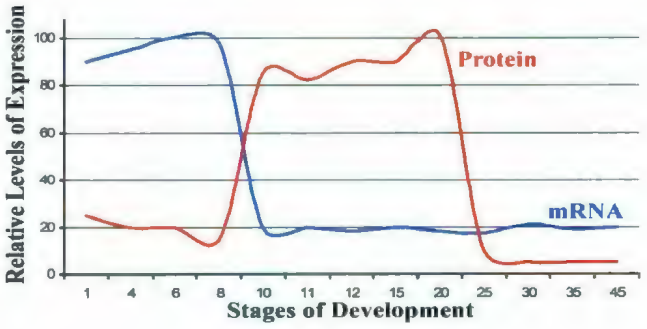
C
Relative Levels of Expression
100
80
60
40
20
0
Protein
mRNA
1 4 6 8 10 11 12 15 20 25 30 35 45
Stages of Development

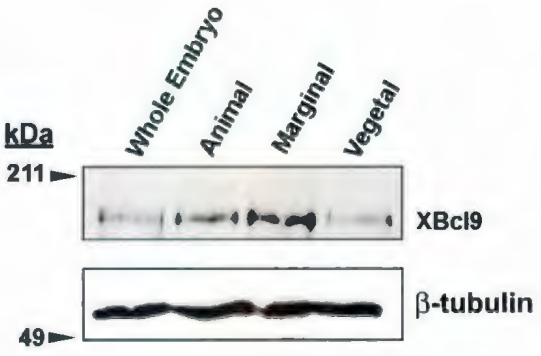
D
Whole Embryo
Animal
Marginal
Vegetal
kDa
211
XBcl9
β-tubulin
49

next determined whether or not the subcellular expression of XBcl9 correlated with embryonic polarity.

Embryos from stages 7, 8, 8.5 and 9.5 were fixed and bisected into dorsal and ventral halves. Embryos were tilted orthogonally to the animal-vegetal axis within 30-40 minutes following fertilization until they completed the first cell division, to ensure the position of the plane of bilateral symmetry (Black and Gerhart 1985). Immediately after tilting, the surface of the equatorial zone was marked with Nile Blue crystals so that the presumptive dorsal region could be identified at later stages. Embryo halves were then processed for immunofluorescence using XBcl9 antiserum and visualized by scanning confocal microscopy (Figure 3.6A-C). At stage 7, the low XBcl9 levels were detected diffusely in both dorsal and ventral sections (Figure 3.6A). By stage 8.5, XBcl9 was present at the periphery of both dorsal and ventral cells but in the nuclei of dorsal marginal and vegetal cells only (Figure 3.6B(ii, iv, vi and viii)). Between stages 8-8.5, 24-30% of dorsal nuclei expressed XBcl9 compared to 2-5% of ventral nuclei (Figure 3.6D). This dorsal-ventral asymmetry in nuclear expression of XBcl9 remained until late stage 9 when XBcl9 was expressed at cell boundaries and in nuclei throughout the entire embryo (Figure 3.6C(ii-iv and vi-viii)), coincident with the overall elevated levels of XBcl9 protein (Figure 3.5C). This dorsal-ventral nuclear staining pattern suggests an association of XBcl9 with dorsal cell fate during early development.

The activities of Wnt pathway components, Xβ-catenin, Dishevelled and GBP positively correlate with dorsal tissue identity in normal embryos and those that have been hyperdorsalized with deuterium oxide (D_2O)

Figure 3.6 XBcl9 subcellular localization and levels correlate with dorsal development.

A) Stage 7, B) 8.5 and C) 9.5 embryos bisected into dorsal and ventral halves. Endogenous XBcl9 protein (green) was detected by immunofluorescence using polyclonal antiserum. A(ii, iv), B(ii, iv) and C(ii, vi)) Pre-immune serum negative controls for XBcl9 staining. C (iii, iv, vii and viii) Magnified view of nuclei expressing XBcl9. DAPI staining specifically identifies nuclei. D) Quantitative representation of the fraction of nuclei expressing XBcl9 in 8-12 dorsal (blue) and ventral (red) embryo halves. E) XBcl9, Xβ-catenin and XGSK3β levels in D_2O dorsalized or UV ventralized whole embryos. Total protein was standardized to β-tubulin levels. (DAI = dorsoanterior index. n = sample size). (A,B and C(i-ii and v-vi) scale bar = 150μm; C(iii-iv and vii-viii) scale bar = 200μm)

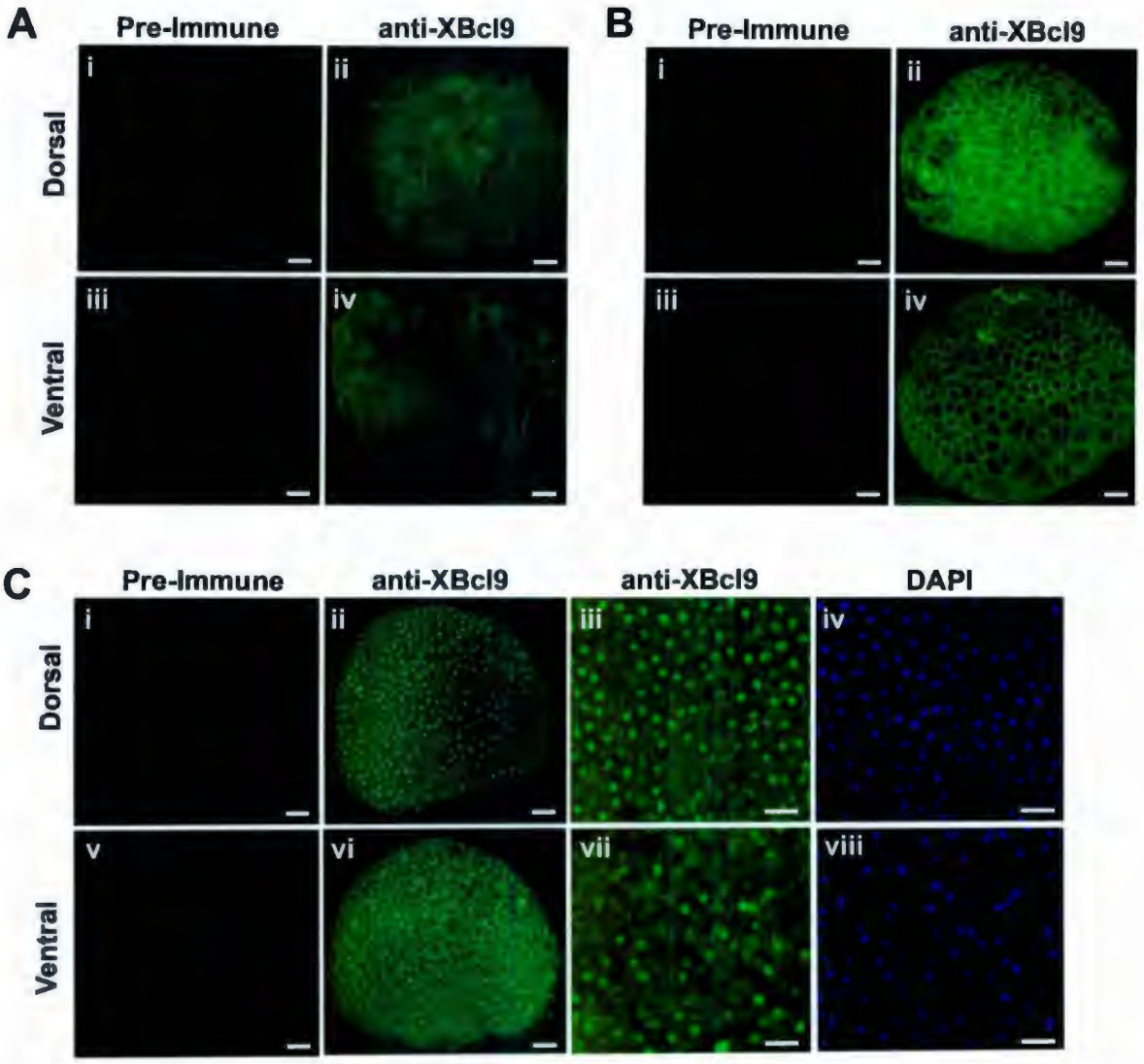
A
Pre-Immune
anti-XBcl9
Dorsal
Ventral
i
ii
iii
iv
B
Pre-Immune
anti-XBcl9
i
ii
iii
iv
C
Pre-Immune
anti-XBcl9
anti-XBcl9
DAPI
Dorsal
Ventral
i
ii
iii
iv
v
vi
vii
viii
D
Dorsal
Ventral
Fraction of Nuclei Expressing XBcl9
0.7
0.6
0.5
0.4
0.3
0.2
0.1
0
Stage 8
Stage 8.5
Stage 9.5
E
Ave DAI
(n=)
5.01 (67)
6.72 (47)
6.40 (45)
4.95 (83)
1.72 (75)
0.91 (109)
XBcl9
Xβ-catenin
XGSK-3β
β-tubulin
Treatment Time (min):
0
4
2
0
2
1
D2O
UV

(Scharf et al. 1989; Miller et al. 1999; Rowning et al. 1997; Weaver et al. 2003). Correspondingly, UV-irradiated, ventralized embryos lack dorsal-ventral polarity in the expression of these dorsal markers and levels of GSK3β, a Wnt pathway inhibitor, negatively correlates with dorsal identity (Dominguez and Green 2000). Based on the observation that XBcl9 is preferentially expressed in dorsal nuclei, I determined if XBcl9 levels correlated with dorsalization of the Xenopus embryo. Embryos were treated with D_2O to hyperdorsalize them, and UV-irradiated to ventralize them. Cohorts of 10 embryos were taken from each treatment for western blot analysis and the remaining ones were left to develop until late tail bud stages for DAI scoring. In D_2O treated embryos XBcl9 and Xβ-catenin levels increased with DAI but surprisingly, no difference was detected in total GSK3β levels in embryos with average DAI ~6.4-6.7 (Figure 3.6E). The lack of detectable reduction in total GSK3β levels compared to previous findings may be explained by the higher degree of hyperdorsalization (DAI ≥7) reported by Dominguez and Green (2000). In UV ventralized embryos, there was no consistently detectable change in either XBcl9 or Xβ-catenin levels, nor in GSK3β levels, as expected (Dominguez and Green 2000). These results confirm that XBcl9 protein levels positively correlate with dorsal but not ventral cell fate.

3.3.6 Ectopic expression of XBcl9 with XPygo induces secondary axis

Consistent with studies in *Drosophila* embryos in which Lgs and Pygo are required together in a complex to activate transcription from Wnt target genes (Kramps et

al. 2002; Parker et al. 2002; Thompson et al. 2002), only when XBcl9 and Xpygo2 are ectopically co-expressed, can they promote axis formation in Xenopus. Embryos injected ventrally, either vegetally or marginally, with either XBcl9 or XPygo2 synthetic mRNA developed normally (Figure 3.7C-D). The lack of any marked phenotype by overexpression of XPygo2 is consistent with previous findings (Lake and Kao 2003b). However, co-injection of XBcl9 *and* XPygo2 mRNAs into the ventral-vegetal region of 2 cell stage embryos frequently caused axis duplication (52/86, 60%) (Figure 3.7E, G).

qPCR analysis of marker genes confirmed the upregulation of many Wnt/dorsal target genes such as *siamois* (~3-3.5 fold increase), *chordin* (~2.5-3 fold increase) and *goosecoid* (~2.5-3 fold increase) as well as a modest reduction in the ventral marker *Bmp4* (~0.4 fold decrease) (Figure 3.7H). In addition, co-expression of XBcl9 and XPygo2β induced or expanded the amount of dorsal endoderm in 14 out of 86 (16%) embryos (Figure 3.7F, G) as suggested by the large increase in the canonical Wnt targets *Xnr5* (~6.5 fold increase) and *Xnr6* (~9 fold increase) (Figure 3.7H). No change was detected in other endodermal markers such as *Xnr1*, *Xnr2* and *Endodermin* (Data not shown) although a modest increase (~0.5 fold) in *Xsox17α* and (~0.75 fold) *mix2* was detected (Figure 3.7H). These results indicate that both XBcl9 and Xpygo2 cooperatively promote dorsal gene expression.

Table 3.2 qPCR primers used to analyze marker gene expression.

qPCR primers	Origin	Sequence
gooscoid	New	U: 5-GTGCTGATTCCACCAGTGCCTCACC-3 D: 5-GCCTCCTCTTCCTCCTGCAG-3
chordin	Belenkaya *et al.*,2002	U: 5-AACTGCCAGGACTGGATGGT-3 D: 5-GGCAGGATTTAGAGTTGCTTC
sox17α	Xanthos *et al.*, 2001	U: 5-GCAAGATGCTTGGCAAGTCG-3 D: 5-GCTGAAGTTCTCTAGACACA
BMP4	New	U: 5-GTCAAGACATCATGATTCCTGG-3 D: 5-AGCTCATTGCTCTGAGGCGA
mix2	New	U: 5-TGCAAGCCATCATTATTCTAGC-3 D: 5-AGGAACCTCTGCCTCGAGACAT-3
Xnr5	New	U: 5-CCAGAACAGCATCATAAGAAGCGG-3 D: 5-GGCTTGAAGTTCTCATCCAGTGG-3
Xnr6	New	U: 5-CCACACCAAAGACCGTCACGAG-3 D: 5-CCAACATGACTCTCTCCGCAAC-3
siamois	Heasman *et al.*, 2000	U: 5-CTGTCCTACAAGAGACTCTG-3 D: 5-TGTTGACTGCAGACTGTTGA-3
ODC	Heasman *et al.*, 2000	U: 5-GCCATTGTGAAGACTCTCTCCATTC-3 D: 5-TTCGGGTGATTCCTTGCCAC-3

Figure 3.7 Dorsalization of *Xenopus* embryos by co-overexpression of XBcl9 and XPygo2β.

A) Uninjected control embryos. B) EGFP mRNA (1ng) injected control. C) EGFP-XBcl9 mRNA (4ng) injected embryos. D) XPygo2β mRNA (2ng) injected embryos. E&F) Co-injection of EGFP-XBcl9 (4ng) and XPygo2β (2ng) (white arrows indicate duplicated axes; black arrow indicates large endodermal mass). G) Frequency of embryos exhibiting axis duplication (blue bars) or enlarged endoderm (purple bars). Sample size is bracketed above bars indicating number of scored embryos. H) qPCR analysis of dorsal, ventral and endodermal markers in stage 10 embryos that were uninjected (i), injected with EGFP mRNA (ii), EGFP-XBcl9 mRNA (iii), XPygo2β mRNA (iv), or EGFP-XBcl9 plus XPygo2β mRNA(v). Relative fold change (Y-axis) as compared to the uninjected controls was calculated using the $2^{-\Delta\Delta Ct}$ method (Livak and Schmittgen 2001; Schmittgen and Livak 2008). All experiments were performed 3 times. A representative experiment is presented in (H).

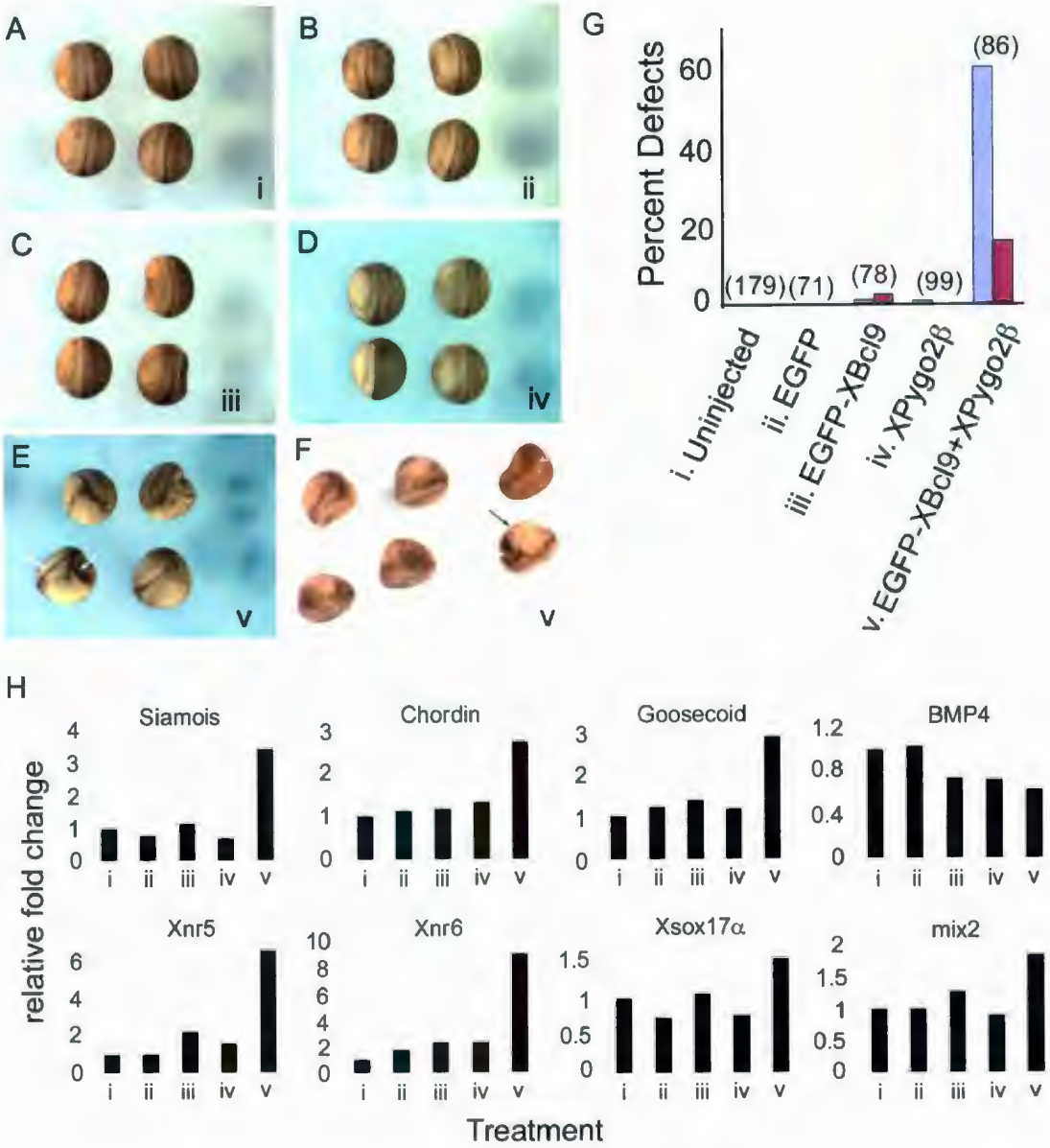
A
B
C
D
E
F
G
H
i
ii
iii
iv
v
Percent Defects
60
40
20
0
(179)
(71)
(78)
(99)
(86)
i. Uninjected
ii. EGFP
iii. EGFP-XBcl9
iv. XPygo2β
v. EGFP-XBcl9+XPygo2β
relative fold change
Siamois
Chordin
Goosecoid
BMP4
Xnr5
Xnr6
Xsox17α
mix2
Treatment

3.3.7 XPygo2 is required for XBcl9 nuclear expression and enhances Xβ-catenin binding

The formation of a secondary axis by the co-injection of XBcl9 and XPygo2 suggested that these two proteins interact with each other, *in vivo*. Furthermore, in 293T cells, Lgs/Bcl9 was shown to be a nuclear protein only when co-expressed with Pygo despite the presence of a putative nuclear localization sequence (KRRK: XBcl9 amino acids 542-545) (Townsley et al. 2004a). Consistent with this previous observation, when expressed alone in stage 9 animal pole explants, EGFP-XBcl9 accumulated in randomly dispersed aggregates throughout the animal cap cells but was never detected in nuclei (Figure 3.8A, top row). However, when co-injected with MT-XPygo2, EGFP-XBcl9 was localized in nuclei (Figure 3.8A, bottom row) indicating that XBcl9 nuclear localization is dependent on the presence of Pygo.

Our above results indicating that XBcl9 activity is augmented by Xpygo2 in embryos was substantiated by *in embryo* protein interaction assays. Combinations of RNAs encoding EGFP-XBcl9, MT-XPygo2β and mRFP-Xβ-catenin were injected into 2 cell stage embryos which were allowed to develop until stage 9 when total protein was harvested from 40-50 whole embryos for co-immunoprecipitation experiments. As demonstrated, *in vitro* (Figure 3.2B), XBcl9 interacted very strongly with XPygo2β but weakly with Xβ-catenin *in vivo* (Figure 3.8B). When co-expressed with XPygo2β, XBcl9 interacted much more strongly with Xβ-catenin (Fig. 7B), indicating that XPygo2β enhances or facilitates their interaction in embryos.

Figure 3.8 XPygo2β localizes XBcl9 to nuclei and enhances its interaction with Xβ-catenin.

A) Enhanced green fluorescent protein tagged (EGFP) XBcl9 (2ng) was injected alone or in combination with MT-XPygo2β (1ng) into animal caps. Animal caps were explanted at stage 8 and cultured until stage9. XBcl9 localization was detected by EGFP fluorescence (green); Myc tagged (MT)-XPygo2β was detected by immunostaining for the Myc tag (Cy5; red) and visualized by confocal microscopy. Nuclei were identified by counterstaining with DAPI. B) Co-immunoprecipitation of monomeric red fluorescent protein (mRFP) tagged Xβ-catenin and/or MT-XPygo2β with EGFP or EGFP-XBcl9. Equal amounts of input protein per co-IP was confirmed by Western blot of total protein extracts and further standardized by β-tubulin as a loading control.

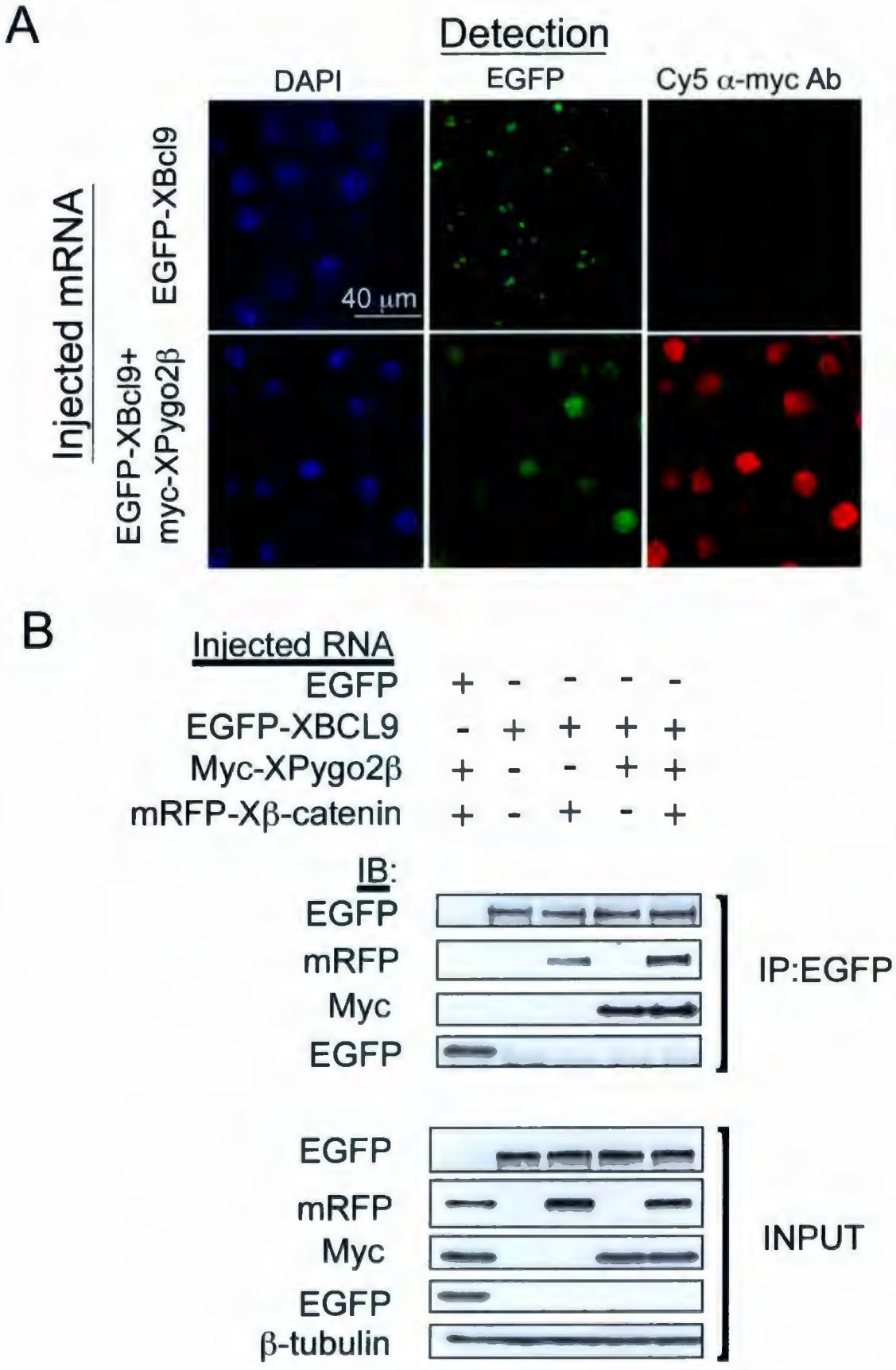
A
Detection
DAPI
EGFP
Cy5 α-myc Ab
Injected mRNA
EGFP-XBcl9
EGFP-XBcl9+
myc-XPygo2β
40 μm
B
Injected RNA
EGFP + - - - -
EGFP-XBCL9 - + + + +
Myc-XPygo2β + - - + +
mRFP-Xβ-catenin + - + - +
IB:
EGFP
mRFP
Myc
EGFP
IP:EGFP
EGFP
mRFP
Myc
EGFP
β-tubulin
INPUT

3.3.8 Maternal XBcl9 is required for axis formation

The Wnt signaling pathway is essential for formation of the dorsal body axis during *Xenopus* development. Therefore, we next determined if maternally expressed XBcl9 was required for axis formation. For this analysis, we depleted maternal XBcl9 transcripts using a phosphothioated antisense oligonucleotide (oligo) from oocytes harvested from three female wildtype frogs, which were subsequently matured *in vitro* and processed for embryonic development using the host-transfer technique (Mir and Heasman 2008). XBcl9 mRNA was reduced by approximately 70% and XBcl9 protein was reduced to nearly undetectable levels, when as much as 4ng of the antisense oligo was injected into fully grown oocytes as compared to uninjected, control oocytes (Figure 3.9A, B).

When fertilized using the host-transfer technique, XBcl9 depleted oocytes developed severe axis abnormalities. Injection of 1ng and 2ng of the antisense oligo resulted in ventralization defects in 3/26 (12%) and 6/38 (16%) embryos, respectively, when scored at tailbud stages (Figure 3.9C). At 4ng, ventralization defects were present in 16/31 (52%) embryos (Figure 3.9C). The control cohort all developed normally (0/43, 0%) (Figure 3.9C). qPCR analysis of Wnt/dorsal molecular markers revealed significant reductions in the levels of *siamois*, *Xnr3*, *Chordin*, and *Goosecoid* at stage 9 and stage10, in XBcl9 depleted embryos (Figure 3.9D). There were no observable changes in the levels of the ventral markers, *Bmp4* and *XWnt8*, or the endodermal marker, *Xsox17α* (Figure 3.9D).

Figure 3.9 XBcl9 is required for dorsal axis formation.

A) qPCR analysis of XBcl9 mRNA levels in 1ng, 2ng and 4ng antisense oligo injected, progesterone-matured stage VI oocytes relative to uninjected (UI) controls. B) Western blot analysis of XBcl9 protein levels corresponding to (A). Protein levels were standardized using β-tubulin as a loading control. C) Phenotype analysis of embryos with reduced XBcl9 mRNA and protein levels from host-transfer. Phenotypes were scored at stage 24. Embryos appear as different colours due to vital staining during the host-transfer protocol. D) qPCR analysis of molecular markers at stage 9 and stage 10 in XBcl9 depleted (*XBcl9*$^{-}$) embryos. qPCR analysis was performed on 2 independent batches of embryos. Results shown in (D) were consistent in both batches of embryos. The *XBcl9*$^{-}$ embryos illustrated were injected with 4ng antisense oligos.

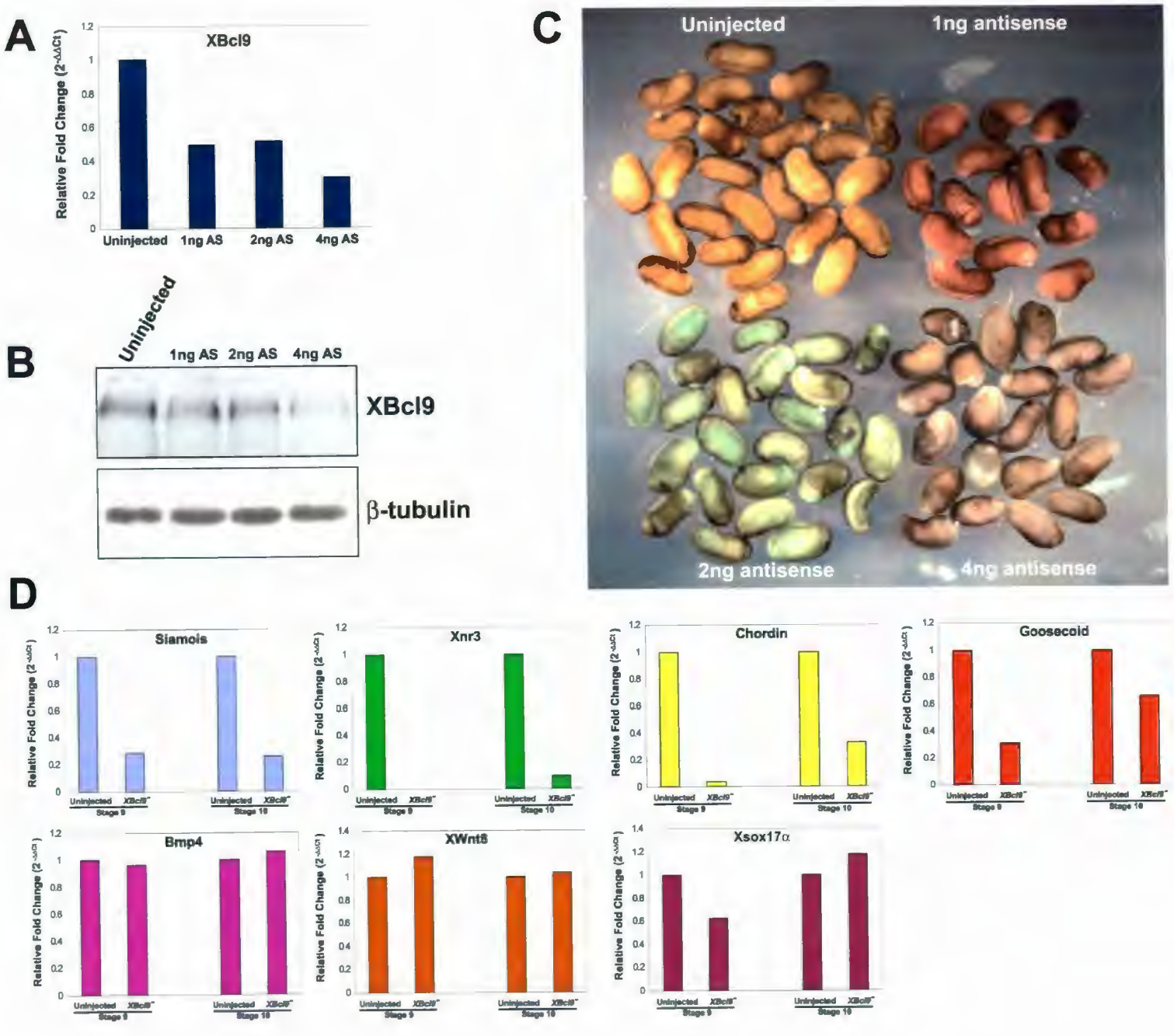
A
XBcl9
Relative Fold Change (2^-ΔΔCt)
1.2
1
0.8
0.6
0.4
0.2
0
Uninjected
1ng AS
2ng AS
4ng AS
B
Uninjected
1ng AS
2ng AS
4ng AS
XBcl9
β-tubulin
C
Uninjected
1ng antisense
2ng antisense
4ng antisense
D
Siamois
Xnr3
Chordin
Goosecoid
Bmp4
XWnt8
Xsox17α
Relative Fold Change (2^-ΔΔCt)
Uninjected
XBcl9-
Stage 9
Stage 10

To confirm specificity of the XBcl9 antisense oligo mediated ventralization, we injected manually, defolliculated oocytes with 2ng of XBcl9-specific antisense oligo and cultured for 48hrs at 18°C to rescue normal development; restoration of XBcl9 would not rescue non-specific/off-target effects. While 4ng of oligo caused a greater frequency of ventralization, we used 2ng to limit the total amount of exogenous nucleic acids being introduced into the oocytes. Thus, before progesterone-induced *in vitro* maturation, *XBcl9*$^{-}$ oocytes were injected with either 500pg of XBcl9 mRNA alone or co-injected with 250pg of XPygo2 mRNA since injection of both mRNAs were necessary for ectopic axis formation (as shown in Figure 3.7E, F). Uninjected control embryos developed normally in 64/69 (93%) cases. Ventralization defects were observed in 20/87 (23%) embryos derived from oocytes injected with 2ng XBcl9 antisense oligos. Injection of XBcl9 rescuing mRNA alone into XBcl9^{-} oocytes was sufficient to restore normal axis formation in 31/37 (84%) and cause dorsal-anteriorization in 5/37 (14%) embryos (Figure 3.10). Co-injection of XBcl9 and XPygo2 rescuing mRNAs into XBcl9^{-} oocytes, caused excessive dorsal-anteriorization in 43/43 (100%) (Figure 3.10) These results indicate that maternal XBcl9 is required for normal axis development.

Figure 3.10 XBcl9 mRNA restores development to axial defective, XBcl9$^-$ embryos.

A) Embryos depleted of maternal XBcl9 mRNA by injection of 2ng of XBcl9 antisense oligonucleotides (αs Bcl9) were co-injected with 500 pg XBcl9 mRNA (αs Bcl9+Bcl9 RNA) or additionally, with 250pg XPygo2 mRNA (+Pygo2 RNA). Data shown are for embryos generated from three females (1-3). Oocytes from female 3 were injected with antisense oligos and co-injected with XBcl9 and Xpygo2 mRNA. B) Examples of maternal XBcl9-depleted embryos (upper right panel) co-injected with XBcl9 (lower left panel) and XBcl9 plus XPygo2 (lower right panel) mRNA. Green arrow heads indicate ventralized embryos lacking either complete axis or dorsal-anterior head structures.

A

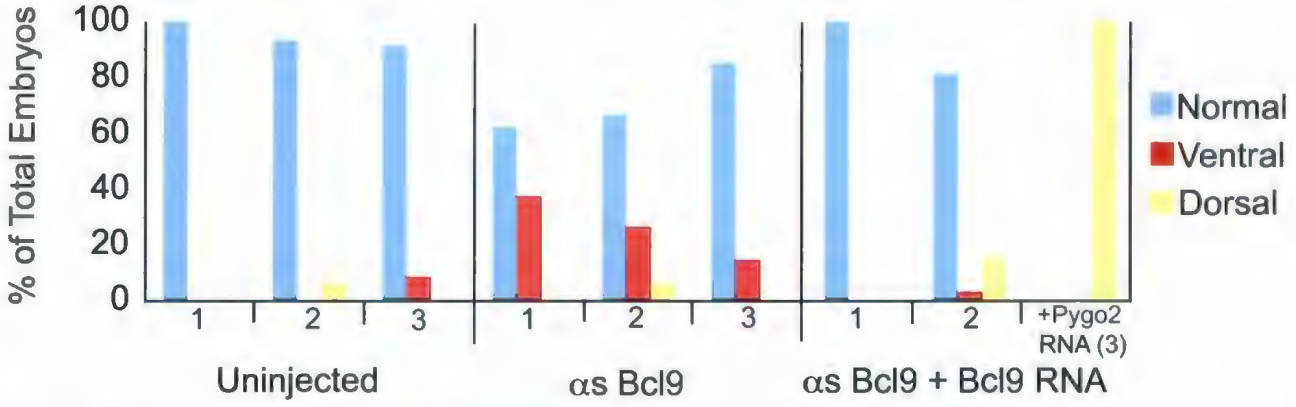
% of Total Embryos
100
80
60
40
20
0
1
2
3
1
2
3
1
2
+Pygo2 RNA (3)
Uninjected
αs Bcl9
αs Bcl9 + Bcl9 RNA
Normal
Ventral
Dorsal

B


Uninjected
2ng AS
2ng AS + XBcl9
2ng AS + XBcl9 + XPygo2

3.4 Discussion

3.4.1 XBcl9 is required for body axis formation

Specification of the dorsal body axis during *Xenopus* development depends on tightly regulated temporal and spatial activation of the Wnt signaling pathway. Since many of the intracellular components of the Wnt pathway are present maternally (Heasman 2006), normal development occurs only when these molecules are properly distributed in the developing embryo. Hence, polarization of the embryo into dorsal and ventral regions is initiated by the cortical rotation that results in the stabilization and nuclear accumulation of β-catenin in dorsally fated cells (Larabell et al. 1997; Schneider et al. 1996). These events occur very early in embryogenesis and appear to 'prime' cells to express dorsal target genes several hours later. Hence, the identification of Wnt pathway components that can mediate the β-catenin-Tcf transcription complex is a necessary step towards understanding the dynamics of the complex and how it operates during embryonic development.

Since *lgs/Bcl9* has been described as a core component of Wnt signaling during *Drosophila* embryogenesis as well as important for transcription of synthetic Wnt reporter constructs in mammalian cell lines (Stadeli and Basler 2005; Townsley et al. 2004b; Kramps et al. 2002; Parker et al. 2002; Thompson et al. 2002), we hypothesized that Bcl9 is a necessary transcriptional regulating protein required for Wnt mediated processes during *Xenopus* development. Our results suggested that in Xenopus development, neither Bcl9, nor Pygo are dispensable for Wnt-mediated function. Both proteins strongly interact with each other and both are required to localize to nuclei,

activate dorsal gene targets and promote axis formation. Thus, we propose that while Pygo and possibly Bcl9 may have non-Wnt associated functions, it is their ability to form a complex that defines their function in canonical Wnt-dependent axis formation events.

Temporal gene expression patterns are often indicative of when a gene is required during embryogenesis. Our results confirming XBcl9 as a component that interacts with β-catenin and Pygo in *Xenopus* and the relatively high mRNA levels present maternally, suggested an early requirement for Wnt-mediated dorsal axis formation. However, the highest levels of XBcl9 protein were not detected until gastrulation, when mRNA levels were lowest, suggesting the existence of post-transcriptional regulation of *XBcl9* expression in embryos.

3.4.2 Nuclear localization of XBcl9/XPygo is a determinative step in dorsal gene activation

Nuclear accumulation of maternal β-catenin by the 16-32 cell stage (Larabell et al. 1997) specifies competency in those cells and is required to specifically activate genes that define the dorsal axis. However, many dorsal target genes such as *Xnr3* (Smith et al. 1995), and *siamois* (Lemaire et al. 1995) are not expressed until late stage 8 and early stage 9, several hours later than nuclear accumulation of β-catenin, suggesting that there are additional requirements for transcriptional activation. Based on our observation that XBcl9 is detected in dorsal nuclei immediately prior to the detection of dorsal markers, and that β-catenin requires Bcl9-Pygo for transcriptional activation, we propose that a

Figure 3.11 Schematic representation of canonical Wnt signaling dependency on XBcl9-XPygo for spatio-temporal regulated dorsal gene expression.

A) Radially symmetric *Xenopus* embryo. Dorsal determinants (*i.e.* maternal Wnt11) are associated with vegetal cortex. B) Cortical rotation results in the asymmetric expression of Wnt11 (blue) that C) locally stabilizes β-catenin (red) by 8-16 cell stage. D) XBcl9 (green) localizes to dorsal nuclei at stage 8-8.5, concomitant with the timing of dorsal gene activation. (D, Dorsal; V, Ventral)

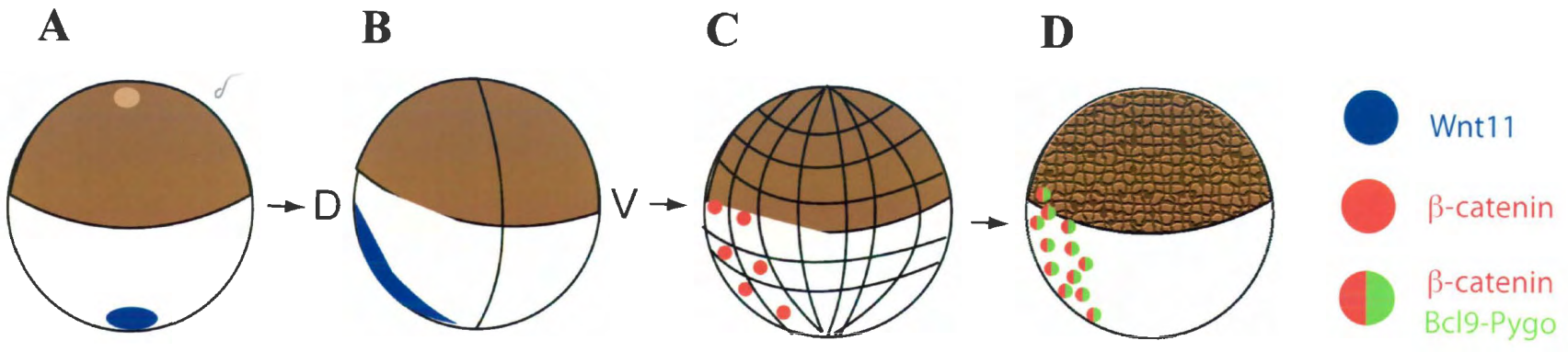
A
B
C
D
D
V
Wnt11
β-catenin
β-catenin
Bcl9-Pygo

determinative step of dorsal cell fate is dependent on the timing of XBcl9 nuclear entry thus completing the link between β-catenin and Pygo2 and the basal transcriptional machinery (Figure 3.11). Interestingly, the detection of pre-MBT β-catenin directed transcription of *Xnr5* and *Xnr6* has been reported (Yang et al. 2002). These results are not inconsistent with my findings. It is possible that XBcl9 is expressed at levels sufficient to stimulate low levels of transcription but undetectable in nuclei by immunofluorescent staining. Furthermore, the large scale activation of dorsal target genes that *comitt* cells to the dorsal lineage may be dependent on the timing of XBcl9 nuclear entry whereas the induction of low levels of *Xnr5* and *Xnr6 specify* dorsal cell fate.

Recently, a novel transactivation region between HD4 and HD5 of Bcl9 was identified. This region augmented β-catenin stimulated transcription from DNA reporter constructs specifically in lymphoid (B and T) cell lines and was largely independent of Pygo2 (Sustmann et al. 2008). We did not find any evidence of such intrinsic activity of XBcl9 since overexpression of XBcl9 did not alter axis development. It is possible, however, that this Pygo-independent function simply isn't required during early embryogenesis, but may be important for later development.

The dual requirement of XBcl9-XPygo for canonical Wnt signaling in Xenopus may provide new insight into β-catenin-mediated transcription in mammalian development. Studies in *Drosophila* have clearly identified a co-dependency for Lgs/Bcl9 and Pygo proteins for Wnt signaling (Kramps et al. 2002; Thompson et al. 2002). In addition to completing the link between Pygo and β-catenin-LEF/TCF bound to target promoters, analysis of the crystal structure of the HD1 domain of Bcl9 and the PHD

region of Pygo demonstrated that the HD1 enhanced the affinity of Pygo's PHD for methylated histones implicating its role in chromatin remodeling (Fiedler et al. 2008). Bcl9-Pygo complexes may function, therefore, at multiple levels to regulate the transcription of Wnt target genes. *Pygo2*$^{-/-}$ null mice die very early and display mild congenital defects (e.g. microopthalmia and exencephaly) compared to mice with defects in other canonical Wnt pathway components (Song et al. 2007), these observations might suggest that Pygo has an evolutionarily diminished Wnt pathway function in mice. It is possible however, that Bcl9 and Pygo are broadly co-dependent for canonical Wnt function in vertebrates. *Bcl9*$^{-/-}$*/Pygo2*$^{-/-}$ developmental models might therefore need to be exploited to distinguish the canonical-Wnt and non-Wnt pathway requirements for *Pygo* in mouse development.

Chapter 4: Post-transcriptional regulation of XBcl9 mRNA: A novel mechanism regulating dorsal axis formation

4.1 Introduction

In the previous chapter, I described experiments that revealed the importance of the Lgs/Bcl9 protein in early axis formation. My experiments demonstrated that translation of XBcl9 occurred not necessarily concomitant with transcription. In this chapter I have identified a novel mechanism, post-transcriptionally regulating XBcl9 that may be important during early embryogenesis.

4.1.1.1 Translational regulation during early embryonic development

Early embryonic development is directed by maternal mRNA and proteins because the egg and zygote are transcriptionally inert. Embryonic genome activation (EGA) occurs after different lengths of time in different organisms. For example, in *Xenopus,* the time point when activation of zygotic transcription occurs (known as mid-blastula transition, or MBT in this genus and in *Drosophila*) is several hours post-fertilization when the embryo reaches about 4000 cells (Newport and Kirschner 1982a; Newport and Kirschner 1982b). In mice and humans, EGA occurs by the end of the 2-cell stage and 4-cell stage, respectively, which can take several days (Telford et al. 1990). Therefore early development must be governed by post-transcriptional and post-translational mechanisms that regulate cell fate prior to EGA.

Of particular interest in this chapter are post-transcriptional mechanisms mediated by protein-RNA interactions that police mRNA translation. A comprehensive treatise of the subject has been published elsewhere (Colegrove-Otero et al., 2005) but I will review the aspects relevant to my thesis. Translation can be divided into 3 phases: initiation,

elongation and termination. Although modes of translational regulation can be applied at any level, all known mechanisms regulate the initiation phase. Such mechanisms include internal ribosome entry site (IRES)-mediated translation, micro RNA (miRNA) and RNA-protein interactions which can repress and/or activate translation by controlling the formation of the so-called 'closed-loop' conformation necessary for efficient ribosome loading and/or which regulate transcript polyadenylation status (Bettegowda and Smith 2007; Colegrove-Otero et al. 2005).

4.1.1.2 Overview of translation: The Initiation Phase

During the initiation phase of translation, the immature, 43S ribosomal subunit is recruited to the 5' untranslated region (UTR) of mRNAs. The preinitiation 43S complex is composed of the 40S ribosomal subunit, the initiator methionyl tRNA and the eukaryotic initiation factor 2 (eIF2) (Algire and Lorsch 2006; Colegrove-Otero et al. 2005; Pestova et al. 2001). The scanning 43S complex is recruited to AUG start codons by eIF5 which triggers hydrolysis of GTP associated with eIF2 (Huang et al. 1997; Majumdar and Maitra 2005) and the release of factors associated with the 40S subunit (Colegrove-Otero et al. 2005; Algire and Lorsch 2006; Mitchell and Lorsch 2008). The initiation phase then concludes when the 60S and 40s subunits unite and the elongation phase begins.

4.1.1.3 The "closed-loop model" of translation

The "closed-loop model" promotes translation and explains the translational synergism of the 7-methylguanosine (m^7G) cap and the poly-A tail (Jacobson 1996; Kahvejian et al. 2001; Wells et al. 1998). Stimulation of translation, for example by growth factors, is dictated by a complex network of m^7G cap and 3'UTR binding proteins that mediate the formation of the 'pseudocircular' conformation (Figure 4.1A).

The eIF4F complex binds directly to the m^7G cap and recruits the 43S preinitiation complex to mRNA molecules. The eIF4F assembly is composed of the eIF4E cap-binding protein (Edery et al. 1983; Tahara et al. 1981), the eIF4G scaffold (Browning et al. 1987; Pyronnet et al. 1999) and Poly(A) binding protein (PABP) (Imataka et al. 1998; Tarun, Jr. and Sachs 1996) and the eIF4A DEAD-box RNA helicase (Ray et al. 1985). eIF4E anchors the eIF4F complex to the m^7G cap; eIF4G interacts with eIF3 which directly recruits the 43S preinitiation complex and simultaneously binds to PABP; eIF4A unwinds or dissolves secondary structure in the 5'UTR of mRNA species (Colegrove-Otero et al. 2005).

Cytoplasmic Poly (A) element binding protein (CPEB) binds to sequence-specific elements (*i.e.* CPEs) in the 3'UTR to regulate the length of Poly(A) tails (Hake and Richter 1994; Stebbins-Boaz et al. 1996). PABPs simultaneously bind to elongated Poly(A) tails and to eIF4G thus inducing the so-called "closed-loop" conformation which facilitates translation (Wakiyama et al. 2000; Imataka et al. 1998; Tarun, Jr. and Sachs 1996; Wells et al. 1998). As such, the regulation of the interactions necessary for the circularization of mRNA molecules is a common strategy of translational control.

Figure 4.1 Regulation of translation by RNA-protein interactions.

A) 'Closed' Loop model of translational activation. The association of PABP proteins with the poly(A) tail and with the eIF-4G of the 5'cap binding complex causes a pseudocircularization of the mRNA, synergistically enhancing translation initiation efficiency. B) The interaction of Maskin/Cup with sequence specific, RNA binding proteins disrupts proper pseudocircularization by interfering with combinatorial association of 5'cap binding proteins, effectively inhibiting translation initiation.

A

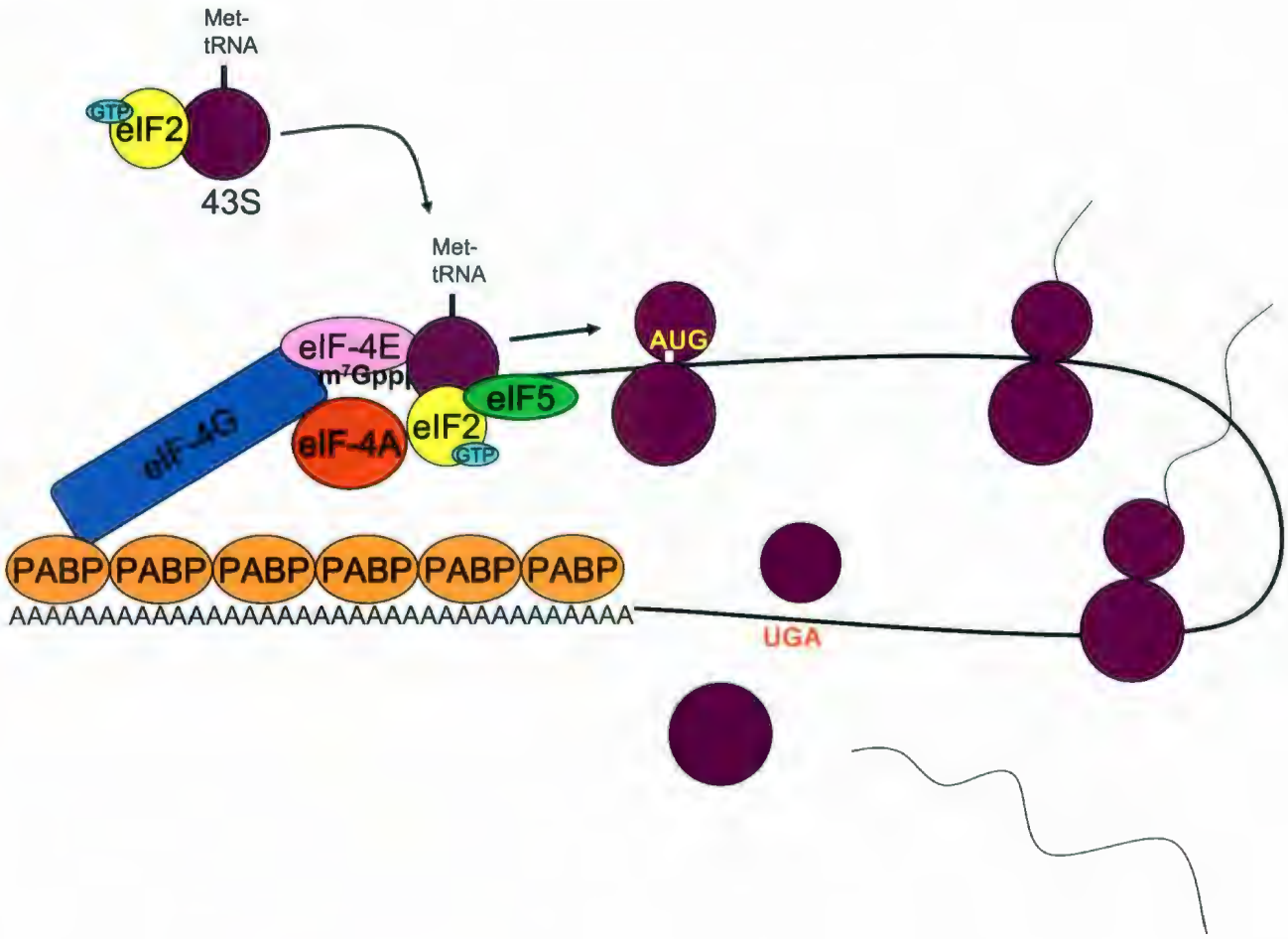
Met-
tRNA
GTP
eIF2
43S
Met-
tRNA
eIF-4E
eIF5
AUG
eIF-4G
eIF-4A
eIF2
GTP
PABP
PABP
PABP
PABP
PABP
PABP
AAAAAAAAAAAAAAAAAAAAAAAAAAAAAAAAAAAA
UGA

B

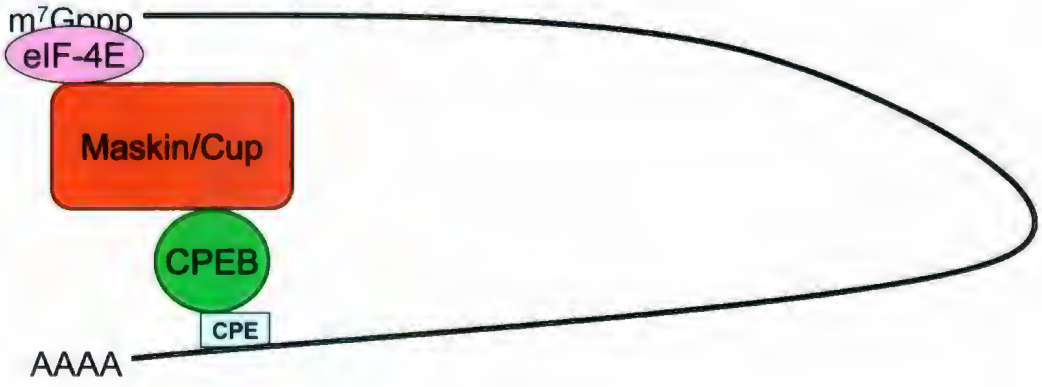
m7Gppp
eIF-4E
Maskin/Cup
CPEB
CPE
AAAA

Several eIF4E binding proteins (4E-BPs) have been described which interfere with the interaction between eIF4E and eIF4G and subsequently inhibit translation. For example, the Cup/Maskin (invertebrate/vertebrate) proteins function as inhibitory 4E-BPs (Figure 4.1B). In *Drosophila*, Cup binds to Bruno and Smaug proteins (analogous to CPEB) bound to BRE and SRE response elements in the 3'UTR, respectively, to prevent the translation of genes such as *oskar* (Wilhelm et al. 2003; Dahanukar et al. 1999; Kim-Ha et al. 1995). In *Xenopus* and mammals, Maskin binds to CPEB loaded onto the CPE to regulate translation of *cyclin B1* , *wee-1*, and *c-mos* in *Xenopus* (Stebbins-Boaz et al. 1996; Charlesworth et al. 2000; Groisman et al. 2000), *tissue type plasminogen activator* (*tPA*) in rats (Shin et al. 2004), and *c-mos* and *cyclin B1* in mice (Gebauer and Richter 1996; Tay et al. 2000).

4.1.1.4 IRES and miRNA modes of translational regulation

Most eukaryotic RNAs are translated by a cap-dependent mechanism whereby the 40S ribosomal subunit is recruited to the m^7G cap on the 5' tip of mRNA by proteins such as eIF4E, and eIF4G. IRES sites were discovered as sequences in the 5' untranslated regions (5'UTR) of the picornavirus RNA genome that mediated cap-independent translation (Jang et al. 1990; Jang et al. 1988; Pelletier et al. 1988; Pelletier and Sonenberg 1988). Since this discovery, several cellular mRNAs have been described to be post-transcriptionally regulated by IRES sites. Examples include the human insulin receptor (Spriggs et al. 2009), the c-, L- and N- myc protooncogenes (Jopling and Willis 2001; Jopling et al. 2004; Stoneley et al. 1998) and p53 (Ray et al. 2006).

miRNAs are short, RNA molecules about 21-23 nucleotides in length, transcribed from intragenic regions which are not translated but which function as a form of RNA interference (RNAi) (Lee et al. 2004; Lee et al. 1993; Bushati and Cohen 2007). The most recognized mode of action of miRNAs is through destabilizing target mRNAs by inducing their degradation via RNA-induced silencing complex (RISC) activity (Lee et al. 2004; Bushati and Cohen 2007). More recently, various classes of miRNAs, such as *let-7* and miR-2, have been shown to repress translation without affecting mRNA stability in a mammalian cell-free system and *Drosophila* embryos respectively (Wakiyama et al. 2007; Thermann and Hentze 2007). *Let-7* was shown to induce deadenylation of target mRNA, whereas miR-2 inhibited loading the 40S ribosomal subunit on to mRNA.

4.1.1.5 RNA-Protein interactions regulate the "closed-loop model" of translation

The most well-studied post-transcriptional mechanisms are mediated by RNA-protein interactions and have been shown to have critical requirements during invertebrate and vertebrate development (Bettegowda and Smith 2007; Colegrove-Otero et al. 2005; Vasudevan et al. 2006). In *Drosophila*, maternal effect genes induce the transcription of maternal mRNA encoding RNA-binding proteins such as *bicoid*, *hunchback*, *nanos* and *caudal*, which become localized in the egg. The activity of these genes create protein gradients which regulate the zygotic transcription of Gap genes, Pair-rule genes, segment polarity and homeotic genes which generate the anterior-posterior body axis (Gilbert 2003). In *Xenopus* oocytes, RNA-protein interactions

regulate meiotic maturation in the oocyte by regulating polyadenylation/deadenylation of maternally expressed mRNAs, thus controlling protein levels. Furthermore, in mammalian cells, iron metabolism, for example, is governed by RNA-protein interactions that regulate the translation of ferritin mRNA in response to cellular iron levels (Pantopoulos 2004; Wallander et al. 2006).

The maternal fly *bicoid* and *hunchback* transcripts establish the anterior region of the embryo, whereas *nanos* and *caudal* establish the posterior region. Bicoid mRNA is localized to the presumptive anterior-most region and nanos mRNA is localized in the presumptive posterior-most region of *Drosophila* eggs. Hunchback and caudal transcripts are distributed throughout the egg. Prior to MBT/EGA, Bicoid protein binds to the m^7G cap protein, eIF4E, and the 3'UTR of caudal mRNA, independently of CPEB, Bruno or Smaug proteins, thus disrupting the association of eIF4E with eIF4G and repressing its translation anteriorly (Niessing et al. 2002). Similarly, nanos protein binds to the 3'UTR of hunchback mRNA through the RNA-binding protein, Pumilio. Nanos-Pumilio direct the deadenylation of hunchback mRNA thus repressing its translation in the posterior region (Irish et al. 1989; Wharton and Struhl 1991; Wreden et al. 1997). In this way, caudal protein is translated posteriorly and hunchback protein is expressed anteriorly, marking an early step in body plan formation in *Drosophila*.

4.1.1.6 Translational control regulates meiotic maturation

The best-studied example of polyadenylation-mediated translation control in vertebrates is of *cyclinB1* and *c-mos* transcripts, which are sequentially required for

meiotic maturation during oogenesis. Mature oocytes are arrested at metaphase II (MII) until fertilization. However, fully-grown oocytes are first arrested in prophase I (PI). PI meiotic arrest is mediated by high levels of cyclic-Adenosine monophosphate (cAMP) produced by follicle cells of the ovary, which activate protein kinase A (PKA) in the oocyte. PKA maintains the meiotic arrest through suppression of the maturation promoting factor (MPF), itself composed of cyclinB1 and cdc2. cAMP levels are reduced in response to the gonadotropin, luteinizing hormone, which further induces the release of steroid hormones (e.g. Progesterone), which culminate in reduced PKA activity and subsequently stimulating MPF. MPF causes the resumption of meiosis, marked by germinal vesicle breakdown (GVBD), and increased c-mos protein levels which activates the Map Kinase Kinase (MEK) pathway, necessary to maintain MII arrest (Dekel 2005).

In Progesterone-induced rat and *Xenopus* oocytes, *c-mos* transcripts are polyadenylated by a CPE-CPEB dependent mechanism (Sheets et al. 1994; de Moor and Richter 1997; Sheets et al. 1995; Lazar et al. 2004; Josefsberg et al. 2003; Lazar et al. 2002). However, in rat oocytes activation of MPF promotes c-mos translation (Lazar et al. 2004; Josefsberg et al. 2003; Lazar et al. 2002), whereas in *Xenopus* oocytes activation of c-mos translation promotes MPF activity (Sheets et al. 1994; de Moor and Richter 1997; Sheets et al. 1995).

Cyclin B1 mRNA is polyadenylated by a CPEB and Pumilio dependent pathway (Nakahata et al. 2003; Groisman et al. 2002; Barkoff et al. 2000). Coincidently, cyclinB1, a component of MPF, is translated prior to c-mos in rat oocytes to promote cell cycle progression (Dekel 2005; Josefsberg et al. 2003; Lazar et al. 2002; Lazar et al. 2004), but

in *Xenopus* oocytes, c-mos stimulates *cyclinB1* polyadenylation during meiotic maturation (de Moor and Richter 1997; Howard et al. 1999). Together, these results suggest that either the sequential activity of MPF and c-mos proteins differ amongst vertebrates, though both are required, or that potentially, an autocatalytic feedback loop sustains MPF and c-mos activity during meiotic maturation.

4.1.1.6 Chapter overview

In this chapter, I build on the observation in chapter 3 (Figure 3.5A-B) that XBcl9 mRNA and proteins were expressed in a non-reciprocal fashion, which suggested the possibility of post-transcriptional control of XBcl9 transcripts during embryogenesis. I have determined that translation of XBcl9 mRNA is regulated by its 5'UTR. These results suggest a novel level of regulation governing vertebrate embryonic axis formation, by limiting the translation of a key component using a previously unidentified mechanism.

4.2 Materials and Methods

4.2.1 Embryo collection and manipulation

Wild type embryos were obtained from female *Xenopus laevis* using standard techniques as described (Lake et al. 2001; Kao and Lockwood 1996). Fertilized eggs were injected in 50% Normal Amphibian Medium (NAM) supplemented with 2-4% Ficoll and cultured in 5% NAM. Embryos were staged according to Nieuwkoop and Faber (1994). Embryos were photographed for phenotype analysis using a Leica MZ FLIII microdissection microscope fitted with 'Cool Snap' camera and software.

4.2.2 In silico analysis of Bcl9 5'UTR sequences

Alignment of the 5'UTR sequences was performed online using the ClustalW2 internet based software (http://www.ebi.ac.uk/Tools/clustalw2/index.html). The 5'UTR sequences were derived from cDNA encoding XBcl9 (Accession no. GQ891057), hBcl9 (Accession no NM_004326), hBcl9-L (Accession no. NM_182557), mBcl9 (Accession no. NM_029933) and dLgs (Accession no. 143665).

Secondary structure predictions were made using OligoTech (http://www.oligosetc.com/) and RNAFold web server (http://rna.tbi.univie.ac.at/) free online software.

4.2.3 Plasmid construction and RNA synthesis

pCS2+/XBcl9 5'UTR and pCS2+/XBcl95'UTR-Xβ-catenin were constructed by PCR amplification of the 290nt, 5'UTR sequence from stage 1, embryonic cDNA, restriction digested and ligated into the BamHI/ClaI sites of pCS2+ and pCS2+/Xβ-catenin (described in Chapter 3, section 3.2.2) expression vectors, respectively. pCS2+/EGFP-Xβ-catenin and pCS2+/XBcl9 5'UTR-EGFP were generated by PCR amplification of the EGFP coding region (lacking a stop codon), using pEGFP-C2 (Addgene) as template. The EGFP amplicon was then restriction digested and inserted into the BamHI/ClaI sites of pCS2+/Xβ-catenin (described in Chapter 3, section 3.2.2) or ClaI/EcoRI sites of pCS2+/XBcl9 5'UTR. pCS2+/EGFP is described in Chapter 3, section 3.2.2. pCS2+/XBcl9$^{\Delta 5'UTR}$ was constructed by PCR amplification of the 3'UTR, restriction digestion and ligation into the XhoI/XbaI sites of pCS2+/XBcl9^{coding} (described in Chapter 3, section 3.2.2). pCS2+/XBcl9$^{F.L.}$ and pCS2+/XBcl9$^{\Delta 3'UTR}$ were made by PCR amplification of the 290nt 5'UTR sequence with the N-terminal EcoRI fragment of XBcl9 cDNA. This fragment as well as pCS2+/XBcl9^{coding} and pCS2+/XBcl9$^{\Delta 5'UTR}$ were restriction digested with ClaI/EcoRI. The 5'UTR+XBcl9 EcoRI fragment was then inserted to pCS2+/XBcl9^{coding} and pCS2+/XBcl9$^{\Delta 5'UTR}$ to generate pCS2+/XBcl9$^{\Delta 3'UTR}$ and pCS2+/XBcl9$^{F.L.}$, respectively. Serial deletions of the XBcl9 5'UTR sequence of pCS2+/XBcl9$^{\Delta 3'UTR}$ expression plasmid were generated by PCR amplification of selected XBcl9 5'UTR regions with the XBcl9 EcoRI fragment described above. These 5'UTR serial deletion fragments were then inserted into the ClaI/EcoRI sites of pCS2+/XBcl9$^{\Delta 3'UTR}$. pCS2+/Luciferase and pCS2+/XBcl9 5'UTR-

Luciferase constructs were generated by PCR amplification of the Luciferase coding cDNA using the pGL3 vector (Promega) as template. The Luciferase cDNA was then restriction digested and inserted into the ClaI/EcoRI sites of pCS2+ and pCS2+/XBcl9 5'UTR. All primers used for the construction of plasmids in this chapter are listed in Table 4.1.

In vitro transcription of all mRNAs used in this chapter were synthesized using the SP6 mMessage mMachine RNA synthesis kit, as per manufacturer's protocol (Ambion).

4.2.4 RNA-EMSA/Gel Retardation Assay

RNA probe was labeled by incorporation of UTP-[α-^{32}P] (Perkin Elmer) during *in vitro* transcription as per manufacturer's protocol using the Sp6 mMessage mMachine RNA synthesis kit (Ambion). Cold (competitor) RNA was *in vitro* transcribed in the absence of UTP-[α-^{32}P]. The entire 290nt 5'UTR was used as template to generate the RNA probe.

Approximately 10μg of total protein (as describe below, 4.2.6) were incubated with ~20,000 cpm of radiolabelled probes in binding buffer (5mM Tris pH 7.5, 15mM KCl, 0.25mM DTT, 5mM $MgCl_2$, 10μg torula RNA, 10% glycerol) with 40 units of RNAseOut (Invitrogen), in a final volume of 20μl, at 30°C for 30 minutes. Protein-bound RNA complexes were resolved on a 5% Native PAGE in 0.5x Tris-borate EDTA (TBE) buffer for 1.5hrs at 100volts.

4.2.5 β-Galactosidase and Luciferase Assays

All embryos used for luciferase assays were co-injected with 50pg each of 5'UTR-Luciferase plasmid and β-galactosidase (β-gal) mRNA for each experiment. β-Gal assays were performed as per manufacturer's protocol (Clontech). Approximately 10μl of total protein extracted from cohorts of 5 embryos were incubated in 200μl of Z-buffer (60mM $Na_2HPO_4 \bullet 7H_2O$, 40mM $NaH_2PO_4 \bullet {}_2O$, 10mM KCl, 1mM $MgSO_4 \bullet 7H_2O$, pH 7.0) with 4g/L ONPG (2-Nitrophenyl β-D-galactopyranoside) (SIGMA) and β-Mercaptoethanol (0.27%) at 37°C until yellow color developed. Reactions were then stopped by the addition of equal volume of 1M Tris (pH 11) and colour intensity was measured using a BioRad 3550 microplate reader. Luciferase assays were performed as per manufacturer's protocol. Ten microliters of total protein extracts were used per luciferase reaction. Samples were read in a Monolight 2010 Luminometer.

4.2.6 RNA Analysis and Western Blotting

Total RNA was extracted from cohorts of 10-12 embryos using the Nucleospin II RNA Extraction Kit (Clontech). For RT-PCR analysis, ~1μg of total RNA was reverse transcribed to cDNA using either 100ng of Random hexamers or an 18mer oligo dT primer (IDTDNA) and MMLV-RT (Invitrogen) as per manufacturer's protocol. cDNA was diluted 1:10 and 2 μl was used per PCR reaction. XBcl9 was PCR amplified for 28 cycles from Random primed cDNA and 29 cycles from Oligo dT primed cDNA. XBcl9 primers: forward primer: 5'-GAGGCGCTACCGGTAATT-3'; reverse primer: 5'-

GGGTCACGATACAGCAGTGCTCATC-3'. Levels were normalized to the housekeeping gene Ornithine Decarboxylase (ODC). ODC was PCR amplified for 23 cycles. ODC primers: forward 5'-GCCATTGTGAAGACTCTCTCCATTC-3'; reverse 5'-TTCGGGTGATTCCTTGCCAC-3' (Heasman et al. 2000).

Approximately 5μg of total RNA, extracted as described above, was used for northern blots essentially as described (Kao and Hopwood 1991). The H4 probe was generated by PCR amplification of a fragment of Histone 4 (Lake and Kao 2003b) from embryonic cDNA. Probes specific to 5'UTR-Xβ-catenin and EGFP-Xβ-catenin were also generated by PCR using plasmid DNA as template. 5'UTR-Xβ-catenin probe: Forward primer: 5'-GGGAGTCTAAAGCTGCCG-3'; EGFP-Xβ-catenin probe: Forward primer: 5'-GCGCGATCACATGGTCCTGC-3'. Both probes used an internal Xβ-catenin reverse primer: 5'-TGGTCCTCGTCATTAAGC-3'. PCR products were gel purified (Ultrafree-DA, Millipore Corp.) and used for random labeling (Prime-a-Gene, Promega) with ATP-[α-^{32}P] (Perkin-Elmer). Radiolabelled probes were hybridized at 58-60°C and visualized by autoradiography.

Whole embryo protein was extracted by homogenization in 1XTm (10mM Tris (pH 7.5), 1% Triton-X 100, 10 mM EDTA, 0.02% NaN_3) with protease inhibitors, and incubated on ice, 30min. Total protein was extracted from 293T cells in 1XTm with protease inhibitors (as above). Homogenate was then passed through a 1cc syringe 8-10 times and centrifuged at ~14,000 rpm at 4°C, 10 minutes to pellet cellular debris. Soluble protein extract/supernatant was transferred to sterile tubes. Protein samples were resolved by denaturing SDS-PAGE and transferred to nitrocellulose membrane (Amersham).

Membranes were then probed with affinity purified XBcl9 antibody (section 3.2.6 and Figure 3.4) (1:750 dilution), EGFP antibody (1:3000 dilution) (Abcam) or β-tubulin antibody (1:3000 dilution) (Developmental Studies Hybridoma Bank). HRP-conjugated secondary antibodies (Amersham) were detected using the ECL-Plus (XBcl9) and ECL (EGFP and β-tubulin) (GE Healthcare) western detection systems.

4.2.7 Cell Culture

Human embryonic kidney (293T) cells (American Type Culture Collection, ATCC) were cultured at 37°C, 5% CO_2 in Dulbecco's modified Eagle's medium (DMEM) (Sigma) supplemented with 10% fetal bovine serum (FBS) (Invitrogen). Approximately $2x10^5$ cells were seeded per well in 12-well plates, 24hrs prior to transfection. Approximately 0.4μg of plasmid DNA was transfected using Lipofectamine and Plus reagent as per manufacturer's protocol (Invitrogen). Cells were then cultured for 24hrs before protein extraction as describe above (section 4.2.6).

4.3 Results

4.3.1.1 Identification of a novel mechanism regulating XBcl9 protein expression

In chapter 3 (Figure 3.5A-B), I demonstrated that XBcl9 mRNA and protein are expressed in a non-reciprocal fashion; the levels of XBcl9 mRNA began to decrease to relatively low levels as the amount of detectable protein increased during late blastula stages or just prior to the onset of gastrulation. Furthermore, I demonstrated that XBcl9 mRNA was ubiquitously distributed in the early embryo at this time but that XBcl9 protein preferentially accumulates in dorsal nuclei (Figure 3.6). In other experiments, I attempted to overexpress XBcl9 protein in early embryos, but injection of RNA synthesized from full length XBcl9 cDNA either failed to be translated or was inefficiently translated when injected into embryos. Based on these observations I hypothesized that XBcl9 mRNA may be post-transcriptionally regulated.

Many RNAs are post-transcriptionally regulated by mechanisms involving the 3'UTR. One such mechanism is through the selective addition/removal of the poly(A) tract on the 3' end of messenger RNAs. I first tested, therefore, whether poly(A) XBcl9 mRNA was asymmetrically localized in embryos compared to total XBcl9 mRNA (Figure 3.5C). I extracted total RNA from dissected embryos at stage 6 when the total XBcl9 mRNA expression is relatively high, (Figure 3.5A) and at stage 8.5 when the total XBcl9 mRNA levels decline (Figure 3.5A). XBcl9 cDNA was generated by reverse transcription using either random hexamers or oligo dT primers which selects for poly(A) mRNA. The distribution of total and poly(A) XBcl9 mRNA inferred from RT-PCR

Figure 4.2 XBcl9 mRNA is ubiquitously expressed in *Xenopus* embryos.

A) Relative distribution of total XBcl9 transcripts in embryo halves by RT-PCR analysis of cDNA generated using random hexamer primers. B) Relative distribution of Poly(A) XBcl9 mRNA in embryo halves by RT-PCR analysis of cDNA generated using Oligo dT primers. XBcl9 mRNA levels are normalized to *ornithine decarboxylase* (*ODC*) levels. An = animal; Vg = vegetal; D = dorsal; V = ventral.

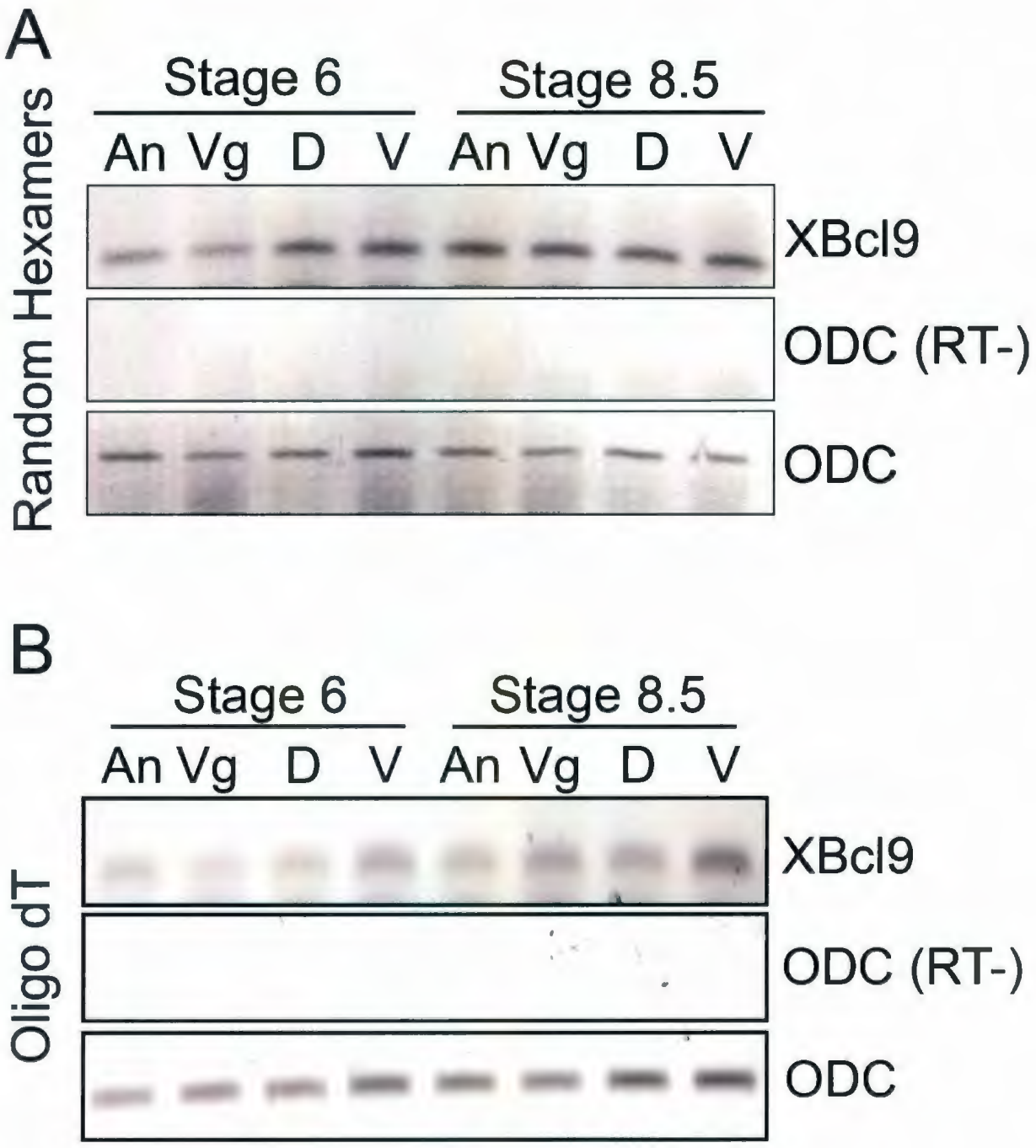
A
Stage 6
Stage 8.5
An Vg D V An Vg D V
Random Hexamers
XBcl9
ODC (RT-)
ODC
B
Stage 6
Stage 8.5
An Vg D V An Vg D V
Oligo dT
XBcl9
ODC (RT-)
ODC

revealed approximately equal levels in dorsal and ventral cells as well as in animal and vegetal cells (Figure 4.2). The lack of localized poly(A) XBcl9 mRNA expression suggested that endogenous XBcl9 protein levels are likely regulated by nucleotide (nt) sequences in the untranslated regions of XBcl9 mRNA. Interestingly, a comparison of the poly(A) XBcl9 transcript levels to that of total XBcl9 mRNA levels, indicated that only a fraction of maternal XBcl9 messages are polyadenylated. Thus, the level of poly(A) XBcl9 mRNA may also play a role in limiting XBcl9 protein levels. However, this experiment was only performed once and needs to be repeated.

To determine if sequences from the non-coding regions of XBcl9 mRNA were regulating translation, I next generated XBcl9 expression constructs that lacked either the 290nt 5'UTR, the 672nt 3'UTR or both. Molar equivalents of synthetic mRNA, based on 2ng of XBcl9 coding mRNA, transcribed from the XBcl9 deletion constructs (Figure 4.3A) were injected into both cells near the animal pole at the 2 cell stage. Embryos were cultured until stage ~8.5 when endogenous XBcl9 protein levels are relatively low (Figure 3.5B). Total protein from ten (10) homogenized embryos was extracted and XBcl9 protein levels in these pooled samples were analyzed by western blot. Compared to uninjected, endogenous control levels, overexpressed XBcl9 protein was only detected in embryos injected with XBcl9 mRNA that lacked the 5'UTR sequence (*i.e.* $XBcl9^{coding}$ and $XBcl9^{\Delta 5'UTR}$) (Figure 4.3B).

The mechanism regulating the observed pattern of endogenous XBcl9 protein levels in early development is not known (Figure 3.5B and Figure 3.6A-D). Given that the 5'UTR appears to influence translation, I asked if the repression of exogenous XBcl9

Table 4.1 Polymerase chain reaction and cloning primers

Plasmid Name	Primer Sequences (5'→3')
pCS2+/ XBcl9 5'UTR	F: GCGGATCCGGGAGTCTAAAGCTGCCG R: GCATCGATTCTTCGGACATGTGCCTC
pCS2+/EGFP-Xβ-catenin	F: CGGGATCCATGGTGAGCAAGGGCGAG R: GCATCGATCTTGTACAGCTCGTCCATGC
pCS2+/XBcl9 5'UTR-Xβ-catenin	F: GCGGATCCGGGAGTCTAAAGCTGCCG R: GCATCGATTGTTCGGACATGTGCCTC
pCS2+/XBcl9$^{F.L.}$	F: GCATCGATGGGAGTCTAAAGCTGCCGTG R: GCGAATTCTGGGGGTTCATGC
pCS2+/XBcl9$^{\Delta 5'UTR}$	F: CGCTCGAGGCTGCTACGAACGGACA R: GCTCTAGACTGTATGAGGTCATAG
pCS2+/XBcl9$^{\Delta 3'UTR}$	F: GCATCGAGGCTGCTACGAACGGACA R: GCGAATTCTGGGGGTTCATGC
pCS2+/XBcl9$^{5'UTR\ (94-290)}$	F: GCATCGATCGGAGAGTACGAGCGCCC R: GCGAATTCTGGGGGTTCATGC
pCS2+/XBcl9$^{5'UTR\ (191-290)}$	F: GCATCGATCTAGACAAGATGAGCACTGC R: GCGAATTCTGGGGGTTCATGC
pCS2+/XBcl9$^{5'UTR\ (232-290)}$	F: CGATCGATCCTGTGTGCCTTGGCGAT R: GCGAATTCTGGGGGTTCATGC
pCS2+/XBcl9$^{5'UTR\ (262-290)}$	F: GCATCGATCTCTGCAGCGAGAGGCAC R: GCGAATTCTGGGGGTTCATGC
pCS2+/XBcl9 5'UTR-EGFP	F: GCATCGATATGGTGAGCAAGGGCGAG R: GCGAATTCCTTGTACAGCTCGTCCATGC
pCS2+/Luciferase	F: GCATCGATATGGAAGACGCCAAAAAC R: GCGAATTCTTACACGGCGATCTTTCC
pCS2+/XBcl9 5'UTR-Luciferase	F: GCATCGATATGGAAGACGCCAAAAAC R: GCGAATTCTTACACGGCGATCTTTCC

Figure 4.3 5'UTR represses translation of XBcl9.

A) Schematic representation of XBcl9 constructs generated by deleting various non-coding sequences from the XBcl9 cDNA. B) Western blot analysis of total XBcl9 protein levels in stage 8.5 and C) stage 10.5 embryos injected with ~2ng of synthetic mRNA transcribed by the XBcl9 constructs illustrated in A). Total protein levels were normalized using β-tubulin as a loading control.

A


XBcl9 Full length cDNA
5'UTR
3'UTR
XBcl9Δ3'UTR
5'UTR
XBcl9Δ5'UTR
3'UTR
XBcl9 coding

B

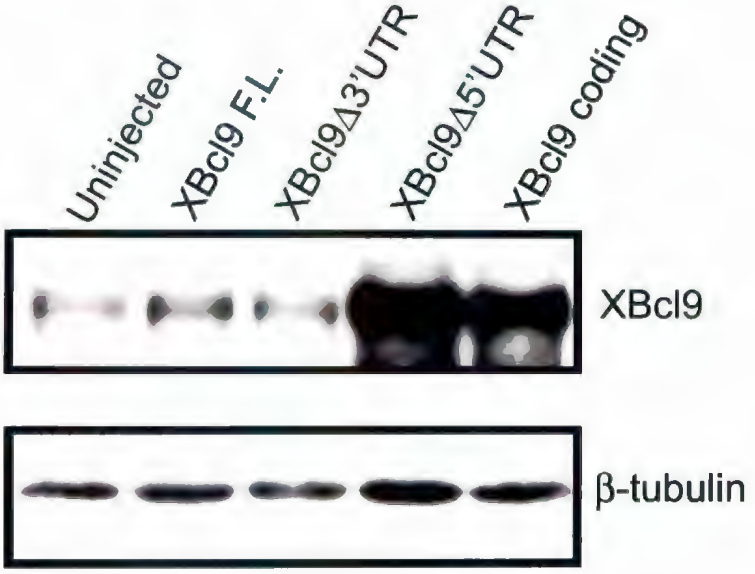
Uninjected
XBcl9 F.L.
XBcl9Δ3'UTR
XBcl9Δ5'UTR
XBcl9 coding
XBcl9
β-tubulin

C

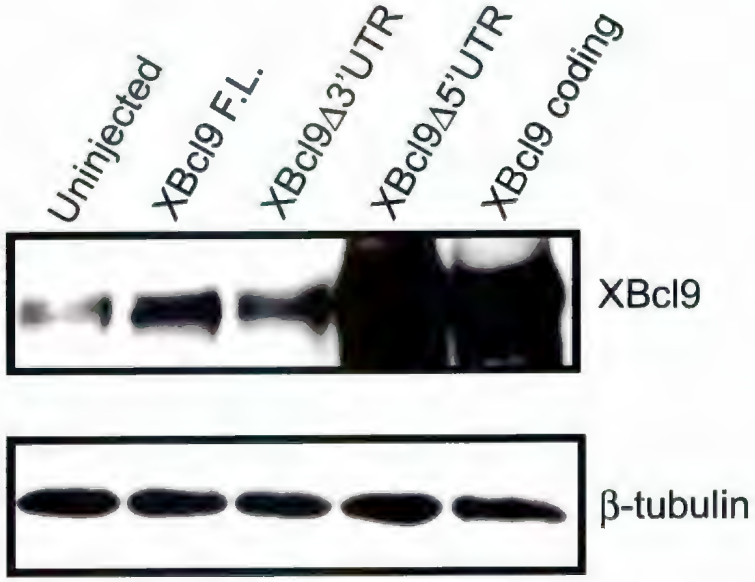
Uninjected
XBcl9 F.L.
XBcl9Δ3'UTR
XBcl9Δ5'UTR
XBcl9 coding
XBcl9
β-tubulin

mRNA was temporally regulated in embryos that mirrored the dynamics of endogenous XBcl9 protein accumulation (Figure 3.5B). Total protein was extracted from ten stage 10.5 embryos injected with mRNA transcribed from each XBcl9 deletion construct as described in Figure 4.3A. XBcl9 protein levels in embryos injected with $XBcl9^{coding}$ or $XBcl9^{\Delta 5'UTR}$ mRNA continued to accumulate to extremely high levels (Figure 4.3C). Interestingly, at this stage, embryos injected with either $XBcl9^{F.L.}$ or $XBcl9^{\Delta 3'UTR}$ mRNA were detected at elevated levels relative to uninjected control levels (Figure 4.3C). These results suggest the existence of a novel repression domain solely dependent on the 5'UTR of XBcl9 mRNA that is temporally regulated in embryos by the same mechanism that regulates endogenous XBcl9.

To determine if the translational repression of XBcl9 mRNA mediated by the 5'UTR sequence is functionally conserved I transfected human embryonic kidney (HEK293T) cells with each of the XBcl9 cDNA expression plasmids described in figure 4.3A. After 24 hrs, total protein was harvested from transfected cells and the levels of XBcl9 were analyzed. Total Bcl9 protein levels in cells transfected with either $XBcl9^{F.L.}$ or $XBcl9^{\Delta 3'UTR}$ cDNA were nearly unchanged (Figure 4.4). Transfection of $XBcl9^{\Delta 5'UTR}$ or $XBcl9^{coding}$ cDNA significantly increased the total Bcl9 protein levels (Figure 4.4), thus demonstrating functional conservation of the 5'UTR of XBcl9.

Figure 4.4 The 5'UTR represses XBcl9 translation in 293T cells.

Western blot analysis of total Bcl9 protein levels in 293T cells transfected with the XBcl9 DNA constructs cartooned in Figure 4.3A. Overexpression of XBcl9 was only detected in cells transfected with expression constructs that lacked the 5'UTR. Total protein levels were normalized using β-tubulin as a loading control. EV = empty vector.

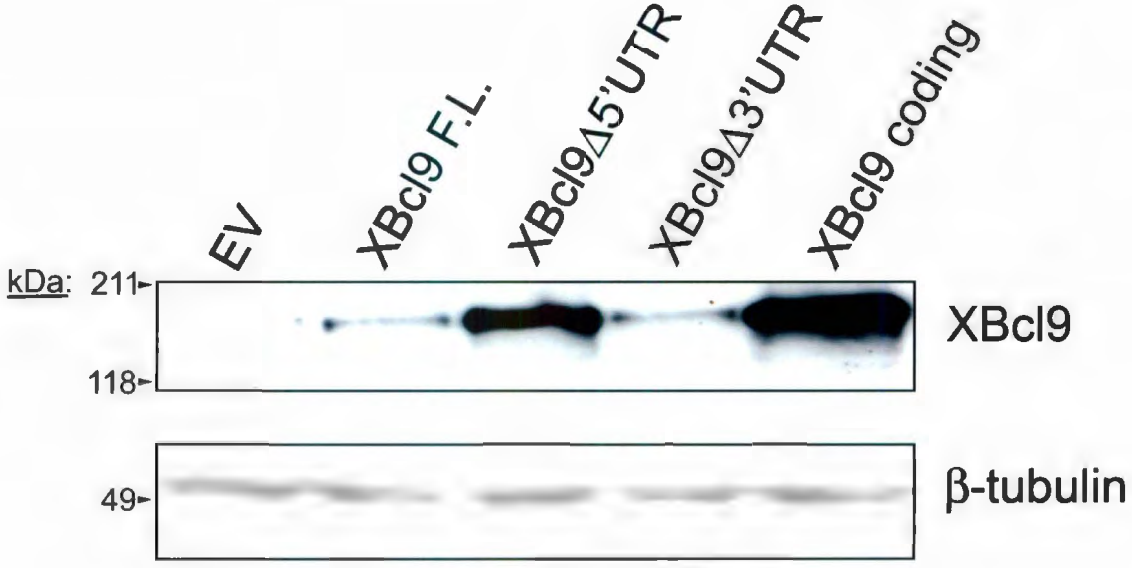
EV
XBcl9 F.L.
XBcl9Δ5'UTR
XBcl9Δ3'UTR
XBcl9 coding
kDa:
211
118
XBcl9
49
β-tubulin

4.3.1.2 XBcl9 5'UTR minimal repression domain

To identify the repression element(s) within the 5'UTR, I systematically deleted 5'UTR sequences from the $XBcl9^{F.L.}$ expression construct described above (Figure 4.3A). Figure 4.5A is the entire 290nt XBcl9 5'UTR sequence. I then injected 2ng of mRNA transcribed, *in vitro,* using templates made from each deletion construct shown in figure 4.5A, into *Xenopus* embryos at the 2 cell stage. The levels of XBcl9 protein in whole protein lysate obtained from ten stage 8.5 embryos were analyzed by western blot. No increase in protein levels were detected in embryos injected with $XBcl9^{5'UTR}$ or $XBcl9^{(94-290)}$ mRNA (Figure 4.5B). Very small increases in XBcl9 protein levels were detected in embryos injected with the mRNA made from serial deletion constructs: $XBcl9^{5'UTR\ (191-290)}$, $XBcl9^{5'UTR\ (232-290)}$ or $XBcl9^{5'UTR\ (262-290)}$. However, deletion of the 29 nucleotides proximal to the putative start of translation, relieved translational repression and XBcl9 protein was detected at levels similar to those obtained in embryos injected with $XBcl9^{coding}$ mRNA (Figure 4.5B). Thus, nucleotides 262-290 of the 5'UTR of XBcl9 mRNA contain the minimal repression domain.

The repression of the 5'UTR of XBcl9 is conserved in *Xenopus* (Figure 4.4) and human cell lines (Figure 4.5), respectively. Mapping of the minimal repression domain (Figure 4.5) raised the question as to whether there was any evolutionary conservation in nucleotide sequence of the 5'UTR of XBcl9 with other Bcl9 orthologues. Using ClustalW2 internet based software, I aligned the XBcl9 5'UTR 29nt minimal repression sequence with the 5'UTR of the human (h) and mouse (m) Bcl9, and *Drosophila* (d) Legless (Lgs)

Figure 4.5 Mapping the 5'UTR minimal repression element.

A) Complete 290 nucleotide sequence of the XBcl9 5'UTR. N-terminal deletions were made at each residue indicated in red. Start codon is highlighted green. B) Western blot analysis of total XBcl9 protein levels in embryos injected with synthetic XBcl9 mRNA with each serial 5'UTR deletion indicated in A). Total protein levels were normalized to β-tubulin levels.

A

1 - gggagucuaaagcugccgugauaccggcugugagaggcggaggagaaacc

51 - cgggacaggcccggccggcgcgucacaccucacccccaacccc[94]ggagag

101 - uacgagcgcccccucccuccgcgcgcuccuccuguucuacccgaggcgcu

151 - accgguaauuacguuucuguugcacgggcccucacugacu[191]ucuagacaag

201 - augagcacugcuguaucgugaccccaggggac[232]cugugugccuuggcgaug

251 - cacaacguucc[262]cucugcagcgagaggcacauguccgaaga ATG

B

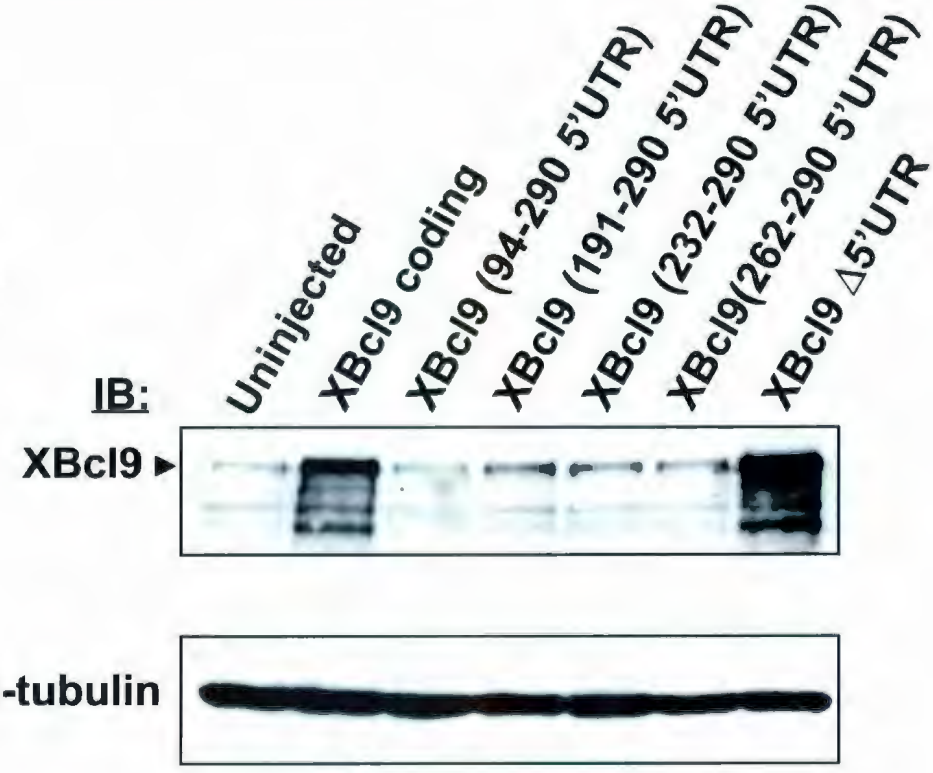

cDNA sequences, as well as the closely related human (h) Bcl9-L sequence.

This *in silico* analysis identified significant similarity between the 29nt repression element and a region in each 5'UTR sequence. The 29nt repression domain was most highly conserved with human Bcl9 5'UTR where 22/29 (76%) nucleotides were perfectly conserved in a nearly contiguous stretch of sequence (Figure 4.6A) as compared to 17/29 (59%), 14/29 (48%) and 13/29 (45%) with hBcl9-L, mBcl9 5'UTR and dLgs RNA sequences, respectively (Table 4.2). These results suggest the possibility that the 29nt repression domain or some part of it may be evolutionarily conserved.

Since I had mapped the repression domain to the 29nt proximal to the putative translational start codon, I next determined if this sequence is predicted to form any stable secondary structure(s). I analyzed the 29nt repression domain using two different online software programs, OligoTech (http://www.oligosetc.com/) and RNAfold web server (http://rna.tbi.univie.ac.at/). Both programs predicted the formation of a stable stem-loop structure in the XBcl9 5'UTR from 29nt – 15nt (Figure 4.6B). The free energy associated with the stem-loop ranged from -2.2 (OligoTech) to -3.8 (RNAfold web server) joules suggesting that the stem-loop structure readily forms and requires an input of energy to resolve the secondary structure. Furthermore, OligoTech predicted the stem-loop to have a melting temperature (T_m) of 56°C, well above the ambient body and water/culture medium temperature of *Xenopus* eggs (~18-24°C).

Table 4.2 Comparison of select Bcl9 5'UTR nucleotide sequences.

	% sequence identity				
	XBcl9	hBcl9	hBcl9-2	mBcl9	dLgs
XBcl9	-	76%	59%	48%	45%
hBcl9	76%	-	37%	59%	37%
hBcl9-2	59%	37%	-	55%	37%
mBcl9	48%	59%	55%	-	37%
dLgs	37%	37%	37%	37%	-

Figure 4.6 *In silico* analysis of Bcl9 5'UTR sequences.

A) ClustalW2 sequence alignment of the minimal XBcl9 5'UTR repression element with other Bcl9 5'UTR sequences. Nucleotides conserved between *Xenopus* and human Bcl9 5'UTR sequences are highlighted in red. Residues conserved in all species analyzed are indicated by an asterisk. B) Prediction of secondary structure in the minimal XBcl9 5'UTR sequence. Base-pairing of complementary sequence producing the secondary structure is outlined by the box. The color bar indicates the predicted entropy associated with each ribonucleotide; the higher the entropy the greater the free energy produced upon folding.

A

```
XBcl9 5′UTR:          260...CUCUG-CAGC-GAGAGGCACAUGUCCGAAGA...290
hBcl9 5′UTR:          507...CUCUGGCAGCAG-GAGGCACGCACCCAGAGA...537
hBcl9-L 5′UTR :       536...C-CUGGGUGAGGGGCGCGUCUGGGAGCAGGA...566
mBcl9 5′UTR:           11...C-CAGCACUAAGGGACGCACCAAGCA-AACA...40
dLgs 5′UTR:            73...CUCUU-AUUAUGCGAGCUGUUUAUUCCAAAG...102
                          * *           * *
```

B

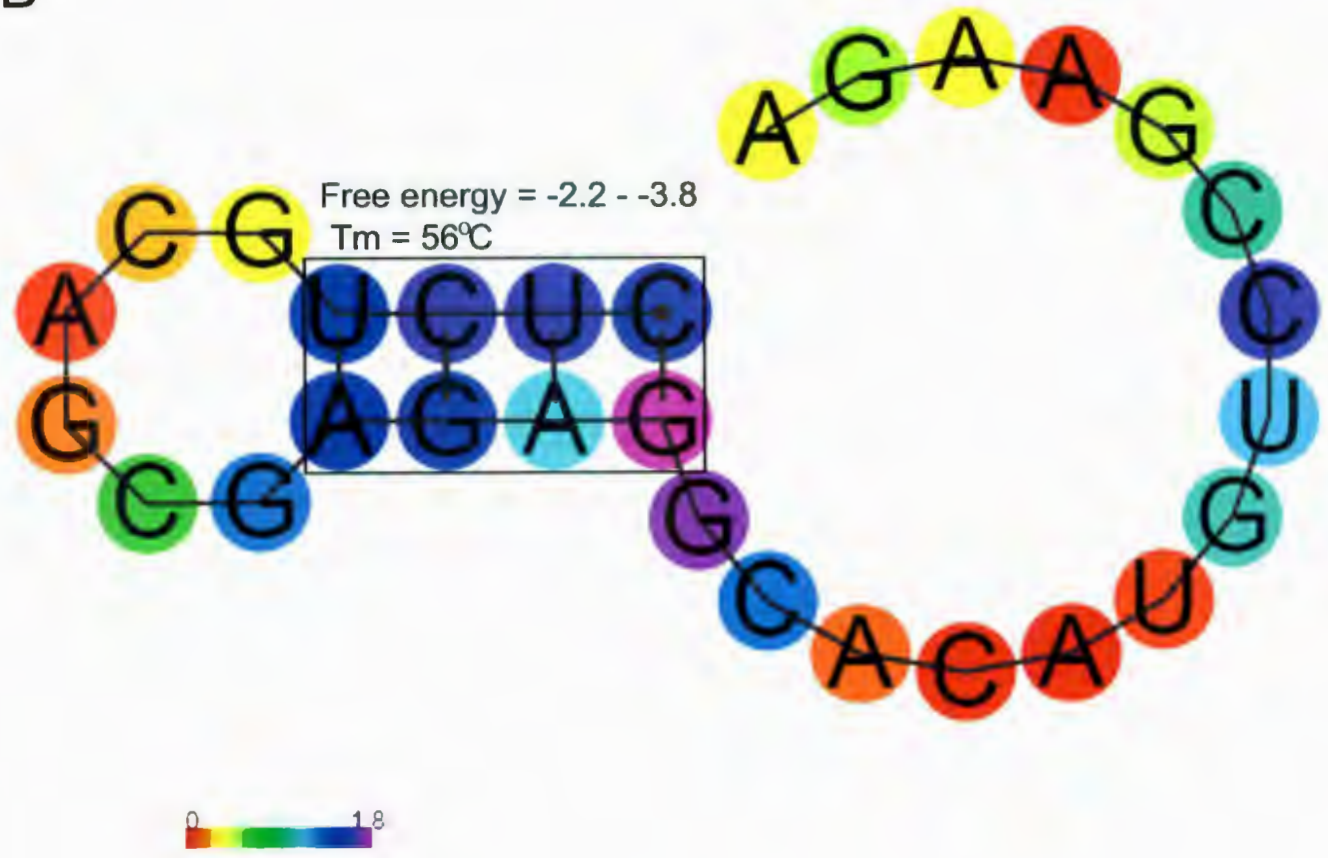

4.3.1.3 Intrinsic repression activity of the 5'UTR sequence of XBcl9

Based on the observation that the 5'UTR of *XBcl9* mRNA could effectively prevent the translation of XBcl9 protein, I next determined if the repression activity of the 5'UTR was intrinsic or if it required additional nucleotide sequence present in the XBcl9 coding region. I created a chimeric expression construct by fusing the 5'UTR cDNA sequence of XBcl9 to the N-terminus of the β-catenin coding region cDNA. To prevent confusion of referring to the 5'UTR of XBcl9 when fused with other genes, I will heretofore call it BUTR. Ectopic expression of β-catenin mRNA in the ventral marginal region of 2-4 cell stage *Xenopus* embryos induces a complete secondary axis (Funayama et al. 1995; Lavery and Hoppler 2008). Therefore, I hypothesized that if the BUTR suppressive activity is intrinsic to the nucleotide sequence itself, then it should be capable of reducing or inhibiting the translation of any mRNA (e.g. β-catenin) to which it is fused. I exploited the secondary axis induction bioassay by injecting β-catenin mRNA or chimeric BUTR-β-catenin mRNA into the ventral marginal zone of *Xenopus* embryos at the 2 cell stage. The frequency of induction of partial and complete secondary embryonic axes by β-catenin mRNA increased with increasing dose (Figure 4.7Aii-iv and B). At 100pg, 200pg and 400pg of β-catenin mRNA, the observed frequency of induction of complete/partial secondary axes was 20%/9%, 45%/21% and 61% /18%, respectively (Figure 4.7B). Supernumerary axis formation (*i.e.* secondary axis formation was significantly reduced when 100pg (0%/0%), 200pg (4%/4%) and 400pg 39%/14%) of BUTR-β-catenin mRNA was injected (Figure 4.7B). These results suggested that the

Figure 4.7 Chimeric BUTR-β-catenin has reduced twinning activity.

A (i)) Uninjected control embryos. A (ii-iv)) Ventral over-expression of increasing amounts of β-catenin or (v-vii) BUTR-β-catenin mRNA. B) Graphical representation of the observed frequency of axial duplication from A. The total number of analyzed embryos from 2 experiments is indicated in brackets. Complete secondary axis defined by having a full complement of dorsoanterior structures; partial axis duplication refers to embryos with two body axes but lacked head structures on one. Red arrow heads point to the anterior ends of duplicated body axes.

A

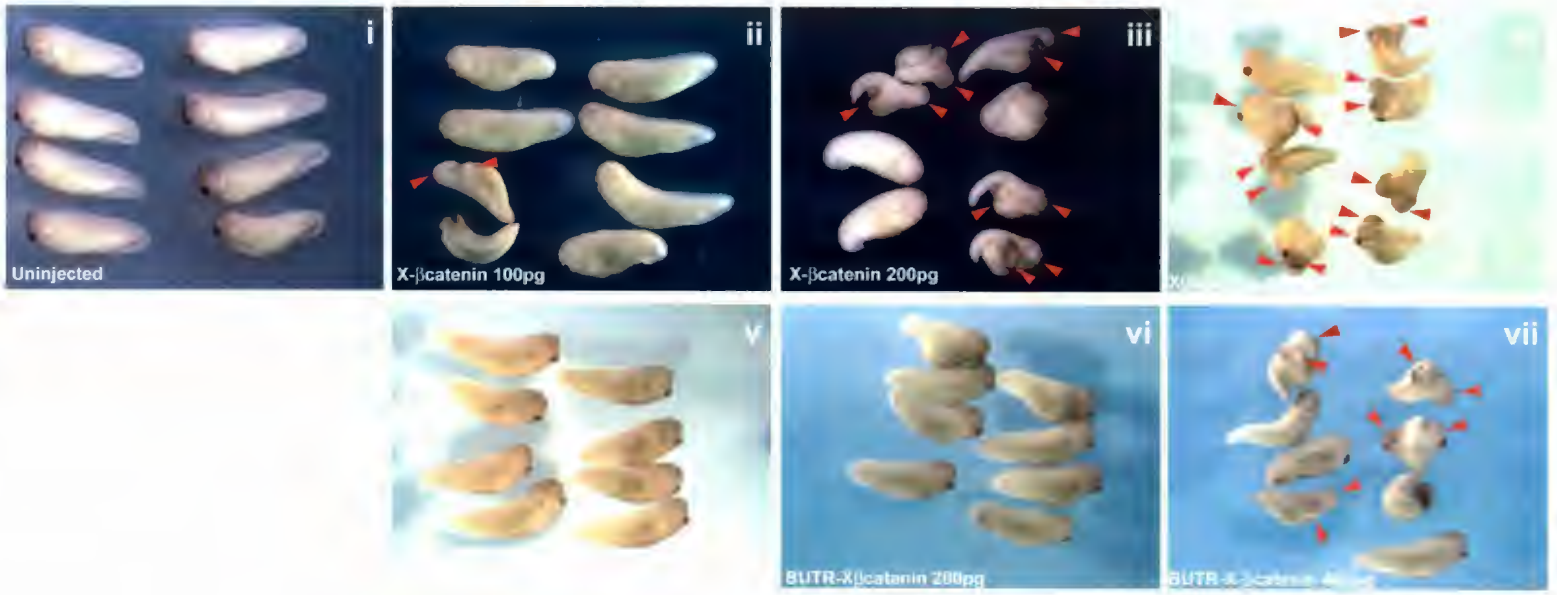
i
Uninjected
ii
X-βcatenin 100pg
iii
X-βcatenin 200pg
v
vi
BUTR-Xβcatenin 200pg
vii

B

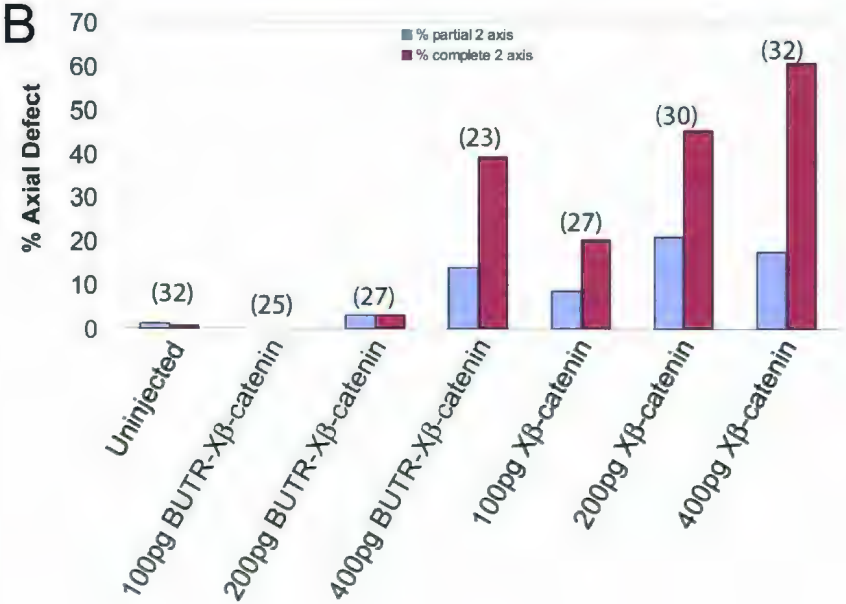
% Axial Defect
70
60
50
40
30
20
10
0
% partial 2 axis
% complete 2 axis
(32)
(25)
(27)
(23)
(27)
(30)
(32)
Uninjected
100pg BUTR-Xβ-catenin
200pg BUTR-Xβ-catenin
400pg BUTR-Xβ-catenin
100pg Xβ-catenin
200pg Xβ-catenin
400pg Xβ-catenin

repressive activity of the 5'UTR of XBcl9 is intrinsic to the BUTR sequence. The observation of moderate frequency of twinned embryos observed in batches of embryos injected with BUTR-β-catenin mRNA is probably a result of injecting an overwhelming amount of message or more simply, a result of 'leaky' translation of our reporter construct.

I developed two additional BUTR reporter constructs for quantitative analysis of regulated XBcl9 mRNA translation. The first reporter contains BUTR cloned into the N-terminus of the Enhanced Green Fluorescent Protein (EGFP) gene, called BUTR-EGFP. To verify the ability of the 5'UTR to suppress translation from EGFP mRNA, I injected 200pg of either EGFP mRNA or synthetic chimeric mRNA transcribed from the BUTR-EGFP reporter construct into the animal pole at the 2 cell stage. Total protein was harvested from 10 embryos at stages 6.5, 8, 10.5 and 19, to monitor EGFP protein accumulation. In embryos injected with EGFP mRNA, EGFP protein was detected at very high levels that continued to accumulate throughout development (Figure 4.8A). In contrast, the amount of EGFP protein detected at the same stages in embryos injected with BUTR-EGFP mRNA was much lower. It should also be noted that there appeared to be a spike in detected XBcl9 protein levels at stage 10.5 in BUTR-EGFP mRNA injected embryos, corroborating our observation in figure 3.5B, possibly reflecting the elevated levels of endogenous protein detected at stage 10.

For the second reporter, I subcloned the XBcl9 5'UTR adjacent to the N-terminus of the firefly Luciferase gene in a pCS2+ expression plasmid, thus creating a BUTR-

Figure 4.8 Testing additional BUTR reporter constructs.

A) Levels of EGFP protein at several stages of development from embryos injected with either EGFP or BUTR-EGFP mRNA. Total protein levels were normalized to β-tubulin as a loading control. B) Luciferase assay using total stage 8 protein from 3 independent batches of embryos performed in triplicate to infer the relative levels of protein translation from BUTR-Luciferase or Luciferase mRNA co-injected into 2-cell embryos with β-gal mRNA. Error bars represent the standard error of 3 combined experiments. Luciferase assay was normalized by β-gal assay. AP, animal pole; VP, vegetal pole.

A

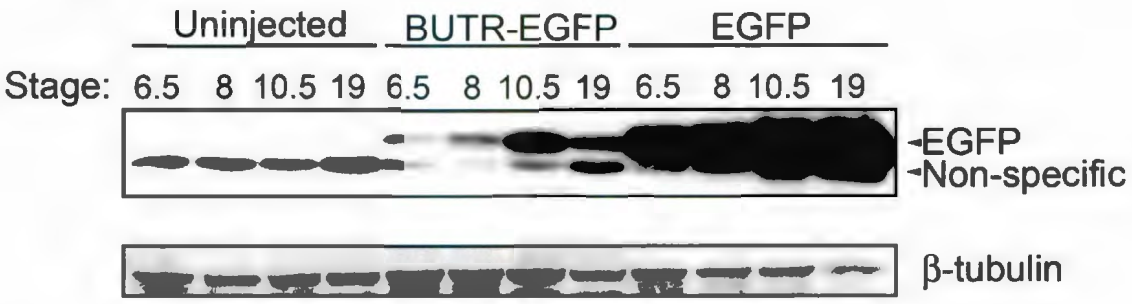
Uninjected
BUTR-EGFP
EGFP
Stage: 6.5 8 10.5 19 6.5 8 10.5 19 6.5 8 10.5 19
EGFP
Non-specific
β-tubulin

B

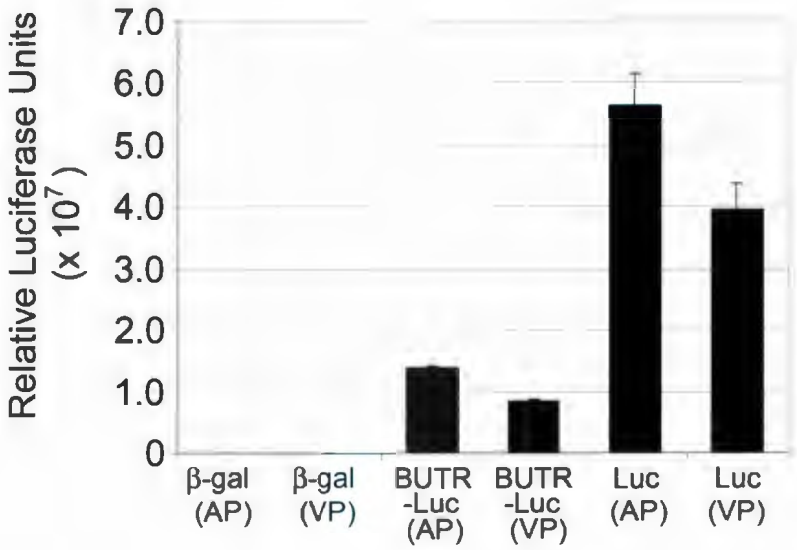
Relative Luciferase Units
(x 10^7)
7.0
6.0
5.0
4.0
3.0
2.0
1.0
0
β-gal (AP)
β-gal (VP)
BUTR -Luc (AP)
BUTR -Luc (VP)
Luc (AP)
Luc (VP)

Luciferase reporter construct. To verify the ability of the BUTR sequence to suppress translation of the Luciferase gene, I injected 50pg of BUTR-Luciferase mRNA into embryos at either the animal pole or vegetal pole. β-galactosidase mRNA (50pg) was co-injected in each embryo to control for mRNA delivery. Luciferase assays performed on total protein harvested from stage ~8.5 embryos demonstrated the suppression of translation of BUTR-Luciferase mRNA to ~25% that of Luciferase in animal cells and ~20% in vegetal cells, as inferred from reduced levels of Luciferase activity (Figure 4.8B). These results verify both the BUTR-EGFP and BUTR-Luciferase as viable reporter constructs that can be used to further study the mechanism of translational repression by the 5'UTR of XBcl9 mRNA.

4.3.1.4 Mode of XBcl9 5'UTR regulation

Mechanisms of mRNA translational regulation are generally imposed by protein interactions that either block translation or destabilize transcripts, micro RNA (miRNA) down-regulation of mRNA levels or the stimulation of translation due by internal ribosomal entry sites (IRES) in untranslated sequences (Abaza and Gebauer 2008; Bettegowda and Smith 2007; Colegrove-Otero et al. 2005; Piccioni et al. 2005; van der Velden and Thomas 1999; Vasudevan et al. 2006). Because the BUTR represses translation of XBcl9 and chimeric reporter mRNAs, it is unlikely to be governed by IRES-mediated mechanisms. Therefore, to determine if XBcl9 translation was regulated

by mRNA stability, I asked if the BUTR affected the stability of exogenous chimeric mRNAs.

Since I found that translational repression is dependent on the nucleotide sequence of BUTR, it is possible that the BUTR destabilizes the mRNA and I would therefore observe a faster rate of turnover of messages containing the BUTR. To test this hypothesis, I injected either 250pg of BUTR-Xβ-catenin mRNA or EGFP-Xβ-catenin mRNA into embryos at the 2 cell stage. Total RNA was collected at stages 6, 8.5 and 11.5 and the expression of exogenous mRNAs was analyzed by Northern blotting. Exogenous mRNAs were specifically detected using probes that significantly overlapped the BUTR or EGFP sequence with the Xβ-catenin coding region. Figure 4.9 illustrates that both the BUTR-Xβ-catenin and EGFP-Xβ-catenin mRNA levels were similar at various post-injection time points. Hence it is unlikely that the BUTR represses translation by accelerating the rate of mRNA turnover.

4.3.1.5 XBcl9 5'UTR mRNA binding proteins

Protein translation is regulated by RNA-binding proteins which interact with the 3'UTR as well as with the methylated 5'cap structure and 5'UTR. My above results have effectively eliminated the likelihood of other known modes of post-transcriptional regulation, such as IRES or mRNA stability. Hence I investigated whether any expressed embryonic protein(s) could interact with the BUTR mRNA as evidence for protein mediated activity.

Figure 4.9 XBcl9 5'UTR does not affect mRNA stability.

Northern blot analysis for XBcl9 5'UTR-β-catenin (Top panel) and EGFP-β-catenin mRNA (Bottom panel). Total RNA levels were normalized by blotting for Histone 4 (H4). Both exogenous mRNAs had similar rates of turnover. Experiment was performed twice.

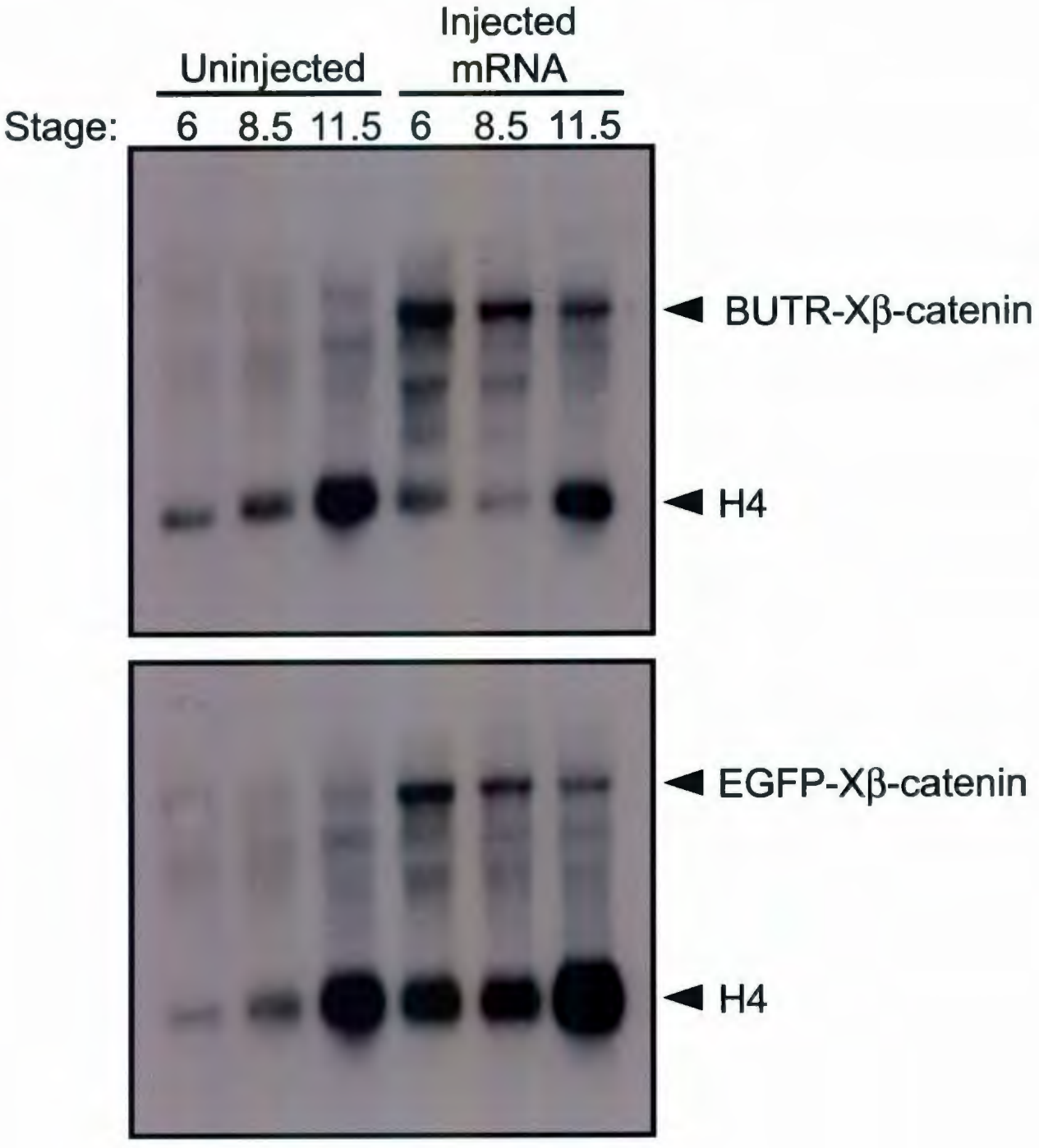
Uninjected
Injected mRNA
Stage: 6 8.5 11.5 6 8.5 11.5
BUTR-Xβ-catenin
H4
EGFP-Xβ-catenin
H4

BUTR mRNA radiolabelled with UTP-[α-^{32}P] was used to probe for interacting proteins from *Xenopus* whole embryo protein extracts. Radiolabelled RNA probes were incubated with stage 6 and stage 10 whole protein extracts. The BUTR mRNA probe formed protein-RNA complexes with endogenous proteins, as shown in figure 4.10. Proteins that bound to the RNA probe were competed off with non-radiolabelled BUTR mRNA, confirming the specificity of the protein-mRNA interaction. Interestingly, stage 10 protein-RNA complexes were more easily competed than those detected from stage 6 protein extracts possibly suggesting differential protein binding at these stages.

Figure 4.10 Identification of BUTR RNA-protein interactions.

RNA-electrophoretic mobility shift assay (RNA-EMSA) using the entire BUTR mRNA, with incorporated α-P^{32}-UTP, as a probe. NB. The relatively small shift was due to the massive size of the probe (290nt). The lack of competed probe detected at similar distances as the free probe is presumably due to RNAse-mediated degradation.

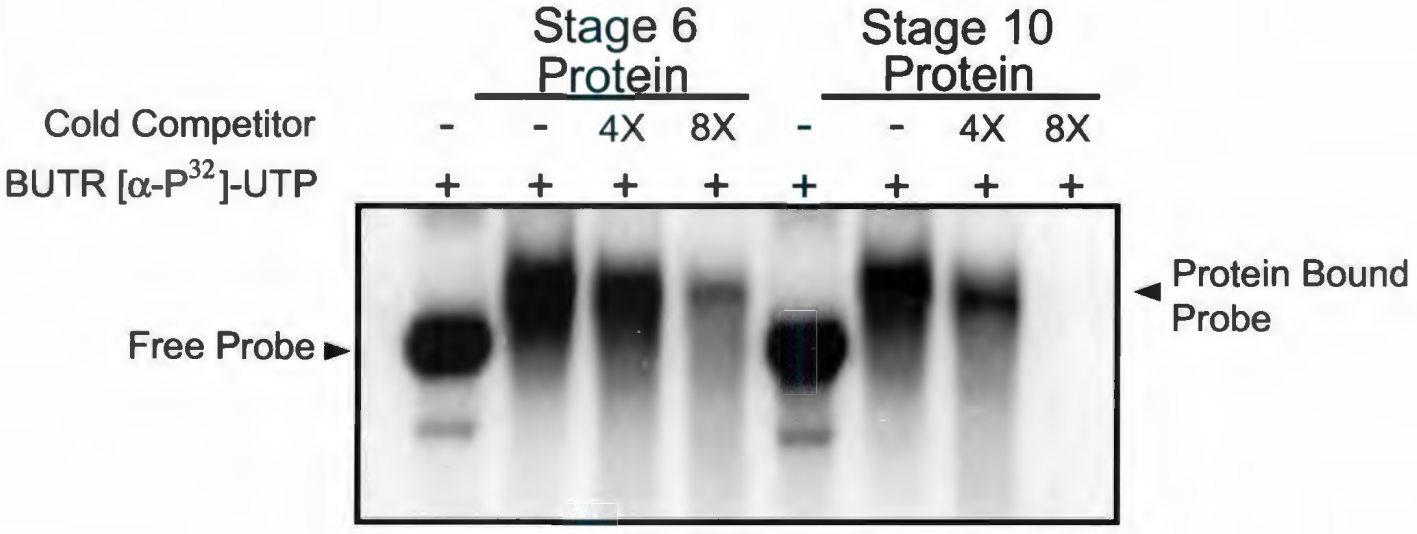
Stage 6 Protein
Stage 10 Protein
Cold Competitor
- - 4X 8X - - 4X 8X
BUTR [α-P32]-UTP
+ + + + + + + +
Free Probe
Protein Bound Probe

4.4 Discussion

4.4.1.1 XBcl9 mRNA is post-transcriptionally regulated

Early embryogenesis occurs in the relative absence of transcription of the zygotic genome. As such, developmental processes, such as body axis formation, are governed largely by maternally inherited proteins and messenger RNAs that are post-transcriptionally regulated, which in turn mediate zygotic gene expression at the MBT/EGA. In chapter 3, I demonstrated that XBcl9 is a maternal factor required for body axis formation and suggested, based on its non-reciprocal mRNA and protein temporal expression pattern, that XBcl9 may be post-transcriptionally regulated in the oocyte and/or embryo. In this chapter, I have determined that XBcl9 mRNA is indeed regulated at the level of translation and have identified a novel, conserved element in the 5'UTR that forms a stable secondary structure capable of repressing translation.

4.4.1.2 XBcl9 translation repressed by 5'UTR secondary structure.

XBcl9 translation is not repressed by destabilizing the XBcl9 mRNA since the transcript is very stable during early development when protein levels are low. If the 5'UTR destabilized the message, then it seems likely that both mRNA and proteins levels would have been expressed in similarly low levels. As well, chimeric BUTR-Xβ-catenin transcripts were equally as stable as chimeric EGFP-Xβ-catenin mRNA ectopically expressed in *Xenopus* embryos. Furthermore, because miRNAs typically regulate transcript levels to control protein expression, they cannot be strictly ruled out as

contributing to a possible mechanism of XBcl9 post-transcriptional regulation. Very few examples of miRNAs that inhibit translation without affecting transcript stability, however, have been reported and are highly controversial (Kozak 2008). Together, these results effectively eliminate transcript instability as a possible mechanism of translational repression of XBcl9.

I reasoned that IRES-mediated translation is not a likely scenario as it normally results in the activation of cap-independent translation. Since I observed translational repression only in BUTR-containing constructs and not in others, all of which were synthesized with a 5' methylated cap, translational regulation of XBcl9 occurs in 5' capped messages but dictated by transcript sequence.

In silico analysis of the minimal repression domain identified a reasonably well-conserved sequence element that was predicted to form a stable secondary structure under ambient conditions. I have, therefore, proposed that XBcl9 translation is uniquely regulated by sequence elements in the BUTR that likely form stable secondary structures interfering with the ability of ribosomes to be recruited to XBcl9 transcripts. Furthermore, the ability to detect protein(s) binding to the BUTR suggests the attractive hypothesis that dissolution of secondary structure may by enzymatically mediated to activate XBcl9 translation. Additional mutational analysis may be necessary to more precisely refine the minimal repression element and to identify potential sequence-specific RNA-binding proteins.

Interestingly, a recent study identified a mechanism whereby secondary structure in the 5'UTR of *junD*, which encodes a member of the AP-1 transcription factor family,

facilitates cap-dependent translation (Hartman et al. 2006; Tettweiler and Lasko 2006). In this report, investigators identified RNA Helicase A (RHA), a DEAD-box RNA binding protein previously demonstrated to function as an enhancer of translation of several viral RNAs (Butsch et al. 1999; Roberts and Boris-Lawrie 2003; Hull and Boris-Lawrie 2002), as possibly facilitating pseudocircularization mRNA (Hartman et al. 2006). In the absence of RHA, mRNAs were suggested to be inefficiently translated or degraded (Hartman et al. 2006; Tettweiler and Lasko 2006).

Studies of iron homeostasis have revealed unique 5'UTR sequences, called iron responsive elements (IRE), that fold into stable secondary structures forming 'docking sites' for RNA-binding proteins which repress translation (Pantopoulos 2004; Wallander et al. 2006; Leipuviene and Theil 2007). IREs have been described in at least ten genes, such as *H-ferritin*, *L-ferritin* (Aziz and Munro 1987; Leibold and Munro 1988; Hentze et al. 1987) and *m-aconitase* (Gray et al. 1996). Two IRE binding proteins, IRP1 and IRP2, have been to shown to bind with high affinity to IREs when cellular iron levels are low, thus blocking translation of IRE-containing mRNAs. When iron levels increase, IRP1 for example, forms a [4Fe-4S] iron cluster that reduces IRP1-RNA binding affinity, effectively relieving translational repression (Pantopoulos 2004; Wallander et al. 2006).

Hence, XBcl9 translation may be similarly regulated to that of either *junD* or IRE-containing mRNAs. That is to say that an XBcl9 5'UTR RNA-binding protein may be required to overcome the secondary structure effects to initiate translation. Alternatively, a unique secondary structure in the XBcl9 5'UTR sequence may recruit maternally

expressed repressor proteins that limit/inhibit translation in cleavage stage embryos, but is de-repressed subsequent to MBT.

Many proto-oncogenes with relatively long 5'UTR sequences are able to form secondary structures that likely reduce translation efficiency (Kozak 1986; Kozak 1987; Kozak 1989). *c-Myc*, *cyclinA2* and *Histones* are examples of genes whose transcripts are translationally regulated by secondary structures (Fraser et al. 1996; Strugnell and Browder 1997; Fu et al. 1991). The translation of human *c-myc* and *Xenopus cyclinA2* 5'UTR reporter constructs were reported to be efficiently repressed in *Xenopus* embryos due to the formation of stem-loops in the 5'UTR sequence (Fraser et al. 1996; Strugnell and Browder 1997). However, it is not clear how the problem of secondary structure is overcome. Intriguingly, Histone mRNAs form a stem loop in the 3'UTR which is bound by stem-loop binding proteins (SLBPs) that mediate pre-mRNA processing into a mature translatable message (Sanchez and Marzluff 2002; Dominski and Marzluff 2007). Hence it is possible that similar SLBPs exist that can mediate the translation of c-myc, cyclinA2 and XBcl9 mRNAs, for example, in response to physiological cues when needed during development.

4.4.1.3 Potential novel mechanism regulating Bcl9 in oncogenesis

Deregulation of canonical Wnt signaling has been implicated in several types of cancer such as breast cancer, leukemia and colon cancer (MacDonald et al. 2009). Aberrant activation of canonical Wnt signaling has often been shown to be a mutagenic

effect of inhibiting pathway components that destabilize β-catenin protein, such as APC (Munemitsu et al. 1995; Rubinfeld et al. 1993), or those that directly render β-catenin insensitive to phosphorylation and subsequent degradation (Palacios and Gamallo 1998).

Recently, Bcl9 has been shown to be over expressed in colon cancer (Mani et al. 2009) and breast and ovarian cancer (Kennedy and Kao, unpublished observations). As a result, Bcl9 has been classified as an oncogene due to its requirement for β-catenin-dependent transcription in human multiple myeloma and colon carcinoma (Mani et al. 2009). Based on my observations that a minimal 29nt region of the 5'UTR is conserved in both human and *Xenopus* Bcl9 sequences and that the XBcl9 5'UTR is repressed in human cells, the elevated levels of Bcl9 in cancer cells may be a result of the loss of translation control. As such the regulation of Bcl9 translation by cis- or trans-elements in the 5'UTR may indicate a novel means of tumor suppression.

Chapter 5: Summary: Antagonistic regulation of β-catenin mediates body axis formation

5.1.1 Revised model of body axis formation

The body axis is derived primarily from specification and patterning of the dorsal mesoderm, a morphogenetic field of the embryo generated by overlapping dorsal-ventral asymmetry unto the specified mesoderm germ layer. As outlined in Chapter 1, maternal determinants required for the specification of the dorsal body parts are associated with the vegetal pole cortex which are displaced following fertilization to a more equatorial position as a result of cortical rotation (Darras et al. 1997; Marikawa et al. 1997). These maternal factors are activating components of the canonical Wnt signaling cascade. In this way, the maternal canonical Wnt pathway establishes the dorsal endodermal Nieuwkoop centre that in turn induces the formation of the Spemann organizer in the overlying mesoderm to generate the embryonic body plan (Figure 1.1).

My research, presented and discussed herein, focused on the regulation of Wnt/β-catenin mediated transcription to further elucidate the mechanism that controls the formation of the body axis. Overall, my results suggest that XRel3 and/or XRelA suppress canonical Wnt signaling by transcriptional inactivation of β-catenin at the mesectodermal boundary, whereas β-catenin is dependent on XBcl9 for target gene expression in dorsally fated cells (Figure 5.1C). Furthermore, I determined that XBcl9 mRNA is post-transcriptionally regulated in *Xenopus* embryos.

Taken together, these results can be used to formulate a model whereby XRel3/XRelA in the animal hemisphere limits the territory in which β-catenin can

Figure 5.1 Spatiotemporal regulation of β-catenin mediated transcription defines the body axis morphogenetic domain.

A) The binding of XRel3 to β-catenin abrogates transcription. B) The association of XBcl9 with β-catenin creates a bridge between Pygo and the basal transcriptional machinery (Mediator complex and RNA polymerase). C) Left: β-catenin transcription is repressed in regions of the embryo by XRel factors and stimulated by XBcl9-Pygo duets in others. In this way, the opposing regulation of β-catenin transcription specifies the morphogenetic field that derives the body axis/notochord (Right). **NB:** Right side is dorsal.

A

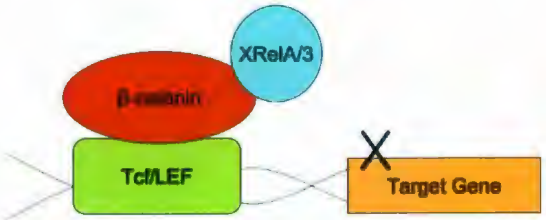
XRelA/3
β-catenin
Tcf/LEF
X
Target Gene

B

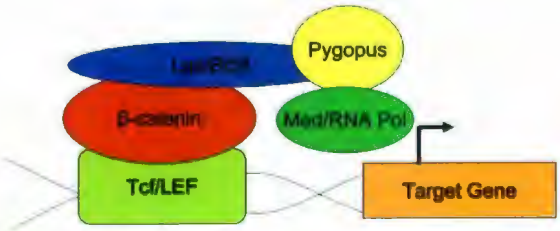
Pygopus
β-catenin
Med/RNA Pol
Tcf/LEF
Target Gene

C

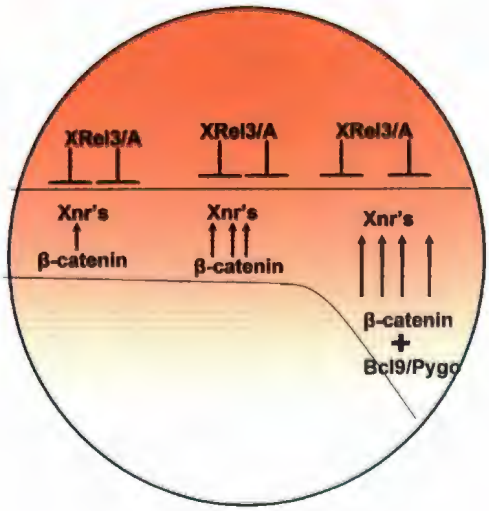
XRel3/A
XRel3/A
XRel3/A
Xnr's
β-catenin
Xnr's
β-catenin
Xnr's
β-catenin
+
Bcl9/Pygo

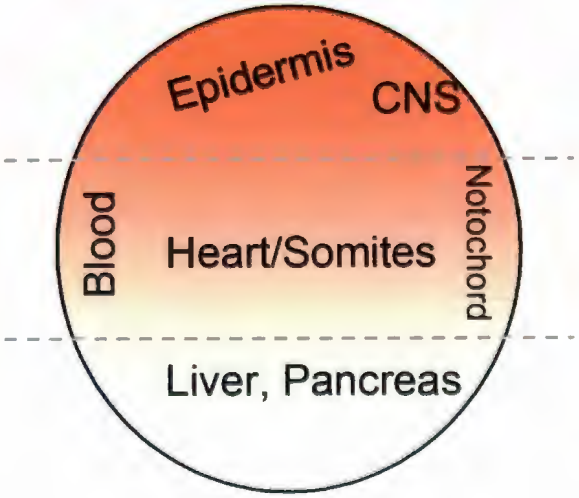
Epidermis
CNS
Blood
Heart/Somites
Notochord
Liver, Pancreas

mediate *Xnr* expression, thus restricting the domain of mesoderm induction, at least dorsally. However, in dorsal mesendodermal cells XBcl9 is required for β-catenin mediated transcription to promote dorsal mesoderm (body axis) formation. Interestingly, the translational regulation of XBcl9 mRNA in embryos may form a novel rate-limiting mechanism during Wnt/β-catenin pathway activation. Taken together, these findings suggest that XRel3/XRelA and XBcl9 proteins function as antagonistic and/or complementary regulators of β-catenin activity to control the space and time during which the body axis is established.

5.1.2 Canonical Wnt signaling: Why should we care?

It is well established that canonical Wnt signaling plays essential roles in embryogenesis and cellular homeostasis in all animals, including mammals. Hence, aberrant canonical Wnt signaling can cause/contribute to congenital birth defects and diseases, such as cancer. Thus, the elucidation of the molecular mechanistic control of β-catenin activity is the key to deciphering the physiological requirements and parameters of canonical Wnt signaling. As such, the determination of core components as well as cell-type/context dependent regulators of β-catenin activity is essential to defining and describing normal canonical Wnt-mediated biological processes as well as the etiology of many birth defects and cancers. The discovery of such basic scientific knowledge would greatly further our understanding of how the parts of the human body are formed and

maintained, as well as provide biological targets for clinical medicine when these basic biological process are misregulated.

Chapter 6: References

6.1 References

Reference List

Abaza I, Gebauer F. 2008. Trading translation with RNA-binding proteins. RNA 14:404-409.

Aberle H, Bauer A, Stappert J, Kispert A, Kemler R. 1997. beta-catenin is a target for the ubiquitin-proteasome pathway. EMBO J 16:3797-3804.

Agius E, Oelgeschlager M, Wessely O, Kemp C, De Robertis EM. 2000. Endodermal Nodal-related signals and mesoderm induction in Xenopus. Development 127:1173-1183.

Algire MA, Lorsch JR. 2006. Where to begin? The mechanism of translation initiation codon selection in eukaryotes. Curr Opin Chem Biol 10:480-486.

Amaya E, Stein PA, Musci TJ, Kirschner MW. 1993. FGF signalling in the early specification of mesoderm in Xenopus. Development 118:477-487.

Amit S, Hatzubai A, Birman Y, Andersen JS, Ben Shushan E, Mann M, Ben Neriah Y, Alkalay I. 2002. Axin-mediated CKI phosphorylation of beta-catenin at Ser 45: a molecular switch for the Wnt pathway. Genes Dev 16:1066-1076.

Andrews PG, He Z, Popadiuk C, Kao KR. 2009. The transcriptional activity of Pygopus is enhanced by its interaction with cAMP-response-element-binding protein (CREB)-binding protein. Biochem J 422:493-501.

Armstrong NJ, Steinbeisser H, Prothmann C, DeLotto R, Rupp RA. 1998. Conserved Spatzle/Toll signaling in dorsoventral patterning of Xenopus embryos. Mech Dev 71:99-105.

Asashima M, Nakano H, Uchiyama H, Davids M, Plessow S, Loppnow-Blinde B, Hoppe P, Dau H, Tiedemann H. 1990. The vegetalizing factor belongs to a family of mesoderm-inducing proteins related to erythroid differentiation factor. Naturwissenschaften 77:389-391.

Aziz N, Munro HN. 1987. Iron regulates ferritin mRNA translation through a segment of its 5' untranslated region. Proc Natl Acad Sci U S A 84:8478-8482.

Balinsky BI. 1951. On the eyecup-lens correlation in some South African amphibians. Experientia 7:180-181.

Barkoff AF, Dickson KS, Gray NK, Wickens M. 2000. Translational control of cyclin B1 mRNA during meiotic maturation: coordinated repression and cytoplasmic polyadenylation. Dev Biol 220:97-109.

Bearer EL. 1994. Distribution of Xrel in the early Xenopus embryo: a cytoplasmic and nuclear gradient. Eur J Cell Biol 63:255-268.

Beck CW, Sutherland DJ, Woodland HR. 1998. Involvement of NF-kappaB associated proteins in FGF-mediated mesoderm induction. Int J Dev Biol 42:67-77.

Beg AA, Ruben SM, Scheinman RI, Haskill S, Rosen CA, Baldwin AS, Jr. 1992. I kappa B interacts with the nuclear localization sequences of the subunits of NF-kappa B: a mechanism for cytoplasmic retention. Genes Dev 6:1899-1913.

Belenkaya TY, Han C, Standley HJ, Lin X, Houston DW, Heasman J, Lin X. 2002. pygopus Encodes a nuclear protein essential for wingless/Wnt signaling. Development 129:4089-4101.

Bettegowda A, Smith GW. 2007. Mechanisms of maternal mRNA regulation: implications for mammalian early embryonic development. Front Biosci 12:3713-3726.

Billin AN, Thirlwell H, Ayer DE. 2000. Beta-catenin-histone deacetylase interactions regulate the transition of LEF1 from a transcriptional repressor to an activator. Mol Cell Biol 20:6882-6890.

Black SD, Gerhart JC. 1985. Experimental control of the site of embryonic axis formation in Xenopus laevis eggs centrifuged before first cleavage. Dev Biol 108:310-324.

Bouwmeester T, Kim S, Sasai Y, Lu B, De Robertis EM. 1996. Cerberus is a head-inducing secreted factor expressed in the anterior endoderm of Spemann's organizer. Nature 382:595-601.

Branney PA, Faas L, Steane SE, Pownall ME, Isaacs HV. 2009. Characterisation of the fibroblast growth factor dependent transcriptome in early development. PLoS ONE 4:e4951.

Brannon M, Gomperts M, Sumoy L, Moon RT, Kimelman D. 1997. A beta-catenin/XTcf-3 complex binds to the siamois promoter to regulate dorsal axis specification in Xenopus. Genes Dev 11:2359-2370.

Brantjes H, Roose J, van de WM, Clevers H. 2001. All Tcf HMG box transcription factors interact with Groucho-related co-repressors. Nucleic Acids Res 29:1410-1419.

Brown DD, Littna E. 1966. Synthesis and accumulation of low molecular weight RNA during embryogenesis of Xenopus laevis. J Mol Biol 20:95-112.

Browning KS, Maia DM, Lax SR, Ravel JM. 1987. Identification of a new protein synthesis initiation factor from wheat germ. J Biol Chem 262:538-541.

Bushati N, Cohen SM. 2007. microRNA functions. Annu Rev Cell Dev Biol 23:175-205.

Butsch M, Hull S, Wang Y, Roberts TM, Boris-Lawrie K. 1999. The 5' RNA terminus of spleen necrosis virus contains a novel posttranscriptional control element that facilitates human immunodeficiency virus Rev/RRE-independent Gag production. J Virol 73:4847-4855.

Cadigan KM. 2008. Wnt-beta-catenin signaling. Curr Biol 18:R943-R947.

Carrera I, Janody F, Leeds N, Duveau F, Treisman JE. 2008. Pygopus activates Wingless target gene transcription through the mediator complex subunits Med12 and Med13. Proc Natl Acad Sci U S A 105:6644-6649.

Cha SW, Tadjuidje E, Tao Q, Wylie C, Heasman J. 2008. Wnt5a and Wnt11 interact in a maternal Dkk1-regulated fashion to activate both canonical and non-canonical signaling in Xenopus axis formation. Development 135:3719-3729.

Charlesworth A, Welk J, MacNicol AM. 2000. The temporal control of Wee1 mRNA translation during Xenopus oocyte maturation is regulated by cytoplasmic polyadenylation elements within the 3'-untranslated region. Dev Biol 227:706-719.

Cheong SM, Kim H, Han JK. 2009. Identification of a novel negative regulator of activin/nodal signaling in mesendodermal formation of Xenopus embryos. J Biol Chem 284:17052-17060.

Cho HH, Song JS, Yu JM, Yu SS, Choi SJ, Kim DH, Jung JS. 2008. Differential effect of NF-kappaB activity on beta-catenin/Tcf pathway in various cancer cells. FEBS Lett 582:616-622.

Cho KW, Blumberg B, Steinbeisser H, De Robertis EM. 1991. Molecular nature of Spemann's organizer: the role of the Xenopus homeobox gene goosecoid. Cell 67:1111-1120.

Cho M, Gwak J, Park S, Won J, Kim DE, Yea SS, Cha IJ, Kim TK, Shin JG, Oh S. 2005. Diclofenac attenuates Wnt/beta-catenin signaling in colon cancer cells by activation of NF-kappaB. FEBS Lett 579:4213-4218.

Christen B, Slack JM. 1999. Spatial response to fibroblast growth factor signalling in Xenopus embryos. Development 126:119-125.

Christian JL, McMahon JA, McMahon AP, Moon RT. 1991. Xwnt-8, a Xenopus Wnt-1/int-1-related gene responsive to mesoderm-inducing growth factors, may play a role in ventral mesodermal patterning during embryogenesis. Development 111:1045-1055.

Clements D, Friday RV, Woodland HR. 1999. Mode of action of VegT in mesoderm and endoderm formation. Development 126:4903-4911.

Cliffe A, Hamada F, Bienz M. 2003. A role of Dishevelled in relocating Axin to the plasma membrane during wingless signaling. Curr Biol 13:960-966.

Colegrove-Otero LJ, Minshall N, Standart N. 2005. RNA-binding proteins in early development. Crit Rev Biochem Mol Biol 40:21-73.

Cornell RA, Kimelman D. 1994. Activin-mediated mesoderm induction requires FGF. Development 120:453-462.

Cornell RA, Musci TJ, Kimelman D. 1995. FGF is a prospective competence factor for early activin-type signals in Xenopus mesoderm induction. Development 121:2429-2437.

Croce JC, McClay DR. 2006. The canonical Wnt pathway in embryonic axis polarity. Semin Cell Dev Biol 17:168-174.

Cuykendall TN, Houston DW. 2009. Vegetally localized Xenopus trim36 regulates cortical rotation and dorsal axis formation. Development 136:3057-3065.

Dahanukar A, Walker JA, Wharton RP. 1999. Smaug, a novel RNA-binding protein that operates a translational switch in Drosophila. Mol Cell 4:209-218.

Dale L, Matthews G, Colman A. 1993. Secretion and mesoderm-inducing activity of the TGF-beta-related domain of Xenopus Vg1. EMBO J 12:4471-4480.

Dale L, Slack JM. 1987. Regional specification within the mesoderm of early embryos of Xenopus laevis. Development 100:279-295.

Dale L, Smith JC, Slack JM. 1985. Mesoderm induction in Xenopus laevis: a quantitative study using a cell lineage label and tissue-specific antibodies. J Embryol Exp Morphol 89:289-312.

Daniels DL, Weis WI. 2005. Beta-catenin directly displaces Groucho/TLE repressors from Tcf/Lef in Wnt-mediated transcription activation. Nat Struct Mol Biol 12:364-371.

Darras S, Marikawa Y, Elinson RP, Lemaire P. 1997. Animal and vegetal pole cells of early Xenopus embryos respond differently to maternal dorsal determinants: implications for the patterning of the organiser. Development 124:4275-4286.

de Moor CH, Richter JD. 1997. The Mos pathway regulates cytoplasmic polyadenylation in Xenopus oocytes. Mol Cell Biol 17:6419-6426.

De Robertis EM. 2006. Spemann's organizer and self-regulation in amphibian embryos. Nat Rev Mol Cell Biol 7: 296-302.

De Robertis EM. 2009. Spemann's organizer and the self-regulation of embryonic fields. Mech Dev.

De Robertis EM, Kuroda H. 2004. Dorsal-ventral patterning and neural induction in Xenopus embryos. Annu Rev Cell Dev Biol 20:285-308.

Dekel N. 2005. Cellular, biochemical and molecular mechanisms regulating oocyte maturation. Mol Cell Endocrinol 234:19-25.

Deng J, Miller SA, Wang HY, Xia W, Wen Y, Zhou BP, Li Y, Lin SY, Hung MC. 2002. beta-catenin interacts with and inhibits NF-kappa B in human colon and breast cancer. Cancer Cell 2:323-334.

DiDonato JA, Hayakawa M, Rothwarf DM, Zandi E, Karin M. 1997. A cytokine-responsive IkappaB kinase that activates the transcription factor NF-kappaB. Nature 388:548-554.

Dominguez I, Green JB. 2000. Dorsal downregulation of GSK3beta by a non-Wnt-like mechanism is an early molecular consequence of cortical rotation in early Xenopus embryos. Development 127:861-868.

Dominguez I, Itoh K, Sokol SY. 1995. Role of glycogen synthase kinase 3 beta as a negative regulator of dorsoventral axis formation in Xenopus embryos. Proc Natl Acad Sci U S A 92:8498-8502.

Dominguez I, Mizuno J, Wu H, Imbrie GA, Symes K, Seldin DC. 2005. A role for CK2alpha/beta in Xenopus early embryonic development. Mol Cell Biochem 274:125-131.

Dominguez I, Mizuno J, Wu H, Song DH, Symes K, Seldin DC. 2004. Protein kinase CK2 is required for dorsal axis formation in Xenopus embryos. Dev Biol 274:110-124.

Dominski Z, Marzluff WF. 2007. Formation of the 3' end of histone mRNA: getting closer to the end. Gene 396:373-390.

Dubnicoff T, Valentine SA, Chen G, Shi T, Lengyel JA, Paroush Z, Courey AJ. 1997. Conversion of dorsal from an activator to a repressor by the global corepressor Groucho. Genes Dev 11:2952-2957.

Dupont S, Zacchigna L, Cordenonsi M, Soligo S, Adorno M, Rugge M, Piccolo S. 2005. Germ-layer specification and control of cell growth by Ectodermin, a Smad4 ubiquitin ligase. Cell 121:87-99.

Edery I, Humbelin M, Darveau A, Lee KA, Milburn S, Hershey JW, Trachsel H, Sonenberg N. 1983. Involvement of eukaryotic initiation factor 4A in the cap recognition process. J Biol Chem 258:11398-11403.

Elinson RP, Rowning B. 1988. A transient array of parallel microtubules in frog eggs: potential tracks for a cytoplasmic rotation that specifies the dorso-ventral axis. Dev Biol 128:185-197.

ELSDALE TR, Fischberg M, SMITH S. 1958. A mutation that reduces nucleolar number in Xenopus laevis. Exp Cell Res 14:642-643.

ELSDALE TR, Gurdon JB, Fischberg M. 1960. A description of the technique for nuclear transplantation in Xenopus laevis. J Embryol Exp Morphol 8:437-444.

Fan MJ, Gruning W, Walz G, Sokol SY. 1998. Wnt signaling and transcriptional control of Siamois in Xenopus embryos. Proc Natl Acad Sci U S A 95:5626-5631.

Fiedler M, Sanchez-Barrena MJ, Nekrasov M, Mieszczanek J, Rybin V, Muller J, Evans P, Bienz M. 2008. Decoding of methylated histone H3 tail by the Pygo-BCL9 Wnt signaling complex. Mol Cell 30:507-518.

Fisher AL, Caudy M. 1998. Groucho proteins: transcriptional corepressors for specific subsets of DNA-binding transcription factors in vertebrates and invertebrates. Genes Dev 12:1931-1940.

Fletcher RB, Harland RM. 2008. The role of FGF signaling in the establishment and maintenance of mesodermal gene expression in Xenopus. Dev Dyn 237:1243-1254.

Franzoso G, Carlson L, Xing L, Poljak L, Shores EW, Brown KD, Leonardi A, Tran T, Boyce BF, Siebenlist U. 1997. Requirement for NF-kappaB in osteoclast and B-cell development. Genes Dev 11:3482-3496.

Fraser SD, Wilkes-Johnston J, Browder LW. 1996. Effects of c-myc first exons and 5' synthetic hairpins on RNA translation in oocytes and early embryos of Xenopus laevis. Oncogene 12:1223-1230.

Fu LN, Ye RQ, Browder LW, Johnston RN. 1991. Translational potentiation of messenger RNA with secondary structure in Xenopus. Science 251:807-810.

Fujisue M, Kobayakawa Y, Yamana K. 1993. Occurrence of dorsal axis-inducing activity around the vegetal pole of an uncleaved Xenopus egg and displacement to the equatorial region by cortical rotation. Development 118:163-170.

Funayama N, Fagotto F, McCrea P, Gumbiner BM. 1995. Embryonic axis induction by the armadillo repeat domain of beta-catenin: evidence for intracellular signaling. J Cell Biol 128:959-968.

Garcia-Fernàndez J, D'Aniello S, Escrivà H. 2007. Organizing chordates with an organizer. Bioessays 29: 619-624.

Gebauer F, Richter JD. 1996. Mouse cytoplasmic polyadenylylation element binding protein: an evolutionarily conserved protein that interacts with the cytoplasmic polyadenylylation elements of c-mos mRNA. Proc Natl Acad Sci U S A 93:14602-14607.

Gerhart JC, Vincent JP, Scharf SR, Black SD, Gimlich RL, Danilchik M. 1984. Localization and induction in early development of Xenopus. Philos Trans R Soc Lond B Biol Sci 307:319-330.

Gerondakis S, Grumont R, Gugasyan R, Wong L, Isomura I, Ho W, Banerjee A. 2006. Unravelling the complexities of the NF-kappaB signalling pathway using mouse knockout and transgenic models. Oncogene 25:6781-6799.

Gilbert SF. 2003. Developmental Biology. Sunderland, Massachusetts: Sinauer Associates, Inc.p 268-278.

Gillespie LL, Paterno GD, Slack JM. 1989. Analysis of competence: receptors for fibroblast growth factor in early Xenopus embryos. Development 106:203-208.

Gilmore TD. 2006. Introduction to NF-kappaB: players, pathways, perspectives. Oncogene 25:6680-6684.

Gimlich RL. 1986. Acquisition of developmental autonomy in the equatorial region of the Xenopus embryo. Dev Biol 115:340-352.

Gimlich RL, Gerhart JC. 1984. Early cellular interactions promote embryonic axis formation in Xenopus laevis. Dev Biol 104:117-130.

Gonzalez-Sancho JM, Brennan KR, Castelo-Soccio LA, Brown AM. 2004. Wnt proteins induce dishevelled phosphorylation via an LRP5/6- independent mechanism, irrespective of their ability to stabilize beta-catenin. Mol Cell Biol 24:4757-4768.

Gray NK, Pantopoulos K, Dandekar T, Ackrell BA, Hentze MW. 1996. Translational regulation of mammalian and Drosophila citric acid cycle enzymes via iron-responsive elements. Proc Natl Acad Sci U S A 93:4925-4930.

Groisman I, Huang YS, Mendez R, Cao Q, Theurkauf W, Richter JD. 2000. CPEB, maskin, and cyclin B1 mRNA at the mitotic apparatus: implications for local translational control of cell division. Cell 103:435-447.

Groisman I, Jung MY, Sarkissian M, Cao Q, Richter JD. 2002. Translational control of the embryonic cell cycle. Cell 109:473-483.

Gugasyan R, Voss A, Varigos G, Thomas T, Grumont RJ, Kaur P, Grigoriadis G, Gerondakis S. 2004. The transcription factors c-rel and RelA control epidermal development and homeostasis in embryonic and adult skin via distinct mechanisms. Mol Cell Biol 24:5733-5745.

Gurdon JB, ELSDALE TR, Fischberg M. 1958. Sexually mature individuals of Xenopus laevis from the transplantation of single somatic nuclei. Nature 182:64-65.

Gurdon JB, Lane CD, Woodland HR, Marbaix G. 1971. Use of frog eggs and oocytes for the study of messenger RNA and its translation in living cells. Nature 233:177-182.

Habas R, Dawid IB. 2005. Dishevelled and Wnt signaling: is the nucleus the final frontier? J Biol 4:2.

Hake LE, Richter JD. 1994. CPEB is a specificity factor that mediates cytoplasmic polyadenylation during Xenopus oocyte maturation. Cell 79:617-627.

Hardin J, Keller R. 1988. The behaviour and function of bottle cells during gastrulation of Xenopus laevis. Development 103: 211-230.

Harjola O, Toivonen S. 1949. Finnish experience of the care and use of the clawed frog (Xenopus laevis Daudin) in the diagnosis of pregnancy. Ann Chir Gynaecol Fenn Suppl 38:68-82.

Hart MJ, de los SR, Albert IN, Rubinfeld B, Polakis P. 1998. Downregulation of beta-catenin by human Axin and its association with the APC tumor suppressor, beta-catenin and GSK3 beta. Curr Biol 8:573-581.

Hartman TR, Qian S, Bolinger C, Fernandez S, Schoenberg DR, Boris-Lawrie K. 2006. RNA helicase A is necessary for translation of selected messenger RNAs. Nat Struct Mol Biol 13:509-516.

Hashimoto-Partyka MK, Yuge M, Cho KW. 2003. Nodal signaling in Xenopus gastrulae is cell-autonomous and patterned by beta-catenin. Dev Biol 253:125-138.

Haskill S, Beg AA, Tompkins SM, Morris JS, Yurochko AD, Sampson-Johannes A, Mondal K, Ralph P, Baldwin AS, Jr. 1991. Characterization of an immediate-early gene induced in adherent monocytes that encodes I kappa B-like activity. Cell 65:1281-1289.

Heasman J. 1997. Patterning the Xenopus blastula. Development 124:4179-4191.

Heasman J. 2006. Maternal determinants of embryonic cell fate. Semin Cell Dev Biol 17:93-98.

Heasman J, Crawford A, Goldstone K, Garner-Hamrick P, Gumbiner B, McCrea P, Kintner C, Noro CY, Wylie C. 1994. Overexpression of cadherins and underexpression of beta-catenin inhibit dorsal mesoderm induction in early Xenopus embryos. Cell 79:791-803.

Heasman J, Kofron M, Wylie C. 2000. Beta-catenin signaling activity dissected in the early Xenopus embryo: a novel antisense approach. Dev Biol 222:124-134.

Hentze MW, Caughman SW, Rouault TA, Barriocanal JG, Dancis A, Harford JB, Klausner RD. 1987. Identification of the iron-responsive element for the translational regulation of human ferritin mRNA. Science 238:1570-1573.

Hoffmans R, Basler K. 2004. Identification and in vivo role of the Armadillo-Legless interaction. Development 131:4393-4400.

Hoffmans R, Stadeli R, Basler K. 2005. Pygopus and legless provide essential transcriptional coactivator functions to armadillo/beta-catenin. Curr Biol 15:1207-1211.

Holowacz T, Elinson RP. 1993. Cortical cytoplasm, which induces dorsal axis formation in Xenopus, is inactivated by UV irradiation of the oocyte. Development 119:277-285.

Holowacz T, Elinson RP. 1995. Properties of the dorsal activity found in the vegetal cortical cytoplasm of Xenopus eggs. Development 121:2789-2798.

Hong JW, Hendrix DA, Papatsenko D, Levine MS. 2008. How the Dorsal gradient works: insights from postgenome technologies. Proc Natl Acad Sci U S A 105:20072-20076.

Houliston E, Elinson RP. 1991. Patterns of microtubule polymerization relating to cortical rotation in Xenopus laevis eggs. Development 112:107-117.

Howard EL, Charlesworth A, Welk J, MacNicol AM. 1999. The mitogen-activated protein kinase signaling pathway stimulates mos mRNA cytoplasmic polyadenylation during Xenopus oocyte maturation. Mol Cell Biol 19:1990-1999.

Huang H, He X. 2008. Wnt/beta-catenin signaling: new (and old) players and new insights. Curr Opin Cell Biol 20:119-125.

Huang HK, Yoon H, Hannig EM, Donahue TF. 1997. GTP hydrolysis controls stringent selection of the AUG start codon during translation initiation in Saccharomyces cerevisiae. Genes Dev 11:2396-2413.

Huelsken J, Behrens J. 2002. The Wnt signalling pathway. J Cell Sci 115:3977-3978.

Hull S, Boris-Lawrie K. 2002. RU5 of Mason-Pfizer monkey virus 5' long terminal repeat enhances cytoplasmic expression of human immunodeficiency virus type 1 gag-pol and nonviral reporter RNA. J Virol 76:10211-10218.

Ikeda S, Kishida S, Yamamoto H, Murai H, Koyama S, Kikuchi A. 1998. Axin, a negative regulator of the Wnt signaling pathway, forms a complex with GSK-3beta and beta-catenin and promotes GSK-3beta-dependent phosphorylation of beta-catenin. EMBO J 17:1371-1384.

Imataka H, Gradi A, Sonenberg N. 1998. A newly identified N-terminal amino acid sequence of human eIF4G binds poly(A)-binding protein and functions in poly(A)-dependent translation. EMBO J 17:7480-7489.

Iotsova V, Caamano J, Loy J, Yang Y, Lewin A, Bravo R. 1997. Osteopetrosis in mice lacking NF-kappaB1 and NF-kappaB2. Nat Med 3:1285-1289.

Irish V, Lehmann R, Akam M. 1989. The Drosophila posterior-group gene nanos functions by repressing hunchback activity. Nature 338:646-648.

Isaacs HV. 1997. New perspectives on the role of the fibroblast growth factor family in amphibian development. Cell Mol Life Sci 53:350-361.

Isaacs HV, Pownall ME, Slack JM. 1994. eFGF regulates Xbra expression during Xenopus gastrulation. EMBO J 13:4469-4481.

Israel A, Le Bail O, Hatat D, Piette J, Kieran M, Logeat F, Wallach D, Fellous M, Kourilsky P. 1989. TNF stimulates expression of mouse MHC class I genes by inducing an NF kappa B-like enhancer binding activity which displaces constitutive factors. EMBO J 8:3793-3800.

Itoh K, Brott BK, Bae GU, Ratcliffe MJ, Sokol SY. 2005. Nuclear localization is required for Dishevelled function in Wnt/beta-catenin signaling. J Biol 4:3.

Itoh K, Krupnik VE, Sokol SY. 1998. Axis determination in Xenopus involves biochemical interactions of axin, glycogen synthase kinase 3 and beta-catenin. Curr Biol 8:591-594.

Jacobson A. 1996. Poly(A) metabolism and translation: the closed-loop model. In: Hershey JWBMMBaSN, editor. Translational Control. Cold Spring Harbor Laboratories, New York:p 451-480.

Jang SK, Krausslich HG, Nicklin MJ, Duke GM, Palmenberg AC, Wimmer E. 1988. A segment of the 5' nontranslated region of encephalomyocarditis virus RNA directs internal entry of ribosomes during in vitro translation. J Virol 62:2636-2643.

Jang SK, Pestova TV, Hellen CU, Witherell GW, Wimmer E. 1990. Cap-independent translation of picornavirus RNAs: structure and function of the internal ribosomal entry site. Enzyme 44:292-309.

Jiang J, Struhl G. 1998. Regulation of the Hedgehog and Wingless signalling pathways by the F-box/WD40-repeat protein Slimb. Nature 391:493-496.

Joel C, Rabau E. 1949. The Xenopus test in the diagnosis of pregnancy. Harefuah 36:31.

Jonckheere N, Mayes E, Shih HP, Li B, Lioubinski O, Dai X, Sander M. 2008. Analysis of mPygo2 mutant mice suggests a requirement for mesenchymal Wnt signaling in pancreatic growth and differentiation. Dev Biol 318:224-235.

Jones CM, Armes N, Smith JC. 1996. Signalling by TGF-beta family members: short-range effects of Xnr-2 and BMP-4 contrast with the long-range effects of activin. Curr Biol 6:1468-1475.

Jones CM, Kuehn MR, Hogan BL, Smith JC, Wright CV. 1995. Nodal-related signals induce axial mesoderm and dorsalize mesoderm during gastrulation. Development 121:3651-3662.

Jones EA, Woodland HR. 1987. The develoment of animal cap cells in Xenopus: a measure of the start of animal cap competence to form mesoderm. Development 101:557-563.

Jopling CL, Spriggs KA, Mitchell SA, Stoneley M, Willis AE. 2004. L-Myc protein synthesis is initiated by internal ribosome entry. RNA 10:287-298.

Jopling CL, Willis AE. 2001. N-myc translation is initiated via an internal ribosome entry segment that displays enhanced activity in neuronal cells. Oncogene 20:2664-2670.

Josefsberg LB, Galiani D, Lazar S, Kaufman O, Seger R, Dekel N. 2003. Maturation-promoting factor governs mitogen-activated protein kinase activation and interphase suppression during meiosis of rat oocytes. Biol Reprod 68:1282-1290.

Joseph EM, Melton DA. 1997. Xnr4: a Xenopus nodal-related gene expressed in the Spemann organizer. Dev Biol 184:367-372.

Kageura H. 1990. Spatial distribution of the capacity to initiate a secondary embryo in the 32-cell embryo of Xenopus laevis. Dev Biol 142:432-438.

Kahvejian A, Roy G, Sonenberg N. 2001. The mRNA closed-loop model: the function of PABP and PABP-interacting proteins in mRNA translation. Cold Spring Harb Symp Quant Biol 66:293-300.

Kao KR, Elinson RP. 1988. The entire mesodermal mantle behaves as Spemann's organizer in dorsoanterior enhanced Xenopus laevis embryos. Dev Biol 127:64-77.

Kao KR, Elinson RP. 1989. Dorsalization of mesoderm induction by lithium. Dev Biol 132:81-90.

Kao KR, Hopwood ND. 1991. Expression of a mRNA related to c-rel and dorsal in early Xenopus laevis embryos. Proc Natl Acad Sci U S A 88:2697-2701.

Kao KR, Lockwood A. 1996. Negative regulation of dorsal patterning in early embryos by overexpression of XrelA, a Xenopus homologue of NF-kappa B. Mech Dev 58:129-139.

Kao KR, Masui Y, Elinson RP. 1986. Lithium-induced respecification of pattern in Xenopus laevis embryos. Nature 322:371-373.

Katoh M, Katoh M. 2003. Identification and characterization of human BCL9L gene and mouse Bcl9l gene in silico. Int J Mol Med 12:643-649.

Kawai N, Takahashi H, Nishida H, Yokosawa H. 2005. Regulation of NF-kappaB/Rel by IkappaB is essential for ascidian notochord formation. Dev Biol 277:80-91.

Keller R, Danilchik M. 1988. Regional expression pattern and timing of convergence and extension during gastrulation of Xenopus laevis. Development 103: 193-209.

Keller R, Shook D, Skoglud P. 2008. The forces that shape embryos: physical aspects of convergent extension by cell intercalatioon. Phys Biol 5: 1-22.

Kennedy MW, Green KA, Ford RL, Andrews PG, Paterno GD, Gillespie LL, Kao KR. 2007. Regulation of the response to Nodal-mediated mesoderm induction by Xrel3. Dev Biol 311:383-395.

Kim-Ha J, Kerr K, Macdonald PM. 1995. Translational regulation of oskar mRNA by bruno, an ovarian RNA-binding protein, is essential. Cell 81:403-412.

Kimelman D. 2006. Mesoderm induction: from caps to chips. Nat Rev Genet 7:360-372.

Kimelman D, Abraham JA, Haaparanta T, Palisi TM, Kirschner MW. 1988. The presence of fibroblast growth factor in the frog egg: its role as a natural mesoderm inducer. Science 242:1053-1056.

Kimelman D, Kirschner M. 1987. Synergistic induction of mesoderm by FGF and TGF-beta and the identification of an mRNA coding for FGF in the early Xenopus embryo. Cell 51:869-877.

Kishida S, Yamamoto H, Ikeda S, Kishida M, Sakamoto I, Koyama S, Kikuchi A. 1998. Axin, a negative regulator of the wnt signaling pathway, directly interacts with adenomatous polyposis coli and regulates the stabilization of beta-catenin. J Biol Chem 273:10823-10826.

Klein PS, Melton DA. 1996. A molecular mechanism for the effect of lithium on development. Proc Natl Acad Sci U S A 93:8455-8459.

Klein SL, Strausberg RL, Wagner L, Pontius J, Clifton SW, Richardson P. 2002. Genetic and genomic tools for Xenopus research: The NIH Xenopus initiative. Dev Dyn 225:384-391.

Kloc M, Etkin LD. 1995. Two distinct pathways for the localization of RNAs at the vegetal cortex in Xenopus oocytes. Development 121:287-297.

Kofron M, Birsoy B, Houston D, Tao Q, Wylie C, Heasman J. 2007. Wnt11/beta-catenin signaling in both oocytes and early embryos acts through LRP6-mediated regulation of axin. Development 134:503-513.

Kofron M, Demel T, Xanthos J, Lohr J, Sun B, Sive H, Osada S, Wright C, Wylie C, Heasman J. 1999. Mesoderm induction in Xenopus is a zygotic event regulated by maternal VegT via TGFbeta growth factors. Development 126:5759-5770.

Kohn AD, Moon RT. 2005. Wnt and calcium signaling: beta-catenin-independent pathways. Cell Calcium 38:439-446.

Kozak M. 1986. Influences of mRNA secondary structure on initiation by eukaryotic ribosomes. Proc Natl Acad Sci U S A 83:2850-2854.

Kozak M. 1987. An analysis of 5'-noncoding sequences from 699 vertebrate messenger RNAs. Nucleic Acids Res 15:8125-8148.

Kozak M. 1989. Circumstances and mechanisms of inhibition of translation by secondary structure in eucaryotic mRNAs. Mol Cell Biol 9:5134-5142.

Kozak M. 2008. Faulty old ideas about translational regulation paved the way for current confusion about how microRNAs function. Gene 423:108-115.

Kramps T, Peter O, Brunner E, Nellen D, Froesch B, Chatterjee S, Murone M, Zullig S, Basler K. 2002. Wnt/wingless signaling requires BCL9/legless-mediated recruitment of pygopus to the nuclear beta-catenin-TCF complex. Cell 109:47-60.

Krasnow SW, Zhang LQ, Leung KY, Osborn L, Kunkel S, Nabel GJ. 1991. Tumor necrosis factor-alpha, interleukin 1, and phorbol myristate acetate are independent activators of NF-kappa B which differentially activate T cells. Cytokine 3:372-379.

Krieghoff E, Behrens J, Mayr B. 2006. Nucleo-cytoplasmic distribution of beta-catenin is regulated by retention. J Cell Sci 119:1453-1463.

Ku M, Melton DA. 1993. Xwnt-11: a maternally expressed Xenopus wnt gene. Development 119:1161-1173.

LaBonne C, Burke B, Whitman M. 1995. Role of MAP kinase in mesoderm induction and axial patterning during Xenopus development. Development 121:1475-1486.

LaBonne C, Whitman M. 1997. Localization of MAP kinase activity in early Xenopus embryos: implications for endogenous FGF signaling. Dev Biol 183:9-20.

Lake BB, Ford R, Kao KR. 2001. Xrel3 is required for head development in Xenopus laevis. Development 128:263-273.

Lake BB, Kao KR. 2003a. Early head specification in Xenopus laevis. ScientificWorldJournal 3:655-676.

Lake BB, Kao KR. 2003b. Pygopus is required for embryonic brain patterning in Xenopus. Dev Biol 261:132-148.

Larabell CA, Torres M, Rowning BA, Yost C, Miller JR, Wu M, Kimelman D, Moon RT. 1997. Establishment of the dorso-ventral axis in Xenopus embryos is presaged by early asymmetries in beta-catenin that are modulated by the Wnt signaling pathway. J Cell Biol 136:1123-1136.

Laurent MN, Blitz IL, Hashimoto C, Rothbacher U, Cho KW. 1997. The Xenopus homeobox gene twin mediates Wnt induction of goosecoid in establishment of Spemann's organizer. Development 124:4905-4916.

Lavery DL, Hoppler S. 2008. Gain-of-function and loss-of-function strategies in Xenopus. Methods Mol Biol 469:401-415.

Lazar S, Galiani D, Dekel N. 2002. cAMP-Dependent PKA negatively regulates polyadenylation of c-mos mRNA in rat oocytes. Mol Endocrinol 16:331-341.

Lazar S, Gershon E, Dekel N. 2004. Selective degradation of cyclin B1 mRNA in rat oocytes by RNA interference (RNAi). J Mol Endocrinol 33:73-85.

Lee R, Feinbaum R, Ambros V. 2004. A short history of a short RNA. Cell 116:S89-92, 1.

Lee RC, Feinbaum RL, Ambros V. 1993. The C. elegans heterochronic gene lin-4 encodes small RNAs with antisense complementarity to lin-14. Cell 75:843-854.

Leibold EA, Munro HN. 1988. Cytoplasmic protein binds in vitro to a highly conserved sequence in the 5' untranslated region of ferritin heavy- and light-subunit mRNAs. Proc Natl Acad Sci U S A 85:2171-2175.

Leipuviene R, Theil EC. 2007. The family of iron responsive RNA structures regulated by changes in cellular iron and oxygen. Cell Mol Life Sci 64:2945-2955.

Lemaire P, Garrett N, Gurdon JB. 1995. Expression cloning of Siamois, a Xenopus homeobox gene expressed in dorsal-vegetal cells of blastulae and able to induce a complete secondary axis. Cell 81:85-94.

Li B, Rheaume C, Teng A, Bilanchone V, Munguia JE, Hu M, Jessen S, Piccolo S, Waterman ML, Dai X. 2007. Developmental phenotypes and reduced Wnt signaling in mice deficient for pygopus 2. Genesis 45:318-325.

Li L, Yuan H, Weaver CD, Mao J, Farr GH, III, Sussman DJ, Jonkers J, Kimelman D, Wu D. 1999. Axin and Frat1 interact with dvl and GSK, bridging Dvl to GSK in Wnt-mediated regulation of LEF-1. EMBO J 18:4233-4240.

Liu C, Li Y, Semenov M, Han C, Baeg GH, Tan Y, Zhang Z, Lin X, He X. 2002. Control of beta-catenin phosphorylation/degradation by a dual-kinase mechanism. Cell 108:837-847.

Livak KJ, Schmittgen TD. 2001. Analysis of relative gene expression data using real-time quantitative PCR and the 2(-Delta Delta C(T)) Method. Methods 25:402-408.

MacDonald BT, Tamai K, He X. 2009. Wnt/beta-catenin signaling: components, mechanisms, and diseases. Dev Cell 17:9-26.

Majumdar R, Maitra U. 2005. Regulation of GTP hydrolysis prior to ribosomal AUG selection during eukaryotic translation initiation. EMBO J 24:3737-3746.

Malacinski GM, Chung HM, Youn B. 1978. Further characterization of the effects of ultraviolet irradiation of the amphibian egg. Experientia 34:883-884.

Mani M, Carrasco DE, Zhang Y, Takada K, Gatt ME, Dutta-Simmons J, Ikeda H, Diaz-Griffero F, Pena-Cruz V, Bertagnolli M, Myeroff LL, Markowitz SD, Anderson KC, Carrasco DR. 2009. BCL9 promotes tumor progression by conferring enhanced proliferative, metastatic, and angiogenic properties to cancer cells. Cancer Res 69:7577-7586.

Mao B, Wu W, Li Y, Hoppe D, Stannek P, Glinka A, Niehrs C. 2001. LDL-receptor-related protein 6 is a receptor for Dickkopf proteins. Nature 411:321-325.

Marikawa Y. 2006. Wnt/beta-catenin signaling and body plan formation in mouse embryos. Semin Cell Dev Biol 17:175-184.

Marikawa Y, Elinson RP. 1998. beta-TrCP is a negative regulator of Wnt/beta-catenin signaling pathway and dorsal axis formation in Xenopus embryos. Mech Dev 77:75-80.

Marikawa Y, Elinson RP. 1999. Relationship of vegetal cortical dorsal factors in the Xenopus egg with the Wnt/beta-catenin signaling pathway. Mech Dev 89:93-102.

Marikawa Y, Li Y, Elinson RP. 1997. Dorsal determinants in the Xenopus egg are firmly associated with the vegetal cortex and behave like activators of the Wnt pathway. Dev Biol 191:69-79.

Masui O, Ueda Y, Tsumura A, Koyanagi M, Hijikata M, Shimotohno K. 2002. RelA suppresses the Wnt/beta-catenin pathway without exerting trans-acting transcriptional ability. Int J Mol Med 9:489-493.

McCrea PD, Brieher WM, Gumbiner BM. 1993. Induction of a secondary body axis in Xenopus by antibodies to beta-catenin. J Cell Biol 123:477-484.

McMahon AP, Moon RT. 1989. Ectopic expression of the proto-oncogene int-1 in Xenopus embryos leads to duplication of the embryonic axis. Cell 58:1075-1084.

Medina A, Wendler SR, Steinbeisser H. 1997. Cortical rotation is required for the correct spatial expression of nr3, sia and gsc in Xenopus embryos. Int J Dev Biol 41:741-745.

Meinhardt H. 2006. Primary body axes of vertebrates: generation of a near-Cartesian coordinate system and role of Spemann-type organizer. Dev Dyn 235: 2907-2919.

Mercurio F, Zhu H, Murray BW, Shevchenko A, Bennett BL, Li J, Young DB, Barbosa M, Mann M, Manning A, Rao A. 1997. IKK-1 and IKK-2: cytokine-activated IkappaB kinases essential for NF-kappaB activation. Science 278:860-866.

Meroni G, Diez-Roux G. 2005. TRIM/RBCC, a novel class of 'single protein RING finger' E3 ubiquitin ligases. Bioessays 27:1147-1157.

Miller JR, Rowning BA, Larabell CA, Yang-Snyder JA, Bates RL, Moon RT. 1999. Establishment of the dorsal-ventral axis in Xenopus embryos coincides with the dorsal enrichment of dishevelled that is dependent on cortical rotation. J Cell Biol 146:427-437.

Mir A, Heasman J. 2008. How the mother can help: studying maternal Wnt signaling by anti-sense-mediated depletion of maternal mRNAs and the host transfer technique. Methods Mol Biol 469:417-429.

Mir A, Kofron M, Zorn AM, Bajzer M, Haque M, Heasman J, Wylie CC. 2007. FoxI1e activates ectoderm formation and controls cell position in the Xenopus blastula. Development 134:779-788.

Mitchell SF, Lorsch JR. 2008. Should I stay or should I go? Eukaryotic translation initiation factors 1 and 1A control start codon recognition. J Biol Chem 283:27345-27349.

Molenaar M, van de WM, Oosterwegel M, Peterson-Maduro J, Godsave S, Korinek V, Roose J, Destree O, Clevers H. 1996. XTcf-3 transcription factor mediates beta-catenin-induced axis formation in Xenopus embryos. Cell 86:391-399.

Moon RT, Kimelman D. 1998. From cortical rotation to organizer gene expression: toward a molecular explanation of axis specification in Xenopus. Bioessays 20:536-545.

Mosimann C, Hausmann G, Basler K. 2006. Parafibromin/Hyrax activates Wnt/Wg target gene transcription by direct association with beta-catenin/Armadillo. Cell 125:327-341.

Mosimann C, Hausmann G, Basler K. 2009. Beta-catenin hits chromatin: regulation of Wnt target gene activation. Nat Rev Mol Cell Biol 10:276-286.

Moussian B, Roth S. 2005. Dorsoventral axis formation in the Drosophila embryo--shaping and transducing a morphogen gradient. Curr Biol 15:R887-R899.

Munemitsu S, Albert I, Souza B, Rubinfeld B, Polakis P. 1995. Regulation of intracellular beta-catenin levels by the adenomatous polyposis coli (APC) tumor-suppressor protein. Proc Natl Acad Sci U S A 92:3046-3050.

Nakahata S, Kotani T, Mita K, Kawasaki T, Katsu Y, Nagahama Y, Yamashita M. 2003. Involvement of Xenopus Pumilio in the translational regulation that is specific to cyclin B1 mRNA during oocyte maturation. Mech Dev 120:865-880.

Nakamura O, Takasaki H. 1970. Further studies on the differentiation capacity of the dorsal marginal zone in the morula of Tritus pyrrhogaster. Proc Jpn Acad 46:700-705.

Newport J, Kirschner M. 1982a. A major developmental transition in early Xenopus embryos: I. characterization and timing of cellular changes at the midblastula stage. Cell 30:675-686.

Newport J, Kirschner M. 1982b. A major developmental transition in early Xenopus embryos: II. Control of the onset of transcription. Cell 30:687-696.

Niessing D, Blanke S, Jackle H. 2002. Bicoid associates with the 5'-cap-bound complex of caudal mRNA and represses translation. Genes Dev 16:2576-2582.

Nieuwkoop PD. 1955. Independent and dependent development in the formation of the central nervous system in amphibians; a review of experimental analysis. Exp Cell Res262-273.

Nieuwkoop PD. 1973. The organization center of the amphibian embryo: its origin, spatial organization, and morphogenetic action. Adv Morphog 10:1-39.

Nishita M, Hashimoto MK, Ogata S, Laurent MN, Ueno N, Shibuya H, Cho KW. 2000. Interaction between Wnt and TGF-beta signalling pathways during formation of Spemann's organizer. Nature 403: 781-785.

Ogryzko VV, Schiltz RL, Russanova V, Howard BH, Nakatani Y. 1996. The transcriptional coactivators p300 and CBP are histone acetyltransferases. Cell 87:953-959.

Orford K, Crockett C, Jensen JP, Weissman AM, Byers SW. 1997. Serine phosphorylation-regulated ubiquitination and degradation of beta-catenin. J Biol Chem 272:24735-24738.

Osborn L, Kunkel S, Nabel GJ. 1989. Tumor necrosis factor alpha and interleukin 1 stimulate the human immunodeficiency virus enhancer by activation of the nuclear factor kappa B. Proc Natl Acad Sci U S A 86:2336-2340.

Palacios J, Gamallo C. 1998. Mutations in the beta-catenin gene (CTNNB1) in endometrioid ovarian carcinomas. Cancer Res 58:1344-1347.

Pantopoulos K. 2004. Iron metabolism and the IRE/IRP regulatory system: an update. Ann N Y Acad Sci 1012:1-13.

Papa S, Bubici C, Zazzeroni F, Pham CG, Kuntzen C, Knabb JR, Dean K, Franzoso G. 2006. The NF-kappaB-mediated control of the JNK cascade in the antagonism of programmed cell death in health and disease. Cell Death Differ 13:712-729.

Parker DS, Jemison J, Cadigan KM. 2002. Pygopus, a nuclear PHD-finger protein required for Wingless signaling in Drosophila. Development 129:2565-2576.

Parker DS, Ni YY, Chang JL, Li J, Cadigan KM. 2008. Wingless signaling induces widespread chromatin remodeling of target loci. Mol Cell Biol 28:1815-1828.

Paterno GD, Gillespie LL, Dixon MS, Slack JM, Heath JK. 1989. Mesoderm-inducing properties of INT-2 and kFGF: two oncogene-encoded growth factors related to FGF. Development 106:79-83.

Paterno GD, Li Y, Luchman HA, Ryan PJ, Gillespie LL. 1997. cDNA cloning of a novel, developmentally regulated immediate early gene activated by fibroblast growth factor and encoding a nuclear protein. J Biol Chem 272:25591-25595.

Pelletier J, Kaplan G, Racaniello VR, Sonenberg N. 1988. Cap-independent translation of poliovirus mRNA is conferred by sequence elements within the 5' noncoding region. Mol Cell Biol 8:1103-1112.

Pelletier J, Sonenberg N. 1988. Internal initiation of translation of eukaryotic mRNA directed by a sequence derived from poliovirus RNA. Nature 334:320-325.

Pereira SG, Oakley F. 2008. Nuclear factor-kappaB1: regulation and function. Int J Biochem Cell Biol 40:1425-1430.

Perkins ND. 2007. Integrating cell-signalling pathways with NF-kappaB and IKK function. Nat Rev Mol Cell Biol 8:49-62.

Pestova TV, Kolupaeva VG, Lomakin IB, Pilipenko EV, Shatsky IN, Agol VI, Hellen CU. 2001. Molecular mechanisms of translation initiation in eukaryotes. Proc Natl Acad Sci U S A 98:7029-7036.

Piao S, Lee SH, Kim H, Yum S, Stamos JL, Xu Y, Lee SJ, Lee J, Oh S, Han JK, Park BJ, Weis WI, Ha NC. 2008. Direct inhibition of GSK3beta by the phosphorylated cytoplasmic domain of LRP6 in Wnt/beta-catenin signaling. PLoS ONE 3:e4046.

Piccioni F, Zappavigna V, Verrotti AC. 2005. Translational regulation during oogenesis and early development: the cap-poly(A) tail relationship. C R Biol 328:863-881.

Piccolo S, Agius E, Leyns L, Bhattacharyya S, Grunz H, Bouwmeester T, De Robertis EM. 1999. The head inducer Cerberus is a multifunctional antagonist of Nodal, BMP and Wnt signals. Nature 397:707-710.

Piccolo S, Sasai Y, Lu B, De Robertis EM. 1996. Dorsoventral patterning in Xenopus: inhibition of ventral signals by direct binding of chordin to BMP-4. Cell 86:589-598.

Polack SS. 1949. The Xenopus pregnancy test. Can J Med Technol 11:140-143.

Popadiuk CM, Xiong J, Wells MG, Andrews PG, Dankwa K, Hirasawa K, Lake BB, Kao KR. 2006. Antisense suppression of pygopus2 results in growth arrest of epithelial ovarian cancer. Clin Cancer Res 12:2216-2223.

Prothmann C, Armstrong NJ, Roth S, Rupp RA. 2006. Vertebrate Rel proteins exhibit Dorsal-like activities in early Drosophila embryogenesis. Dev Dyn 235:949-957.

Pyronnet S, Imataka H, Gingras AC, Fukunaga R, Hunter T, Sonenberg N. 1999. Human eukaryotic translation initiation factor 4G (eIF4G) recruits mnk1 to phosphorylate eIF4E. EMBO J 18:270-279.

Ranganathan S, Liu CX, Migliorini MM, von Arnim CA, Peltan ID, Mikhailenko I, Hyman BT, Strickland DK. 2004. Serine and threonine phosphorylation of the low density lipoprotein receptor-related protein by protein kinase Calpha regulates endocytosis and association with adaptor molecules. J Biol Chem 279:40536-40544.

Ratnaparkhi GS, Jia S, Courey AJ. 2006. Uncoupling dorsal-mediated activation from dorsal-mediated repression in the Drosophila embryo. Development 133:4409-4414.

Ray BK, Lawson TG, Kramer JC, Cladaras MH, Grifo JA, Abramson RD, Merrick WC, Thach RE. 1985. ATP-dependent unwinding of messenger RNA structure by eukaryotic initiation factors. J Biol Chem 260:7651-7658.

Ray PS, Grover R, Das S. 2006. Two internal ribosome entry sites mediate the translation of p53 isoforms. EMBO Rep 7:404-410.

Roberts TM, Boris-Lawrie K. 2003. Primary sequence and secondary structure motifs in spleen necrosis virus RU5 confer translational utilization of unspliced human immunodeficiency virus type 1 reporter RNA. J Virol 77:11973-11984.

Roose J, Molenaar M, Peterson J, Hurenkamp J, Brantjes H, Moerer P, van de WM, Destree O, Clevers H. 1998. The Xenopus Wnt effector XTcf-3 interacts with Groucho-related transcriptional repressors. Nature 395:608-612.

Roth S. 2003. The origin of dorsoventral polarity in Drosophila. Philos Trans R Soc Lond B Biol Sci 358:1317-1329.

Roth S, Stein D, Nusslein-Volhard C. 1989. A gradient of nuclear localization of the dorsal protein determines dorsoventral pattern in the Drosophila embryo. Cell 59:1189-1202.

Rowning BA, Wells J, Wu M, Gerhart JC, Moon RT, Larabell CA. 1997. Microtubule-mediated transport of organelles and localization of beta-catenin to the future dorsal side of Xenopus eggs. Proc Natl Acad Sci U S A 94:1224-1229.

Rubinfeld B, Souza B, Albert I, Muller O, Chamberlain SH, Masiarz FR, Munemitsu S, Polakis P. 1993. Association of the APC gene product with beta-catenin. Science 262:1731-1734.

Saegusa M, Hashimura M, Kuwata T, Hamano M, Okayasu I. 2007. Crosstalk between NF-kappaB/p65 and beta-catenin/TCF4/p300 signalling pathways through alterations in

GSK-3beta expression during trans-differentiation of endometrial carcinoma cells. J Pathol 213:35-45.

Sakanaka C. 2002. Phosphorylation and regulation of beta-catenin by casein kinase I epsilon. J Biochem 132:697-703.

Sampietro J, Dahlberg CL, Cho US, Hinds TR, Kimelman D, Xu W. 2006. Crystal structure of a beta-catenin/BCL9/Tcf4 complex. Mol Cell 24:293-300.

Sanchez R, Marzluff WF. 2002. The stem-loop binding protein is required for efficient translation of histone mRNA in vivo and in vitro. Mol Cell Biol 22:7093-7104.

Scharf SR, Gerhart JC. 1980. Determination of the dorsal-ventral axis in eggs of Xenopus laevis: complete rescue of uv-impaired eggs by oblique orientation before first cleavage. Dev Biol 79:181-198.

Scharf SR, Gerhart JC. 1983. Axis determination in eggs of Xenopus laevis: a critical period before first cleavage, identified by the common effects of cold, pressure and ultraviolet irradiation. Dev Biol 99:75-87.

Scharf SR, Rowning B, Wu M, Gerhart JC. 1989. Hyperdorsoanterior embryos from Xenopus eggs treated with D2O. Dev Biol 134:175-188.

Schmittgen TD, Livak KJ. 2008. Analyzing real-time PCR data by the comparative C(T) method. Nat Protoc 3:1101-1108.

Schneider S, Steinbeisser H, Warga RM, Hausen P. 1996. Beta-catenin translocation into nuclei demarcates the dorsalizing centers in frog and fish embryos. Mech Dev 57:191-198.

Schohl A, Fagotto F. 2002. Beta-catenin, MAPK and Smad signaling during early Xenopus development. Development 129:37-52.

Schohl A, Fagotto F. 2003. A role for maternal beta-catenin in early mesoderm induction in Xenopus. EMBO J 22:3303-3313.

Sen R, Baltimore D. 1986a. Inducibility of kappa immunoglobulin enhancer-binding protein Nf-kappa B by a posttranslational mechanism. Cell 47:921-928.

Sen R, Baltimore D. 1986b. Multiple nuclear factors interact with the immunoglobulin enhancer sequences. Cell 46:705-716.

Sheets MD, Fox CA, Hunt T, Vande WG, Wickens M. 1994. The 3'-untranslated regions of c-mos and cyclin mRNAs stimulate translation by regulating cytoplasmic polyadenylation. Genes Dev 8:926-938.

Sheets MD, Wu M, Wickens M. 1995. Polyadenylation of c-mos mRNA as a control point in Xenopus meiotic maturation. Nature 374:511-516.

Shin CY, Kundel M, Wells DG. 2004. Rapid, activity-induced increase in tissue plasminogen activator is mediated by metabotropic glutamate receptor-dependent mRNA translation. J Neurosci 24:9425-9433.

Singh H, Sen R, Baltimore D, Sharp PA. 1986. A nuclear factor that binds to a conserved sequence motif in transcriptional control elements of immunoglobulin genes. Nature 319:154-158.

Slack JM. 1991. The nature of the mesoderm-inducing signal in Xenopus: a transfilter induction study. Development 113:661-669.

Slack JM, Darlington BG, Gillespie LL, Godsave SF, Isaacs HV, Paterno GD. 1989. The role of fibroblast growth factor in early Xenopus development. Development 107 Suppl:141-148.

Slack JM, Darlington BG, Gillespie LL, Godsave SF, Isaacs HV, Paterno GD. 1990. Mesoderm induction by fibroblast growth factor in early Xenopus development. Philos Trans R Soc Lond B Biol Sci 327:75-84.

Slack JM, Isaacs HV, Darlington BG. 1988. Inductive effects of fibroblast growth factor and lithium ion on Xenopus blastula ectoderm. Development 103:581-590.

Smith JC, Price BM, Van Nimmen K, Huylebroeck D. 1990. Identification of a potent Xenopus mesoderm-inducing factor as a homologue of activin A. Nature 345:729-731.

Smith WC, McKendry R, Ribisi S Jr, Harland RM. 1995. A nodal-related gene defines a physical and functional domain within the Spemann organizer. Cell 82:37-46.

Sokol S, Christian JL, Moon RT, Melton DA. 1991. Injected Wnt RNA induces a complete body axis in Xenopus embryos. Cell 67:741-752.

Song DH, Dominguez I, Mizuno J, Kaut M, Mohr SC, Seldin DC. 2003. CK2 phosphorylation of the armadillo repeat region of beta-catenin potentiates Wnt signaling. J Biol Chem 278:24018-24025.

Song N, Schwab KR, Patterson LT, Yamaguchi T, Lin X, Potter SS, Lang RA. 2007. pygopus 2 has a crucial, Wnt pathway-independent function in lens induction. Development 134:1873-1885.

Spriggs KA, Cobbold LC, Ridley SH, Coldwell M, Bottley A, Bushell M, Willis AE, Siddle K. 2009. The human insulin receptor mRNA contains a functional internal ribosome entry segment. Nucleic Acids Res.

Stadeli R, Basler K. 2005. Dissecting nuclear Wingless signalling: recruitment of the transcriptional co-activator Pygopus by a chain of adaptor proteins. Mech Dev 122:1171-1182.

Staudt LM, Singh H, Sen R, Wirth T, Sharp PA, Baltimore D. 1986. A lymphoid-specific protein binding to the octamer motif of immunoglobulin genes. Nature 323:640-643.

Stebbins-Boaz B, Hake LE, Richter JD. 1996. CPEB controls the cytoplasmic polyadenylation of cyclin, Cdk2 and c-mos mRNAs and is necessary for oocyte maturation in Xenopus. EMBO J 15:2582-2592.

Stoneley M, Paulin FE, Le Quesne JP, Chappell SA, Willis AE. 1998. C-Myc 5' untranslated region contains an internal ribosome entry segment. Oncogene 16:423-428.

Strugnell TD, Browder LW. 1997. Effects of cyclin A2 noncoding regions on reporter gene translation during early development of Xenopus laevis. Dev Genet 21:134-145.

Sun BI, Bush SM, Collins-Racie LA, LaVallie ER, DiBlasio-Smith EA, Wolfman NM, McCoy JM, Sive HL. 1999. derriere: a TGF-beta family member required for posterior development in Xenopus. Development 126:1467-1482.

Suri C, Haremaki T, Weinstein DC. 2005. Xema, a foxi-class gene expressed in the gastrula stage Xenopus ectoderm, is required for the suppression of mesendoderm. Development 132:2733-2742.

Sustmann C, Flach H, Ebert H, Eastman Q, Grosschedl R. 2008. Cell-type-specific function of BCL9 involves a transcriptional activation domain that synergizes with beta-catenin. Mol Cell Biol 28:3526-3537.

Suzuki K, Tsuchida J, Yamamoto T, Inoue J. 1998. Identification and expression of the Xenopus homolog of mammalian p100-NFkappaB2. Gene 206:1-9.

Suzuki K, Yamamoto T, Inoue J. 1995. Molecular cloning of cDNA encoding the Xenopus homolog of mammalian RelB. Nucleic Acids Res 23:4664-4669.

Swiatek W, Kang H, Garcia BA, Shabanowitz J, Coombs GS, Hunt DF, Virshup DM. 2006. Negative regulation of LRP6 function by casein kinase I epsilon phosphorylation. J Biol Chem 281:12233-12241.

Tahara SM, Morgan MA, Shatkin AJ. 1981. Two forms of purified m7G-cap binding protein with different effects on capped mRNA translation in extracts of uninfected and poliovirus-infected HeLa cells. J Biol Chem 256:7691-7694.

Takahashi S, Yokota C, Takano K, Tanegashima K, Onuma Y, Goto J, Asashima M. 2000. Two novel nodal-related genes initiate early inductive events in Xenopus Nieuwkoop center. Development 127:5319-5329.

Takemaru KI, Moon RT. 2000. The transcriptional coactivator CBP interacts with beta-catenin to activate gene expression. J Cell Biol 149:249-254.

Tannahill D, Wardle FC. 1995. Control of axis formation in Xenopus by the NF-kappa B-I kappa B system. Int J Dev Biol 39:549-558.

Tao Q, Yokota C, Puck H, Kofron M, Birsoy B, Yan D, Asashima M, Wylie CC, Lin X, Heasman J. 2005. Maternal wnt11 activates the canonical wnt signaling pathway required for axis formation in Xenopus embryos. Cell 120:857-871.

Tarun SZ, Jr., Sachs AB. 1996. Association of the yeast poly(A) tail binding protein with translation initiation factor eIF-4G. EMBO J 15:7168-7177.

Tay J, Hodgman R, Richter JD. 2000. The control of cyclin B1 mRNA translation during mouse oocyte maturation. Dev Biol 221:1-9.

Telford NA, Watson AJ, Schultz GA. 1990. Transition from maternal to embryonic control in early mammalian development: a comparison of several species. Mol Reprod Dev 26:90-100.

Teplitsky Y, Paterno GD, Gillespie LL. 2003. Proline365 is a critical residue for the activity of XMI-ER1 in Xenopus embryonic development. Biochem Biophys Res Commun 308:679-683.

Tettweiler G, Lasko P. 2006. A new model for translational regulation of specific mRNAs. Trends Biochem Sci 31:607-610.

Thermann R, Hentze MW. 2007. Drosophila miR2 induces pseudo-polysomes and inhibits translation initiation. Nature 447:875-878.

Thompson B, Townsley F, Rosin-Arbesfeld R, Musisi H, Bienz M. 2002. A new nuclear component of the Wnt signalling pathway. Nat Cell Biol 4:367-373.

Thompson BJ. 2004. A complex of Armadillo, Legless, and Pygopus coactivates dTCF to activate wingless target genes. Curr Biol 14:458-466.

Thomsen GH, Melton DA. 1993. Processed Vg1 protein is an axial mesoderm inducer in Xenopus. Cell 74:433-441.

Tolwinski NS, Wehrli M, Rives A, Erdeniz N, DiNardo S, Wieschaus E. 2003. Wg/Wnt signal can be transmitted through arrow/LRP5,6 and Axin independently of Zw3/Gsk3beta activity. Dev Cell 4:407-418.

Townsley FM, Cliffe A, Bienz M. 2004a. Pygopus and Legless target Armadillo/beta-catenin to the nucleus to enable its transcriptional co-activator function. Nat Cell Biol 6:626-633.

Townsley FM, Thompson B, Bienz M. 2004b. Pygopus residues required for its binding to Legless are critical for transcription and development. J Biol Chem 279:5177-5183.

Ubbels GA, Hara K, Koster CH, Kirschner MW. 1983. Evidence for a functional role of the cytoskeleton in determination of the dorsoventral axis in Xenopus laevis eggs. J Embryol Exp Morphol 77:15-37.

van der Velden AW, Thomas AA. 1999. The role of the 5' untranslated region of an mRNA in translation regulation during development. Int J Biochem Cell Biol 31:87-106.

Vasudevan S, Seli E, Steitz JA. 2006. Metazoan oocyte and early embryo development program: a progression through translation regulatory cascades. Genes Dev 20:138-146.

Vincent JP, Gerhart JC. 1987. Subcortical rotation in Xenopus eggs: an early step in embryonic axis specification. Dev Biol 123:526-539.

Vincent JP, Oster GF, Gerhart JC. 1986. Kinematics of gray crescent formation in Xenopus eggs: the displacement of subcortical cytoplasm relative to the egg surface. Dev Biol 113:484-500.

Vincent JP, Scharf SR, Gerhart JC. 1987. Subcortical rotation in Xenopus eggs: a preliminary study of its mechanochemical basis. Cell Motil Cytoskeleton 8:143-154.

Wakiyama M, Imataka H, Sonenberg N. 2000. Interaction of eIF4G with poly(A)-binding protein stimulates translation and is critical for Xenopus oocyte maturation. Curr Biol 10:1147-1150.

Wakiyama M, Takimoto K, Ohara O, Yokoyama S. 2007. Let-7 microRNA-mediated mRNA deadenylation and translational repression in a mammalian cell-free system. Genes Dev 21:1857-1862.

Wallander ML, Leibold EA, Eisenstein RS. 2006. Molecular control of vertebrate iron homeostasis by iron regulatory proteins. Biochim Biophys Acta 1763:668-689.

Wallingford JB, Fraser SE, Harland RM. 2002. Convergent extension: the molecular control of polarized cell movement during embryonic development. Dev Cell 2: 695-706.

Weaver C, Farr GH, III, Pan W, Rowning BA, Wang J, Mao J, Wu D, Li L, Larabell CA, Kimelman D. 2003. GBP binds kinesin light chain and translocates during cortical rotation in Xenopus eggs. Development 130:5425-5436.

Weaver C, Kimelman D. 2004. Move it or lose it: axis specification in Xenopus. Development 131:3491-3499.

Wells SE, Hillner PE, Vale RD, Sachs AB. 1998. Circularization of mRNA by eukaryotic translation initiation factors. Mol Cell 2:135-140.

Wharton RP, Struhl G. 1991. RNA regulatory elements mediate control of Drosophila body pattern by the posterior morphogen nanos. Cell 67:955-967.

Whitman M, Melton DA. 1992. Involvement of p21ras in Xenopus mesoderm induction. Nature 357:252-254.

Wilhelm JE, Hilton M, Amos Q, Henzel WJ. 2003. Cup is an eIF4E binding protein required for both the translational repression of oskar and the recruitment of Barentsz. J Cell Biol 163:1197-1204.

Wreden C, Verrotti AC, Schisa JA, Lieberfarb ME, Strickland S. 1997. Nanos and pumilio establish embryonic polarity in Drosophila by promoting posterior deadenylation of hunchback mRNA. Development 124:3015-3023.

Wu G, Huang H, Garcia AJ, He X. 2009a. Inhibition of GSK3 phosphorylation of beta-catenin via phosphorylated PPPSPXS motifs of Wnt coreceptor LRP6. PLoS ONE 4:e4926.

Wu H, Symes K, Seldin DC, Dominguez I. 2009b. Threonine 393 of beta-catenin regulates interaction with Axin. J Cell Biochem 108:52-63.

Wylie C, Kofron M, Payne C, Anderson R, Hosobuchi M, Joseph E, Heasman J. 1996. Maternal beta-catenin establishes a 'dorsal signal' in early Xenopus embryos. Development 122:2987-2996.

Xanthos JB, Kofron M, Wylie C, Heasman J. 2001. Maternal VegT is the initiator of a molecular network specifying endoderm in Xenopus laevis. Development 128:167-180.

Yang J, Tan C, Darken RS, Wilson PA, Klein PS. 2002. Beta-catenin/Tcf-regulation prior to the midblastula transition. Development 129: 5743-5752.

Yang S, Lockwood A, Hollett P, Ford R, Kao K. 1998. Overexpression of a novel Xenopus rel mRNA gene induces tumors in early embryos. J Biol Chem 273:13746-13752.

Yost C, Torres M, Miller JR, Huang E, Kimelman D, Moon RT. 1996. The axis-inducing activity, stability, and subcellular distribution of beta-catenin is regulated in Xenopus embryos by glycogen synthase kinase 3. Genes Dev 10:1443-1454.

Yuge M, Kobayakawa Y, Fujisue M, Yamana K. 1990. A cytoplasmic determinant for dorsal axis formation in an early embryo of Xenopus laevis. Development 110:1051-1056.

Zandi E, Rothwarf DM, Delhase M, Hayakawa M, Karin M. 1997. The IkappaB kinase complex (IKK) contains two kinase subunits, IKKalpha and IKKbeta, necessary for IkappaB phosphorylation and NF-kappaB activation. Cell 91:243-252.

Zhang C, Basta T, Hernandez-Lagunas L, Simpson P, Stemple DL, Artinger KB, Klymkowsky MW. 2004a. Repression of nodal expression by maternal B1-type SOXs regulates germ layer formation in Xenopus and zebrafish. Dev Biol 273:23-37.

Zhang C, Carl TF, Trudeau ED, Simmet T, Klymkowsky MW. 2006. An NF-kappaB and slug regulatory loop active in early vertebrate mesoderm. PLoS ONE 1:e106.

Zhang C, Klymkowsky MW. 2009. Unexpected functional redundancy between Twist and Slug (Snail2) and their feedback regulation of NF-kappaB via Nodal and Cerberus. Dev Biol 331:340-349.

Zhang J, Houston DW, King ML, Payne C, Wylie C, Heasman J. 1998. The role of maternal VegT in establishing the primary germ layers in Xenopus embryos. Cell 94:515-524.

Zhang J, King ML. 1996. Xenopus VegT RNA is localized to the vegetal cortex during oogenesis and encodes a novel T-box transcription factor involved in mesodermal patterning. Development 122:4119-4129.

Zhang JY, Green CL, Tao S, Khavari PA. 2004b. NF-kappaB RelA opposes epidermal proliferation driven by TNFR1 and JNK. Genes Dev 18:17-22.

Zhang Y, Tomann P, Andl T, Gallant NM, Huelsken J, Jerchow B, Birchmeier W, Paus R, Piccolo S, Mikkola ML, Morrisey EE, Overbeek PA, Scheidereit C, Millar SE, Schmidt-Ullrich R. 2009. Reciprocal requirements for EDA/EDAR/NF-kappaB and Wnt/beta-catenin signaling pathways in hair follicle induction. Dev Cell 17:49-61.

Zhou X, Sasaki H, Lowe L, Hogan BL, Kuehn MR. 1993. Nodal is a novel TGF-beta-like gene expressed in the mouse node during gastrulation. Nature 361:543-547.

Zimmerman LB, Jesus-Escobar JM, Harland RM. 1996. The Spemann organizer signal noggin binds and inactivates bone morphogenetic protein 4. Cell 86:599-606.